Sorption and Diffusion of small molecules in polymeric media

D I S S E R T A T I O N

zur Erlangung des akademischen Grades

doctor rerum naturalium
(Dr. rer. nat.)
im Fach Physik

eingereicht an der
Mathematisch-Naturwissenschaftliche Fakultät
Humboldt-Universität zu Berlin

von
Dipl.-Phys. Federico Camboni

Präsidentin der Humboldt-Universität zu Berlin:
Prof. Dr.-Ing. Dr. Sabine Kunst

Dekan der Mathematisch-Naturwissenschaftliche Fakultät:
Prof. Dr. Elmar Kulke

Gutachter:
1. Prof. Dr. I. M. Sokolov, Humboldt-Universität zu Berlin
2. Prof. Dr. B. Lindner, Humboldt-Universität zu Berlin
3. Prof. Dr. J. Dzubiella, Albert-Ludwigs-Universität Freiburg

Tag der mündlichen Prüfung: 19 September 2019

to my father Massimo
and my parents-in-law
Anna Maria and Alfredo

Abstract

Aim of this work is to analyze two physical processes that take place whenever a solid polymeric medium is put in contact with a gas atmosphere: gas molecules first penetrate the solid through a sorption process and then wander within it giving rise to a diffusion one.
The sorption process is studied within a model which is very close in spirit to the dual mode model. Applying basic thermodynamics principles we obtain the dependence of the penetrant concentration on the pressure of the gas phase and find that this is expressed via the Lambert W-function, as proposed by the gas-polymer matrix model, being a different functional form than the one proposed by dual sorption mode. The Lambert-like isotherms appear universally at low and moderate pressures and originate from the assumption that the internal energy in a polymer-penetrant-void ternary mixture is (in the lowest order) a bilinear form in the concentrations of the three components. Fitting the existing data shows that the Lambert function fits the data equally well.
The diffusion problem is analyzed by using a lattice approach with random site energies and random transition rates. A relation between the effective diffusion coefficient and the macroscopic conductivity in a random resistor network allows for elucidating possible sources of anomalous diffusion in such an environment. We show that subdiffusion is only possible either if the mean Boltzmann factor in the corresponding potential diverges or if the percolation concentration in the system is equal to unity (or both), and that superdiffusion is impossible in our system under any condition.
Properties of the effective diffusion constant are deeper discussed on a second stage taking into account a short range particle-polymer interaction. The system is modeled by a particle diffusion on a ternary lattice where the sites occupied by polymer segments are blocked, the ones forming the hull of the chains correspond to the places at which the interaction takes place, and the rest are voids, in which the diffusion is free. In the absence of interaction the diffusion coefficient shows only a weak dependence on the polymer chain length and its behavior strongly resembles usual site percolation. In presence of interactions the diffusion coefficient (and especially its temperature dependence) shows a non-trivial behavior depending on the sign of interaction and on whether the voids and the hulls of the chains percolate or not. The temperature dependence may be Arrhenius-like or strongly non-Arrhenius, depending on parameters. The analytical results obtained within the effective medium approximation are in qualitative agreement with those of Monte Carlo simulations.

Zusammenfassung

Ziel dieser Arbeit ist die Analyse zweier physikalischer Prozesse, die stattfinden wenn ein festes polymeres Medium in Kontakt mit einer Gas-Atmosphäre kommt:
1) ein Sorptionsprozess, d.h. die Gasmoleküle dringen in den Feststoff ein und
2) ein Diffusionsprozess, d.h. die Gasmoleküle bewegen sich danach innerhalb des Feststoffes.

Der Sorptionsprozess wird als Model analysiert, das in engem Zusammenhang mit dem Dual Mode Model steht. Durch die Anwendung grundlegender thermodynamischer Prinzipien gewinnen wir die Abhängigkeit der Eindringmittel-Konzentration vom Druck der Gasphase, die — wie im Gas-Polymer-Matrix model vorhergesagt — durch eine Lambertsche W-Funktion ausgedrückt werden kann und dadurch von der Vorhersage des Dual Sorption Mode Models abweicht. Lambert-artige Isothermen treten normalerweise bei niedrigen und moderaten Drücken auf und haben ihren Ursprung in der Annahme, dass die innere Energie einer Polymer-Penetrant-Pore Dreifach-Mixtur (in erster Näherung) eine Bilinearform der Konzentrationen der drei Komponenten ist. Ein Fitting von realen Daten zeigt, dass die Lambert-Funktion die Daten gleichermaßen gut modelliert.

Das Diffusionsproblem wird mittels eines Gitter-Modells mit zufälligen Knotenenergien und Übergangsraten analysiert. Die Analogie zwischen dem effektiven Diffusionskoeffizienten und der makroskopischen Leitfähigkeit eines zufälligen Widerstandsnetzwerks ermöglicht es, mögliche Quellen für anomale Diffusion in einer solchen Umgebung zu finden. Wir zeigen, dass Subdiffusion nur möglich ist, wenn der mittlere Boltzmann-Faktor im entsprechenden Potenzial divergiert oder wenn die Perkolationskonzentration im System gegen eins geht (oder beides) und dass Superdiffusion in diesem System unabhängig von den Bedingungen unmöglich ist.

Die Eigenschaften der effektiven Diffusionskonstanten werden genauer in einer zweiten Stufe diskutiert, in der kurzreichweitige Wechselwirkungen zwischen Teilchen und Polymeren berücksichtigt werden. Das System wird durch Teilchendiffusion auf einem Ternär-Gitter modelliert, wo die Gitterplätze blockiert werden, die von Polymerteilen besetzt sind. Diejenigen, die die Hülle der Ketten bilden, entsprechen dabei den Gitterplätzen, an denen die Wechselwirkungen stattfinden. Die übrigen sind Poren, an denen freie Diffusion stattfindet. In Abwesenheit von Wechselwirkungen zeigt der Diffusionskoef-

fizient nur eine schwache Abhängigkeit von der Polymerlänge und sein Verhalten ähnelt stark dem der gewöhnlichen Knotenperkolation. In Anwesenheit von Wechselwirkungen zeigt der Diffusionskoeffizient (im Besonderen seine Temperaturabhängigkeit) ein nicht-triviales Verhalten, abhängig vom Vorzeichen der Wechselwirkung und davon, ob die Poren und die Hüllen perkolieren oder nicht. Die Temperaturabhängigkeit kann in Abhängigkeit der Parameter Arrhenius-artig oder stark nicht Arrhenius-artig sein. Die analytischen Ergebnisse, die aus der Effective Medium Näherung gewonnen wurden, zeigen eine qualitative Übereinstimmung mit Ergebnissen aus Monte-Carlo Simulationen.

Contents

1. Introduction **1**
- 1.1. Sorption . . . 4
- 1.2. Diffusion . . . 7
  - 1.2.1. Einstein Equation . . . 11
  - 1.2.2. Anomalous Diffusion . . . 14

2. Analytical tools **18**
- 2.1. Flory-Huggins Theory . . . 18
  - 2.1.1. Limitations of the Flory-Huggins theory and Bawendi-Freed corrections . . . 23
- 2.2. Effective Medium Theory . . . 27
  - 2.2.1. Kirkpatrick model . . . 27
  - 2.2.2. Yuge adaptation . . . 31

3. Sorption of small molecules in polymeric media **35**
- 3.1. The model . . . 36
- 3.2. The free energy . . . 42
- 3.3. Fits . . . 48
  - 3.3.1. Concave isotherms . . . 49
  - 3.3.2. Convex isotherms . . . 51
- 3.4. List of abbreviations . . . 51

4. Diffusion of small molecules in polymeric media **53**
- 4.1. Normal and anomalous diffusion in random potential landscapes . . . 53
  - 4.1.1. General considerations . . . 54
  - 4.1.2. Effective diffusion coefficient close to equilibrium . . . 56
  - 4.1.3. Two and only two sources of anomalous diffusion . . . 62
- 4.2. Diffusion in a random energy landscape. . . . 67
  - 4.2.1. Effective medium approximation for diffusivity . . . 70
  - 4.2.2. Pure percolation (binary) model . . . 75
  - 4.2.3. Results for ternary model . . . 76

5. Summary and conclusion **86**

A. Appendix **88**
A.1. Smoluchowsky Equation 88
A.2. The Langevin equation 92
A.3. Einstein relation from the Fluctuation Dissipation theorem 95
A.3.1. Time correlation function 95
A.3.2. Fluctuation Dissipation Theorem 97
A.4. Discretization of a continuous Fokker-Planck equation with random potential 99
A.5. Hashin - Shtrikman bounds on the effective diffusivity 101

Bibliography **108**

1. Introduction

It is a long standing problem the one related to the comprehension of the physical and chemical behavior of polymeric materials. The interest around this kind of systems has been continuously growing in the last decades, driven by their extensive usage. Applications range from the use as barrier materials or protective coatings to gas separation membranes. Moreover, biological polymers are strongly present in nature like proteins, DNA, nucleic acids (polynucleotides), polysaccharides or latex rubber.
As a consequence, a deep understanding of their properties became absolutely necessary, presenting an hard challenge for physicists, chemists and engineers of all over the world.

Polymeric materials are really particular substances; they can be considered to be a mix between solids and liquids and in many cases the transition between the solid and liquid states is rather diffuse and quite difficult to localize.
Generally speaking a polymer is a macromolecule, namely a molecule with a high molecular weight, composed of a large number of elementary subunits, which can be small or big molecular groups on their turn and that constitute a repeated unit. These units form a chain which is held together by the repetition of the same covalent bond.
In order to specify a polymer one has to determine the nature of its inner and terminal subunits, the presence of eventual branches or defects in the structural sequence which may alter its mechanical characteristics.

This work is focused on two specific processes that happen whenever a contact is established between a gas atmosphere and a solid polymeric medium. In such a situation we essentially observe two phenomena: a first sorption process by which gas molecules get absorbed into the polymeric medium and a diffusion one originated by the random motion of the sorbed molecules within the medium.
Such a situations is obviously constantly present in every day life and it represents a serious issue that has to be faced in the most different industrial fields.
A typical example is given by the food industries and the need to pack their products in the most efficient way possible in order to avoid moisture and contaminants of whatever kind to penetrate. Packaging films, mostly made of polymeric materials, have to be therefore properly designed to reduce any kind of sorption and to guarantee the longest conservation.
Another example we want to give, since it represents the scenario that has originated this work, is given by the solar energy industry. The efficiency of solar panels is affected

by many factors, but one of the most problematic is the ingress of water molecules from the outside environment. Water molecules, once in the panel, are responsible of altering the working voltages and create corrosions at the electrical junctions. This in turn drastically reduces module performances.
The structure of a solar panel is therefore designed to satisfy several production needs, and among these to prevent moisture sorption. Of course there's a large variety of solar panel models in commerce nowadays, each having their own particular structure and design, but figure 1.1 may give an idea of what a general structure may be: silicon cells are placed between two polymeric layers (usually Ethylene Vinyl Acetate or EVA) that besides providing mechanical support and electrical isolation, work as encapsulant and protect them from water molecules uptake as well as from external contaminations or deterioration factors as UV radiation or temperature stress. A further protective polymeric back sheet is applied and this is usually made of Polyvinyl fluoride or PVF.

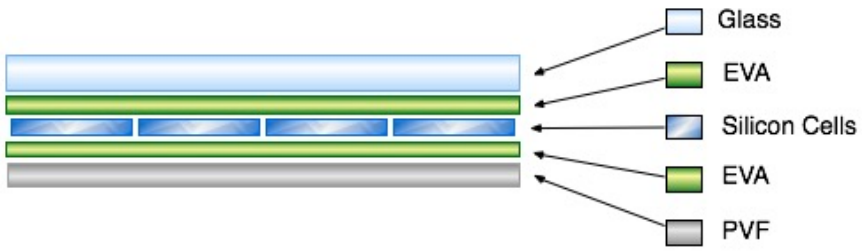

Figure 1.1.: Section of a typical solar panel structure.

The interest around solubility and transport of molecules in polymeric materials is therefore always alive and continuously increasing. This makes the growing of the collection of experimental data and theoretical models an extremely important step for the development of new materials and the increasing of the quality of a huge variety of products.

Aim of this work is to propose two models for the analysis of sorption and transport pf small molecules in a polymeric medium.
We consider a simple ideal experimental set up where we obtain a relation linking the external gas pressure to the equilibrium concentration of gas molecules within the polymeric medium. Later we give an expression for the diffusion constant characterizing their wandering in the same medium.

The results obtained through our models have produced the following publications

- F.Camboni, I.M.Sokolov: "Normal and anomalous diffusion in random potential landscapes", Phys. Rev. E 85, 050104(R) (2012); (arXiv:1205-2543)

- F.Camboni, A.Koher, I.M.Sokolov: "Diffusion of small particles in a solid polymeric medium", Phys. Rev. E 88, 022120 (2013); (arXiv:1210.6816)

- F.Camboni, I.M.Sokolov: "Sorption of small molecules in polymeric media", Physica A 464 (2016) 54–63s

The thesis is structured as follows: a general overview on the history and main features of sorption and diffusion is given in the next sections of this chapter.
Chapter 2 is devoted to the introduction of the analytical tools we mostly used to develop our models: the Flory-Huggins theory, together with the Bawendi and Freed corrections, and the Effective Medium Approximation as presented in the Kirkpatrick model, together with the corrections given by Yuge. This ends the first part of the thesis aimed to provide a comprehensive introduction.
The second part of the thesis is where our results are presented. In chapter 3 we analyze the solubility of gas molecules into a polymeric membrane. By applying basic thermodynamic principles and moving our steps in a scenario similar to the one defining the Dual Mode Sorption model, we obtain a sorption law. This results to be different in shape from the Dual Mode one, being expressed via a Lambert W function and above all showing a fewer number of free parameters. The two isotherms are then compared to several experimental data in the temperature and pressure regimes where the Dual Mode is usually adopted and our fitting quality results to be not inferior to Dual Mode one. More than the originality or prediction capability of the Lambert mode, we will stress its universality, being originated almost exclusively by the (quasi) equilibrium condition, the shape of the free energy in the gas phase and the bilinear dependence on concentrations of the free energy in the solid phase, and being able to reproduce some of the most used sorption laws in proper temperature and pressure limits.
In chapter 4 we face the diffusion problem. We start by proposing a general remark on the possible modes diffusion can occur whenever a random potential landscape model, with random site energies and random transition rates, is used as an approach. Through a relation between the effective diffusion coefficient and the macroscopic conductivity in a random resistor network we will discuss the sufficient and necessary conditions that let the diffusion turn to anomalous. We will show that subdiffusion is only possible either if the mean Boltzmann factor in the corresponding potential diverges or if the percolation concentration in the system is equal to unity (or both), and that superdiffusion is impossible in our system under any condition.
Later we present the calculations that led us to an expression for the diffusion constant of a particle wandering in the random energy landscape. A ternary lattice representation is

used where the sites occupied by polymer segments are considered as blocking. A short range particle-polymer interaction is considered to take place in the nearest neighboring sites of cells occupied by a polymer segment. Sites not occupied by any polymer or particle are considered as voids where diffusion is free.
In the absence of interaction the diffusion coefficient shows only a weak dependence on the polymer chain length and its behavior strongly resembles usual site percolation. On the contrary, in presence of interactions the diffusion coefficient (and especially its temperature dependence) shows a nontrivial behavior depending on the sign of interaction and on whether the voids and the hulls of the chains percolate or not. The temperature dependence may be Arrhenius-like or strongly non-Arrhenius, depending on parameters. The analytical results obtained within the effective medium approximation are in qualitative agreement with those of Monte Carlo simulations.

1.1. Sorption

The term sorption indicates the physical process through which particles or molecules penetrate matter and get absorbed by it until a stable equilibrium situation is reached associated to a precise concentration limit value. This term may include several different mechanisms representing different interactions between particles and the solid medium; for example, the more specific concept of *adsorption* indicates the situation in which particles adhere on the surface of the adsorbing material forming a thin film, or the term *absorption*, for which penetrants get dissolved within the body of it.

In the following we will therefore generally speak about *sorption* without specifying if it is an ad- or absorption process and will not make any difference between the concept of molecules, particles or penetrants, these term will be indistinctly used to mean the elements which get sorbed.
The sorption phenomenon has been extensively studied and observed for situations in which molecules forming a gas phase are sorbed by a polymeric medium. In the last one hundred years a wide literature has been provided on both theoretical and experimental sides with the production of a large series of data referring to several gas-polymer couples. The description and interpretation of experimental data have been built within empirical models combining some simple functions, which the experimental data may be fitted to with a physical explanation of the corresponding choice.

Many sorption laws have been therefore proposed and successfully used. The oldest and simplest one was proposed by William Henry at the beginning of the nineteenth century and was first formulated to analyze a gas-liquid system. Henry's law, states that the amount of sorbed molecules at constant temperature is linearly proportional to

the pressure exerted by the gas on the pressure:

$$C = k_D P \tag{1.1}$$

where C is the gas concentration in the medium, P the external gas pressure and k_D is the proportionality factor known as the solubility coefficient.
Henry's behavior can be observed in rubbery polymers in the ideal gas case at low pressures, or for higher pressures. More generally, Henry's law holds when the interaction between penetrant molecules and polymer ones is negligible respect to the polymer-polymer one.

Deviations from the Henry's law are usually observed in glassy polymers. The analysis of sorption in such media is made far more complex by the intrinsic non equilibrium nature of the glass state. Glassy polymers do not live in a canonical equilibrium condition but rather perform an extremely slow and time-dependent relaxation dynamic to an equilibrium. Polymers in the glass phase are in a pseudo-frozen state in which the mobility of chains is drastically reduced and the whole medium is interrupted by cavities whose effect is to increase the free volume space. The transition from a rubbery phase

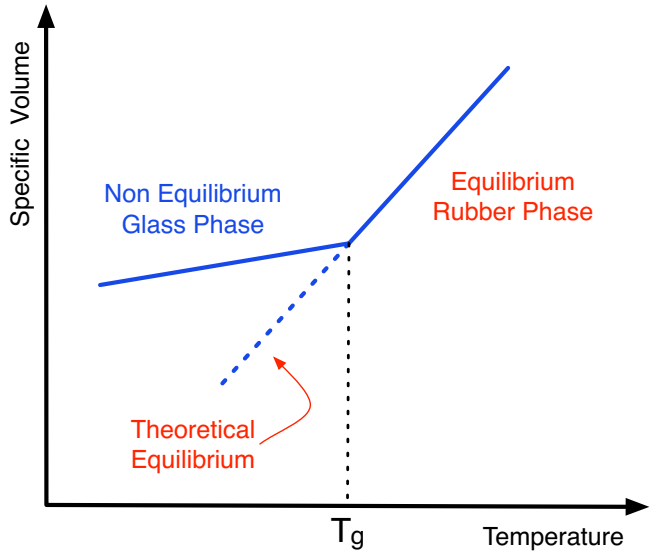

Figure 1.2.: Glass Transition phase diagram. The specific volume of a polymeric material is larger than the theoretical equilibrium one whenever the Glass Transition Temperature is crossed in the low temperature direction.

to a glassy one is encountered whenever a polymer is cooled below a material specific temperature denoted as glass transition temperature.
The transition can be easily observed in any plot showing the relation between the polymer specific volume and the temperature. An example of that is given in figure 1.2, showing a schematic representation of the detachment of the specific volume from the expected usual value at the transition point $T = T_g$ in the limit of low temperatures.

In 1958 Barrer et al. introduced the dual mode of sorption model for glassy polymers (Barrer et al., 1958). This model considers the contemporary existence of two penetrants´populations, one obeying the Henry's law and a second one captured in frozen pores and following a different behavior, identified by a Langmuir term and denoted therefore as Langmuir mode. This Langmuir mode is switched on as soon as the system is cooled below its glass transition temperature and the total sorption law is given by the sum of the two modes,

$$C = k_D P + \frac{C_H b P}{1 + bP}, \tag{1.2}$$

where C_H is the Langmuir's sorption capacity parameter and b is the affinity parameter. The model is probably of the widest use among all models of sorption isotherms. For a more extensive discussion see (Kanehashi and Nagai, 2005).

Later Sefcik and Raucher introduced the Gas-Polymer Matrix Model (Raucher and Sefcik, 1983) in which the relation between concentration and pressure is given by the transcendental equation

$$C = S_0 e^{-\alpha^* C} P \tag{1.3}$$

where α^* is a constant and S_0 the solubility coefficient at zero concentration. This model does not imply the existence of two different populations of solute molecules but the only assumption it needs is an interaction between particles and medium. This interaction modifies the structure of the polymer matrix leading to an enhancing of the motion of molecules through it.

A non equilibrium thermodynamical approach has been recently successfully adopted by Sarti and coworkers to predict sorption of small molecules in glassy polymeric media (Doghieri and Sarti, 1996; Sarti and Doghieri, 1998; Doghieri et al., 2006; De Angelis and Sarti, 2011).
In these models the Lattice Fluid theory of Sanchez and Lacombe, in combination with the Perturbed Hard Sphere Chain theory of Prausnitz is applied and extended to the non equilibrium glassy phase. These include the non equilibrium lattice fluid model (NELF) and the non equilibrium statistical associating fluid theory (NE-SAFT). A crucial point is made by assuming the polymer density to be an additional internal state variable and by considering a proper bulk rheology equation which governs its relaxation to a non

equilibrium value.

Above the glass transition temperature, sorption isotherms also deviate from the Henry straight line at large pressures. This behavior has been successfully reproduced by the Flory-Huggins (Flory, 1953) mode of sorption given by

$$v \cdot \exp\left[(1-v) + \chi(1-v)^2\right] = a \tag{1.4}$$

where v is the penetrant volume fraction, χ is the Flory-Huggins parameter and a is the penetrant activity in the gas phase, connected with the gas pressure. This mode is valid for binary mixtures when the interaction between sorbed molecules is the most relevant one. The sign of χ is known to characterize the shape of the corresponding sorption isotherm: when this is negative, the penetrant is a good solvent for the polymer and the $C(P)$ dependence is convex. In the bad solubility case $\chi > 0$ the corresponding sorption isotherm is concave.

Many variations and combinations of these models have been also proposed, see references (Stern and Kulkarni, 1982; Mauze and Stern, 1982; Chiou and Paul, 1986; Kamiya et al., 1986; Mi et al., 1991; Laatikainen and Lindstrom, 1987) just to name a few. In these models, sorption isotherms show corrections to the principal models discussed above, or appear in form of superpositions of a Matrix Model and Langmuir dependencies, or of two different Langmuir dependencies, etc.

1.2. Diffusion

Generally speaking, diffusion is transport of matter performed via random movements of basic elements, may these be particles, molecules or larger grains, as a reaction to a non equilibrium situation. Such a process can appear in several different ways and can present several different characteristics, mostly depending on the phase of the medium in which this happens, gaseous, liquid or solid, and on the nature of the non equilibrium condition causing it, usually given by a concentration, pressure or temperature gradient. Once an equilibrium state is established, the process is considered terminated even if the random movements of the elements keep on being without altering the equilibrium condition. Among the several classical examples reported in literature to briefly describe what a diffusion process is, we cite the one given by Schrödinger in his famous book "What is Life?" (Schrödinger, 1992), where the basic essence of the process is clearly explained. Let us consider the situation shown in Fig.1.3, where a certain number of molecules of permanganate are dissolved in a vessel filled of water. At the beginning the concentration of the permanganate is made highly asymmetric and larger on the left side of the vessel. What we know to happen in the end is that if we keep the system

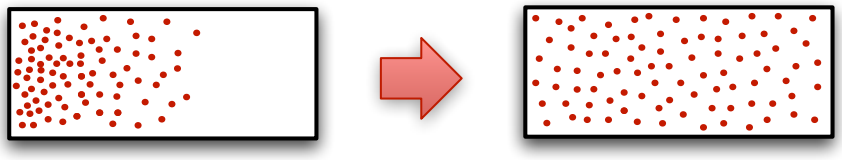

Figure 1.3.: Diffusion of permanganate molecules in a water solution.

isolated and let it evolve, the concentration reaches an homogeneous profile assuming macroscopically the same value in the whole system. There's no net force of course pushing molecules from left to right. Molecules are kept in constant agitation by the temperature and are continuously pushed in random and equally probable directions by the collisions among themselves and with the medium molecules. But, if we consider a vertical surface, or more precisely a surface perpendicular to the direction of the concentration gradient, the probability for the surface to be crossed by a diffusing particle from left to right is proportional to the number of particles on its left, and therefore is larger than the probability to be crossed in the other direction. The final equilibrium is reached when the two probabilities are the same for all possible surfaces, and this happens only if the concentration is constant throughout the vessel.

It is not the task of this book to give a detailed overview on the history of diffusion as a scientific matter, but we would simply like to go through some of the names and moments that have signed our knowledge on this argument.

One of the first considerations on irregular motions of small particles can be found in the "De rerum natura" of Lucretius, a book written in the first century b.C., got lost for more than one thousand years, and finally found again in a german monastery in the 1417[1]. Here's the way Lucretius describes the wandering of dust particles in air when looked through a sun ray:

"*For look closely,whenever rays are let in and pour the sun's light through the dark places in houses: for you will see many tiny bodies mingle in many ways all through the empty space right in the light of the rays, [...] And for this reason it is the more right for you to give heed to these bodies, which you see jostling in the sun's rays, because such jostling hints that there are movements of matter too beneath them, secret and unseen. For you*

[1]The book, or better the three books composing the "De rerum natura", were rediscovered by the humanist Poggio Bracciolini who can be considered as a real book hunter: he also found an essay by Vetruvio and a book by Quintiliano, two mile stones for respectively architecture and law still nowadays.

will see many particles there stirred by unseen blows change their course and turn back, driven backwards on their path, now this way, now that, in every direction everywhere. You may know that this shifting movement comes to them all from the first-beginnings. For first the first-beginnings of things move of themselves; then those bodies which are formed of a tiny union, and are, as it were, nearest to the powers of the first-beginnings, are smitten and stirred by their unseen blows, and they in their turn, rouse up bodies a little larger. And so the movement passes upwards from the first-beginnings, and little by little comes forth to our senses, so that those bodies move too, which we can descry in the sun's light; yet it is not clearly seen by what blows they do it.".

Technically this is not the description of a diffusion process, there's no gradient of any physical quantity, but we can find in these lines some fundamental aspects of the phenomenon. First of all we remark the atomistic vision of matter, that Lucretius derived from Democritus and Leucippus, and that was still a strong matter of debate at the end of the nineteenth century, when a scientific analysis around diffusion was finally produced: "I don't think that atoms do exist" is what Ernst Mach said at the conference held at the Royal Academy of Science in Vienna in the 1897.
Then, no hidden or mysterious force is taken into account in Lucretius' description, but particles are moved by "movements of matter too beneath them", suggesting the idea of the molecular collisions between diffusing and medium molecules which will be one of the interpretations given by Brown to his observations. Finally, motions and collisions are intrinsically generated by "the first beginnings", and this may be seen as an idea of the thermic agitation of molecules.

One of the most important moments in the history of diffusion analysis arrived almost two thousand years later when a Scottish biologist, Robert Brown, based on the previous observations of coal dust particles on the surface of alcohol of Jan Ingenhousz, analyzed the motion of pollen grains in water. The wondering feature of this phenomenon was the complete randomness of the movements of the particles and the fact that these were not due to any current in the fluid or from its evaporation, but that mobility was belonging to the particles them selves. This work can be considered as a milestone in this discipline and signed the history of research in diffusion. What later on would have been called as Brownian Motion, represents the prototipe of any diffusion process and the basis of all those works that, observing it, gave a great insight not only into molecular physics or chemistry, but also to an incredibly large number of different disciplines as mathematics, biology, sociology and economics, just too cite some of them.

The first attempt to perform a quantitative analysis of the diffusion mechanism, was done by the German physicist Adolf Fick around the half of the nineteenth century. Inspired by the experimental results obtained by Tomas Graham on diffusion of salt in water and by the intuition that there may be an analogy between diffusion an heat transmission, he arrived to propose the two basic equations of diffusion that lately became

known as the first and second Fick's laws. These equations still constitute the basis of the formalism adopted nowadays and the starting point for all the new advancements and variations on the diffusion process.

The first law expresses the hypothesis that the number of diffusing particles crossing a unit surface in the unit time is linearly proportional to the gradient of the concentration measured normally to that surface through a parameter denoted as diffusion coefficient

$$J = -D\frac{\partial C}{\partial x} \tag{1.5}$$

where J is the flux, C is the concentration, x is the direction perpendicular to the surface and D is the diffusion coefficient. The minus sign reflects the fact that the flux goes against the gradient. If J and C are expressed in terms of the same units, say gram, it is easy to show that D has the dimensions of a surface divided by a time (usually these are cm^2/sec).

The second law stems from the first one when considering the change in time of the concentration calculated in a certain portion of an isotropic medium. For the sake of simplicity we consider the one dimensional case and take the value C of a linear concentration of particles at point x along a line. The higher dimensional cases can be easily obtained by generalization and do not add anything to this introduction. The change in time of the amount of particles contained in an infinitesimal segment of length $2dx$ and centered at x, is given by the difference between the particle fluxes calculated at its borders $x - dx$ and $x + dx$. Therefore, if J_x is the flux at the central point x, we

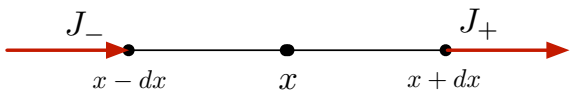

Figure 1.4.: One dimensional example.

have

$$J_- = J_x - \frac{\partial J_x}{\partial x}dx \qquad \text{and} \qquad J_+ = J_x + \frac{\partial J_x}{\partial x}dx. \tag{1.6}$$

The quantity

$$J_- - J_+ = -2dx\frac{\partial J_x}{\partial x} \tag{1.7}$$

is the change in time of the amount of substance in the segment equal to

$$2dx\frac{\partial C}{\partial t} \tag{1.8}$$

where the minus sign takes into account the fact that the two fluxes have different orientations, namely J_- is an entering flux and J_+ is an exiting one.
Collecting things all together and using the first Fick's law, it is straightforward to obatin

$$\frac{\partial C}{\partial t} = D\frac{\partial^2 C}{\partial x^2} \tag{1.9}$$

being the expression of the second Fick's law.

1.2.1. Einstein Equation

A microscopical explanation of the Brownian motion remained unsatisfied for almost one century, until the beginning of the 20th century. In the years between the 1905 and the 1908 Einstein published five papers with the aim to give a solid mathematical form to the Brownian motion phenomenon. Convinced that the motion of small particles suspended in a liquid could represent an evident manifestation of the molecular kinetic theory of heat, he based his analysis on the idea that the basic quantity of this process was not the average velocity of particles, as it was mostly believed at those times, but their mean squared displacement at time t $\langle X^2(t)\rangle$, and that such an approach could allow for a numerical estimation of the Avogadro number and the size of atoms.

We now briefly sketch the guidelines of the seminal paper published in 1905 on the Annalen der Physik. paper that has represented an enormous breakthrough for the physics of atoms and molecules.
Calculations start by considering a certain number of "bodies of microscopically visible size suspended in a liquid" and subject to a force $F(x)$ depending exclusively on space and not on time.[2]

A first equilibrium condition is obtained by balancing the external force contribution to the motion of molecules with the term deriving from the osmotic pressure

$$F\phi = \frac{RT}{N_A}\frac{\partial \phi}{\partial x} \tag{1.10}$$

where ϕ is the number of particles per volume unit, R is the ideal gas constant, N_A is the Avogadro number. A further equilibrium condition is obtained by the superposition

[2] we will omit for brevity the first sections where the osmotic pressure of the solution is obtained and will use a different notation from the original one

of two competitive movements of particles: the one caused by the external force and the one given by the diffusion process.
Assuming a spherical shape of radius ρ for the solute particles and denoting as η the viscosity coefficient of the liquid, each particle is impressed a velocity $v = F/6\pi\eta\rho$ by the external force and therefore, a number

$$n_F = \phi v = \frac{\phi F}{6\pi\eta\rho} \tag{1.11}$$

will be driven by the force F across each unit area perpendicular to the direction of motion. In a static state situation, this number has to be equilibrated by the number of particles traveling across the same area pushed by diffusion. This number is given

$$n_D = -D\frac{\partial\phi}{\partial x} \tag{1.12}$$

therefore it is obtained that

$$\frac{\phi F}{6\pi\eta\rho} = -D\frac{\partial\phi}{\partial x} \tag{1.13}$$

Using equation (1.10) it is easy to obtain an explicit expression for the diffusion constant as

$$D = \frac{RT}{N_A}\frac{1}{6\pi\eta\rho} \tag{1.14}$$

Last equation can be rewritten in a different form if we introduce the Boltzmann constant $K_B = R/N_A$ and identify the product $6\pi\eta\rho$ as the friction constant ζ. Hence,

$$D = \frac{K_B T}{\zeta} \tag{1.15}$$

Last result shows that the diffusion constant is strongly related to the response to an external force here represented by the friction constant. We shall later give a proof that the Einstein relation can be enclosed in the domain of the more general Fluctuation Dissipation Theorem which demonstrates that the main characteristics of the thermal motion of a particle are strictly related to its reaction to an external field.

On a second stage Einstein considered the successive positions of a Brownian particle at time intervals τ and based his analysis on two fundamental assumptions: first, τ is taken to be small but sufficiently large to remove any correlation between the movements of particles on two consecutive time intervals; second, movements of particles are mutually independent.

Being N the total number of solute particles, in the time interval τ the number of particles experiencing a displacement in the x direction between Δ and $\Delta + d\Delta$ is given by

$$dN = N\Phi(\Delta)d\Delta \tag{1.16}$$

where $\Phi(\Delta)$ is the probability distribution function followed by the displacements. A third assumption is made by considering Φ symmetrical respect to the origin and different from zero only for small Δ values.

If the particle number density ϕ is taken as a function of time and space, the following equation is satisfied

$$\phi(x, t+\tau)dx = dx \int \phi(x+\Delta, t)\Phi(\Delta)d\Delta \tag{1.17}$$

Being both τ and Δ small quantities, an expansion is possible in these variables

$$\begin{aligned} \phi(x,t) + \frac{\partial \phi}{\partial t}\tau &= \int \Big(\phi(x,t) + \frac{\partial \phi}{\partial x}\Delta + \frac{1}{2}\frac{\partial^2 \phi}{\partial x^2}\Delta^2\Big)\Phi(\Delta)d\Delta \\ &= \phi(x,t)\int \Phi(\Delta)d\Delta \; + \; \frac{\partial \phi}{\partial x}\int \Delta\Phi(\Delta)d\Delta \\ &+ \; \frac{\partial^2 \phi}{\partial x^2}\int \frac{\Delta^2}{2}\Phi(\Delta)d\Delta \end{aligned} \tag{1.18}$$

The first term on the right hand side gives $\phi(x,t)$ being the distribution Φ normalized; the second one vanishes being Φ symmetric. The second Fick´s law is therefore recovered

$$\frac{\partial \phi}{\partial t} = D\frac{\partial^2 \phi}{\partial x^2} \tag{1.19}$$

having identified the diffusion constant as the average of the squared displacement Δ

divided by twice the time interval τ

$$D = \frac{\langle \Delta^2 \rangle}{2\tau} \tag{1.20}$$

Reverting last equation and considering equation (1.14), it is possible to link an observable quantity like the displacement in time t to the microscopic quantities

$$L_t = \sqrt{2Dt} \tag{1.21}$$

1.2.2. Anomalous Diffusion

The basic laws of the usual Brownian Motion are in deep relationship with the statement of the Central Limit Theorem. Whenever the CLT is not respected for any reason, it is possible to observe deviations from the usual properties of the fundamental physical quantities that lead to anomalous behaviors.
In particular, such situations are encountered whenever the system is affected by broad probability distributions of some relevant quantities with divergent first or second moment, or by long-range correlations (Bouchaud and Georges, 1990a).

Let us consider the simple one dimensional random walk: a walker performs at fixed times τ a step of length l in the positive or negative direction according to a distribution $p(l)$ of the steps.
After N steps, or equivalently a time $t = N\tau$, the position of the walker is given by the sum of the steps

$$x_N = \sum_{n=1}^{N} l_n. \tag{1.22}$$

If the first two moments of $p(l)$ do exist, the mean and the variance of the position are given by

$$\langle x_N \rangle = vt \qquad \text{and} \quad \langle x_N^2 \rangle - \langle x_N \rangle^2 = 2Dt \tag{1.23}$$

where v is a velocity term defined as

$$v = \frac{\langle l \rangle}{\tau} \tag{1.24}$$

and D the diffusion constant defined as

$$D = \frac{\langle l^2 \rangle - \langle l \rangle^2}{2\tau} \tag{1.25}$$

This summarizes the general features of the (biased if we assume that left and right steps are not equally probable making $\langle l \rangle \neq 0$) Brownian Motion. As we can see the variance of the position increases linearly with time. Whenever the dependence of the variance on time has a different scaling we are in the presence of an anomalous diffusion process and will speak about *subdiffusion* if the dependence is lower than linear, or *superdiffusion* if it is larger
These two cases occur whenever one or both of the two conditions we previously mentioned are given: the divergence of at least one of the first two moments of $p(l)$, the presence of long-range correlations among the steps.

As a representative case of anomalous diffusion let us consider a Continuous Time Random Walk problem. This is given by a random walk on a regular d-dimensional lattice where the time between successive steps τ is no more a fixed quantity, but a random variable following a given probability distribution $\psi(\tau)$. The system is taken in its "annealed" version, meaning that each site is associated to a waiting time variable whose value can vary on time according to ψ. The alternative "quenched" version of the system is obtained by "freezing" the environment and associating to each site a fixed τ value, alway according to the ψ distribution.
After N steps or a time t, the mean squared displacement of the walker along the α direction is

$$\langle x_\alpha^2 \rangle = \langle l_\alpha^2 \rangle N \qquad \text{for} \quad N \longrightarrow \infty \tag{1.26}$$

with

$$\langle l_\alpha^2 \rangle = \int p(l) l_\alpha^2 d^d l \tag{1.27}$$

while the total time elapsed t is equal to the sum of the several waiting times

$$t = \sum_{n=1}^{N} \tau_n. \tag{1.28}$$

In the case of finite average of the waiting time $\langle \tau \rangle$, t grows like $N\langle \tau \rangle$ and diffusion is normal

$$\langle x_\alpha^2 \rangle = 2 D_{\alpha\alpha} t \qquad \text{with} \quad D_{\alpha\alpha} = \frac{\langle l_\alpha^2 \rangle}{2\langle \tau \rangle}. \tag{1.29}$$

If on the other hand ψ is a broad distribution as for example

$$\psi(\tau) \propto \tau_0^\mu \tau^{-(1+\mu)} \qquad (\tau \longrightarrow \infty) \tag{1.30}$$

with $0 < \mu \leq 1$, then $\langle \tau \rangle = +\infty$ and t behaves like

$$t \sim \tau_0 N^{1/\mu} \tag{1.31}$$

leading to a subdhiffusive regime with

$$\langle x_\alpha^2 \rangle \sim \langle l_\alpha^2 \rangle \Big(\frac{t}{\tau_0} \Big)^\mu \qquad \text{for} \quad \mu \in (0,1) \tag{1.32}$$

or

$$\langle x_\alpha^2 \rangle \sim \langle l_\alpha^2 \rangle \Big(\frac{t}{\tau_0 \ln(t/\mu)} \Big) \qquad \text{for} \quad \mu = 1 \tag{1.33}$$

As an example for a superdiffusive case we consider the Lorentz gas model where the anomaly of the diffusion is induced by the geometry of the system (Bouchaud and Georges, 1990a): a particle is free to wander in a regular cubic or hypercubic lattice

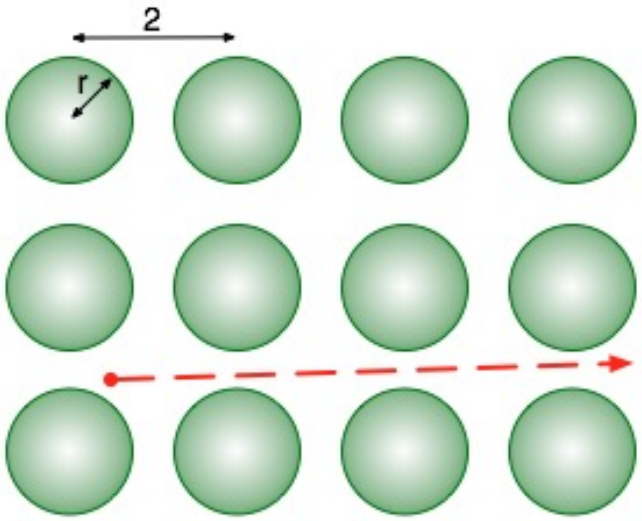

Figure 1.5.: Slnai's billard on a square lattice.

and gets reflected whenever it collides with some spherical obstacles placed at the centre of specific cells (see figure 1.5). This environment is more commonly known as Sinai's Billard (Sinai, 1970).
The length of each path between successive collisions is not a priori limited and distances travelled with one single path can be arbitrarily long. It is possible to estimate the shape of distribution of the length l of the paths in the limit of infinite lengths as

$$p(l) \simeq \frac{1-r}{l^3} \tag{1.34}$$

where r is the radius of the spheres and the lattice spacing has been set to 2. (with this assumption for $r = 1$ the spheres come into contact and no free diffusion is possible anymore).
Diffusion in this environment can then be modeled as a Levy flight showing the following dependence of the mean square displacement on time

$$\langle x_\alpha^2 \rangle \sim t \ln t \tag{1.35}$$

This is of course only a rough approximation, since the dynamics is highly caothic and complicated correlations between successive paths do exist, but still it is enough to give an example of what a super diffusive motion may appear.

2. Analytical tools

After the brief historical overview of the preceding chapter, we are going to open this second section with a more detailed presentation of the analytical tools we used to derivate our results.
Our models are basically fed by two ingredients: the Flory-Huggins model establishing the thermodynamics of molecule-polymer solutions, later reviewed by Bawendi and Freed, and the Effective Medium Approximation used in the scenario of the analogy between conduction and diffusion problems, developed among the others by Kirkpatrick and adapted by Yuge.

2.1. Flory-Huggins Theory

In the early forties of the last century the American physicists Paul J. Flory and Maurice L. Huggins developed independently from each other a statistical mechanical analysis of high polymer solutions moving from a previous qualitative treatment advanced by Meyer (Flory, 1942), (Huggins, 1942). Aim of the works of all of them was to explain the large deviations shown by the entropy of mixing of polymeric solutions from the result predicted by the Raoult's law

$$\Delta S = -R\Big(n_1 \ln X_1 + n_2 \ln X_2\Big) \tag{2.1}$$

where n_i is the number of moles of species i, X_i is the related mole fraction and R is the universal gas constant. Meyer argued that the Raoult's law could hold only in the case of mixing of molecules of the same size. He advanced an idealized model for such solutions based on a quasi-solid lattice different from the one usually adopted for the derivation of eq.(2.1). In Meyer's lattice every site can be occupied by a solvent molecule or by a segment of a polymer chain. A segment does not correspond necessarily to a particular polymer unit identified by a specific sequence of atoms, but it is more easily a polymer section having the same size of the lattice cell. Polymers are therefore represented by a sequence of consecutive cells occupied by segments and arranged in a large variety of ways.

Ideal solutions are mixtures for which two conditions simultaneously hold: the entropy of mixing is given by equation (2.1); the heat of mixing is equal to zero. Whenever one of these conditions is not fulfilled the solution is not ideal. In any case, it has been ob-

served that the heat of mixing plays a secondary role and deviations from ideal behavior are mostly due to the entropy. In particular Flory advanced the idea that for polymeric solutions this should not be expressed via mole fractions as in the Raoult law, but via volume fractions. The difference is crucial: using mole fractions as leading parameter the contribution of each molecule to the entropy does not take into account its dimension; namely, long polymeric chains or small molecules give the same entropic contribution.

We will give now a brief overview on the Flory-Huggins model, sketching its main features, approximations and results. We will follow the steps shown in Flory (1942).

Let us start this argument by considering an ideal mixing of two molecular species having the same size. This situation can be easily visualized in a lattice where each site is occupied by one molecule as shown in figure (2.1).

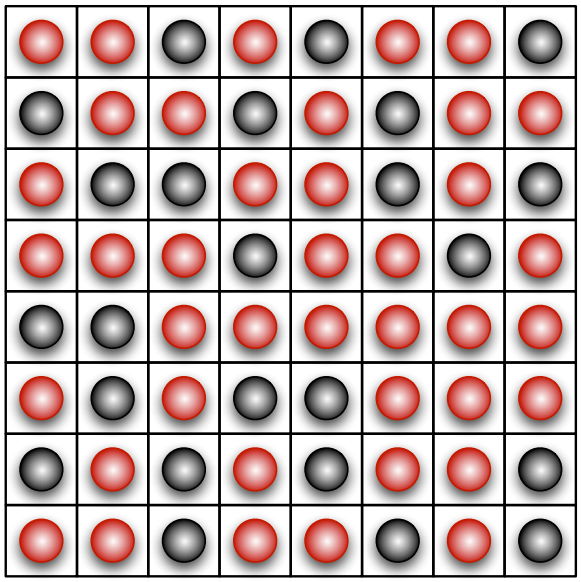

Figure 2.1.: Ideal binary solution lattice scheme.

The entropy of mixing ΔS may be derived by considering the number of ways the molecules can be organized in the lattice. Therefore, taking N_1 molecules of species 1 and $N_2 = N - N_1$ molecules of species 2, with N the total number of sites, the number of all possible configurations simply corresponds to the total number of combinations of N_1 objects in N available places

$$\Omega = \frac{N!}{N_1!N_2!} \tag{2.2}$$

Using the Boltzmann formula

$$\Delta S = K_B \ln \Omega \tag{2.3}$$

and the Stirling approximation $\ln n! = n \ln n - n$, the entropy of mixing is given by

$$\begin{aligned} \Delta S &= K_B\Big(N \ln N - N_1 \ln N_1 - N_2 \ln N_2\Big) = & (2.4)\\ &= -K_B\Big(N_1 \ln \frac{N_1}{N} - N_2 \ln \frac{N_2}{N}\Big). & (2.5) \end{aligned}$$

Introducing the volume fractions (or number concentrations in this case) $\phi_i = N_i/N$, we have

$$\Delta S = -K_B\Big(N_1 \ln \phi_1 - N_2 \ln \phi_2\Big) \tag{2.6}$$

The Raoult law is recovered by converting the Boltzmann constant to the gas constant $R = K_B N_A$ where N_A id the Avogadro number and using the equality in this simple model between volume and mole fractions

$$\begin{aligned} \Delta S &= -R\Big(\frac{N_1}{N_A} \ln X_1 - \frac{N_2}{N_A} \ln X_2\Big) = & (2.7)\\ &= -R\Big(n_1 \ln X_1 - n_2 \ln X_2\Big) & (2.8) \end{aligned}$$

Let us now jump into the polymeric variant of the system. The ideal solution model, strongly based on the assumption of similar size of solvent and solute molecules, can hardly hold for polymer solutions where one component is several order of magnitudes larger than the other one(s). In order to keep the same lattice approach in this new case, specific corrections have to be considered.

The Flory-Huggins model is based on four assumptions which define the nature of the lattice where the solution is placed and the approximations relating to the site occupancy probabilities:
(1) the solution is studied in a Meyer's lattice: each lattice site can host either a solvent molecule or a polymer segment. As previously said a segment is a polymer unit not necessarily corresponding to a given molecular section of the polymer, but simply a chain section of the same size of the solvent molecule. Polymers are therefore modeled as chains of segments arranged in adjacent sites. Segments are identical, indistinguishable and therefore interchangeable. The lattice constant does not depend on composition;
(2) all polymer chains are assumed to have the same length and consist of L segments.

The index L is therefore equal to the molecular volume ratio between polymer and solvent molecules;
(3) the average concentration of segments in cells close to other segments is considered to be equal to the over-all average concentration. This point becomes crucial for the estimation of the total number of possible different configurations of the system.
Let us consider the placement of a polymer chain in a lattice where N_2 polymer molecules have been already placed. We denote with N the total number of sites of the lattice and z its coordination number.[1] After one among the $N - LN_2$ empty sites has been selected as a terminal segment of the chain, according to the third assumption, the expected number of available sites for the second segment to be put is $z(1 - LN_2/N)$. The expected number of available sites for the third segment gives the fourth assumption:
(4) The expected number of available positions for each successive segment is denoted as α and is taken equal to

$$\alpha = \Big(1 - \frac{LN_2}{N}\Big)\Big(z - 1\Big) \tag{2.9}$$

This results to be an overestimate because it includes impossible configurations such those in which two segments of the same chain overlap.
The average number of configurations ν_{N_2+1} for a single chain in the lattice is given by

$$\nu_{N_2+1} = \frac{1}{2}\Big(N - LN_2\Big)\Big(\frac{z}{z-1}\Big)\alpha^{L-1} \tag{2.10}$$

where the factor $1/2$ has been introduced not to count twice equivalent configurations obtained by reverting upside down the chain. The number of all the possible configurations for N_2 chains is therefore

$$\begin{aligned} W &= \frac{1}{N_2!}\prod_{k=1}^{N_2}\nu_k = \Big(\frac{L^{LN_2}}{2^{N_2}N_2!}\Big)\cdot\Big[\frac{(N/L)!}{(N/L-N_2)!}\Big]^L\Big(\frac{z-1}{N}\Big)^{(L-1)N_2} \\ &\simeq \Big(\frac{1}{2}\Big)^{N_2}\cdot\Big[\frac{N^{N_1+N_2}}{N_1^{N_1}N_2^{N_2}}\Big]\cdot\Big(\frac{z-1}{e}\Big)^{(L-1)N_2} \end{aligned} \tag{2.11}$$

where the Stirling formula $N! \simeq (N/e)^N$ has been used again and the number of solvent molecules $N_1 = N - LN_2$ has been introduced.

[1] We are using a different notation from the Flory´s original one in order to be coherent with the rest of the paper.

The configurational entropy of mixing ΔS_m is related to W

$$\begin{aligned}\Delta S_m &= K_B \ln W = \\ &\simeq -K_B \left[N_1 \ln\Big(\frac{N_1}{N_1 + LN_2}\Big) + N_2 \ln\Big(\frac{N_2}{N_1 + LN_2}\Big)\right] + \\ &\quad + K_B N_2 (z-1)\Big(\ln(z-1) - 1\Big) - K_B N_2 \ln 2 \end{aligned} \tag{2.12}$$

Having considered as reference states the pure solvent and pure, perfectly ordered polymer, last expression (2.12) gives the entropy change when mixing N_1 pure solvent molecules with N_2 perfectly arranged and oriented polymer chains. In order to obtain the entropy of mixing for randomly entangled polymers, we have to subtract to eq.(2.12) its $N_1 = 0$ value ΔS_m^* given by

$$\Delta S_m^* = K_B N_2 \ln\Big(\frac{L}{2}\Big) + K_B N_2 (z-1)\Big(\ln(z-1) - 1\Big) \tag{2.13}$$

Hence, we have for the final entropy of mixing ΔS

$$\Delta S = \Delta S_m - \Delta S_m^* = -K_B \left[N_1 \ln\Big(\frac{N_1}{N_1 + LN_2}\Big) + N_2 \ln\Big(\frac{N_2 L}{N_1 + LN_2}\Big)\right] \tag{2.14}$$

which can be rewritten as

$$\Delta S = -K_B\Big(N_1 \ln \phi_1 + N_2 \ln \phi_2\Big) \tag{2.15}$$

if we introduce the volume fractions ϕ_1 and ϕ_2 of respectively the solvent and polymer molecules as

$$\phi_1 = \frac{N_1}{N} \qquad \text{and} \qquad \phi_2 = \frac{N_2 L}{N}. \tag{2.16}$$

Eq.(2.15) is analogous to the Raoult's law of eq.(2.1) with the only difference given by the presence of volume fractions in the place of the molar fractions but the predictions it produces result to be closer to the experimental data.

Let us now move further our presentation and focus on the expression of the free energy. The heat of mixing is calculated as the difference between the energy of the solution and the energy of a reference state that in our case is given by the pure separated components. The only energetic contributions considered are those exchanged by molecules at strict contact. Non nearest neighbor contributions are therefore neglected.
With this assumption the heat of mixing is easily estimated by first considering the energy spent in forming two bonds between molecules of different species starting from

two bonds among molecules of the same kind. It is clear that taken ϵ_{11}, ϵ_{22} and ϵ_{12} as respectively the energy of the solvent-solvent, segment-segment and solvent-segment bond, this difference is given by

$$\Delta\epsilon = \epsilon_{12} - \frac{1}{2}(\epsilon_{11} + \epsilon_{22}) \tag{2.17}$$

The second step is to estimate the number of such bonds. Each polymer chain has an approximate number of free adjacent cells equal to $(z-2)L+2$. The fraction of those occupied by solvent molecules can be in first approximation taken as the whole volume fraction in the lattice. This gives an approximate total number of solvent - segment contacts equal to $zLN_2\phi_1 = zN_1\phi_2$ and a total heat of mixing given by

$$\Delta H = zN_1\phi_2\Delta\epsilon \tag{2.18}$$

Expressing last equation (2.18) in K_BT units we have

$$\Delta H = N_1\phi_2\chi K_BT \tag{2.19}$$

where

$$\chi = \frac{z\Delta\epsilon}{K_BT} = \frac{z(2\epsilon_{12} - \epsilon_{11} - \epsilon_{22})}{2K_BT} \tag{2.20}$$

is the well known Flory-Huggins parameter, the physical interpretation of which is the energy difference between a solvent molecule completely surrounded by segments and another one surrounded only by molecules of its own kind.

The free energy of mixing is finally obtained by coupling equations (2.19) and (2.15)

$$\begin{aligned} \Delta F &= \Delta H - T\Delta S = K_BT\Big(N_1\ln\phi_1 + N_2\ln\phi_2 + \chi N_1\phi_2\Big) \\ &= NK_BT\Big(\phi_1\ln\phi_1 + \frac{\phi_2}{L}\ln\phi_2 + \chi\phi_1\phi_2\Big) \end{aligned} \tag{2.21}$$

2.1.1. Limitations of the Flory-Huggins theory and Bawendi-Freed corrections

The Flory-Huggins theory has represented a guide for several decades for every research on polymer solutions and still nowadays preserves this role of guideline. The model is nonetheless affected by some limitations. These mainly origin from assumptions (3) and (4). The latter, as already said, takes into account impossible arrangements of the chains and overestimates the number of the possible configurations.
Assumption (3) states the mean field approximation character of the model. It affirms that the probability for a site to be occupied by a molecule of kind i is equal to its

number concentration ϕ_i. Therefore, once we have placed a segment in a certain cell, the probability for any nearest neighboring site to be occupied by a solvent molecule is ϕ_1 and by another segment is ϕ_2. This of course neglects to consider that a segment has to be surrounded by at least another segment and, in the case it is not the terminal part of it, at least two. This approximation becomes evident when we give a look at the shape of eq.(2.21) where the energy is seen to be proportional to the product between concentrations $\phi_1 \cdot \phi_2$. This product represents the probability to find a solvent-segment couple in two adjacent sites, regardless of the surroundings and the constraints this produces. Such a model cannot therefore exactly solve the Flory-Huggins lattice itself.

Another limitation is represented by the interaction term containing the well-known Flory-Huggins parameter χ

$$g_{12} = \frac{z}{2}\Big(\frac{\epsilon_{11} + \epsilon_{22} - \epsilon_{12}}{K_B T}\Big). \tag{2.22}$$

In the Flory-Huggins theory this results to be a pure energetic term, concentration independent and proportional to T^{-1}. More careful examinations revealed that g_{12} is not a purely energetic coefficient, but is also concentration dependent via additional entropic contributions.

These issues, that were of course clear and known to Flory and Huggins themselves, have been the topic of several theoretical researches in the last years and gave birth to several models moved by the aim to overcome those limitations.
The first attempts could be generally divided in two categories. The first one contains those models in which assumptions (3) and (4) are reformulated by giving a more accurate definition of the site occupancy probabilities. While managing to obtain a correct energy plus entropy shape of the g_{12} parameter, these theories are still unable to produce a rigorous and systematic correction to the original FH mean field nature of the lattice model.
Models belonging to the second category are usually based on equation of state arguments, and lack the rigor of being derived by statistical mechanical methods which permit the systematic computation of either the parameters of the theory or the corrections to the analytical procedure.
Hence, both types of theories do not provide a real solution of the Flory-Huggins lattice.

Such a solution has been later advanced by M.G.Bawendi, K.F.Freed and coworkers. In their works they presented an exact mathematical solution based on a systematic series expansion in the interaction energy parameters and inverse coordination number which leads to the expression of an effective interaction parameter. This results to have both an entropic and energetic nature, to be a function of the concentrations and to

contain terms proportional to T^{-2}.

It will be sufficient for our scopes to show the expression of the Free Energy of the ternary system void-solvent-segment obtained by Bawendi and Freed (Bawendi and Freed, 1988), since this will be the starting point of our analytical treatments in the next sections.

The model is based on the same Flory-Huggins lattice with the addition of empty sites. Each site can therefore be occupied by one solvent molecule, a polymer segment or simply be empty. The volume fraction, or number concentration of the voids is denoted by $\phi_0 = 1 - \phi_1 - \phi_2$. The Helmholtz free energy of mixing of such a system is given in the Bawendi-Freed model by the following expression

$$F = NK_BT\Big(\phi_0 \ln \phi_0 + \phi_1 \ln \phi_1 + \frac{\phi_2}{L} \ln \phi_2 + \sum_{i<j}^{0,2} g_{ij}\phi_i\phi_j\Big) \tag{2.23}$$

where the interaction functions g_{ij} are made of a mean field energetic factor f^0_{ij}, containing the classical Flory-Huggins term, plus energetic and entropic corrections arising from the series expansion and denoted respectively by f^1_{ij} and s_{ij}

$$g_{ij} = f^0_{ij} + f^1_{ij} + s_{ij} \tag{2.24}$$

Defining $\epsilon = \epsilon_{11} + \epsilon_{22} - \epsilon_{12}$ and $\phi = \phi_1 + \phi_2$, the first mean field factors are expressed as follows

$$f^0_{01} = z\Big[\frac{\epsilon_{11}}{2} - \frac{\epsilon^2_{11}}{4}\phi(1-\phi) + O(\epsilon^3_{11})\Big] \tag{2.25}$$

$$f^0_{02} = z\Big[\frac{\epsilon_{22}}{2} - \frac{\epsilon^2_{22}}{4}\phi(1-\phi) + O(\epsilon^3_{22})\Big] \tag{2.26}$$

$$\begin{aligned} f^0_{12} = z\Big[&\frac{\epsilon}{2} + \frac{\epsilon^2_{11}}{4} + \frac{\epsilon^2_{22}}{4} + \frac{\epsilon^2_{12}}{2} + \\ &+\Big(-\epsilon^2_{11} - \frac{\epsilon^2_{22}}{2} + \epsilon_{11}\epsilon_{12} + \frac{\epsilon^2_{12}}{2}\Big)\phi_1 + \Big(-\epsilon^2_{22} - \frac{\epsilon^2_{11}}{2} + \epsilon_{22}\epsilon_{12} + \frac{\epsilon^2_{12}}{2}\Big)\phi_2 + \\ &+\Big(\frac{3}{4}\epsilon^2_{11} - \frac{1}{4}\epsilon^2_{22} - \epsilon_{11}\epsilon_{12}\Big)\phi_1^2 + \Big(\frac{3}{4}\epsilon^2_{22} - \frac{1}{4}\epsilon^2_{11} - \epsilon_{22}\epsilon_{12}\Big)\phi_2^2 + \\ &+\Big(\frac{3}{4}\epsilon^2_{11} - \frac{3}{4}\epsilon^2_{22} - \frac{1}{2}\epsilon_{11}\epsilon_{22} - \epsilon^2_{12}\Big)\phi_1\phi_2 + O(\epsilon^3_{ij})\Big] \end{aligned} \tag{2.27}$$

where each linear term in ϵ_{ij} represents the Flory-Huggins term while quadratic ones brings a mean field correction. The polynomes are stopped at the order $z\epsilon^2_{ij}$ having implicitly and arbitrarily assumed that the interaction parameters ϵ_{ij} scale as $z^{-2/3}$.

The mean field nature of these corrections stems in the fact that these are originated by the first order of the series expansion performed by Bawendi and Freed where spacial correlations between segments belonging to the same chain are neglected and these are therefore considered as uncorrelated. This is the reason why the polymerization index L does not appear in these expressions.

The corrections to this aspect are produced by the successive terms in the series where the space correlation between consecutive segments are taken into account. This gives rise to the functions f_{ij}^1 and s_{ij}

$$\begin{aligned} f_{01}^1 &= 0 \\ f_{02}^1 &= -\epsilon_{22}\Big(\frac{L-1}{L}\Big)(1-\phi) + O(\epsilon_{22}^2, \epsilon_{22}/z) \qquad (2.28) \\ f_{12}^1 &= \Big(\frac{L-1}{L}\Big)\Big[\epsilon_{22}(\phi_1+\phi_2-2) - \epsilon_{11}\phi_1 + 2\epsilon_{12}(1-\phi_2)\Big] \\ &\quad + O(\epsilon_{ij}^2, \epsilon_{ij}/z) \qquad (2.29) \end{aligned}$$

and

$$\begin{aligned} s_{01} &= 0 \\ s_{02} &= -\frac{1}{z}\Big(\frac{L-1}{L}\Big)^2 - \frac{1}{3z^2}\frac{5(L-1)^4+2(L-1)^3-12(L-1)^2-12(L-1)+3}{L^4} + \\ &\quad + \frac{\phi}{3z^2}\frac{4(L-1)^4-2(L-1)^3-12(L-1)^2}{L^4} - \frac{2\phi^2}{z^2}\Big(\frac{L-1}{L}\Big)^4 + O(z^{-3}) \qquad (2.30) \\ s_{12} &= -\frac{1}{z}\Big(\frac{L-1}{L}\Big)^2 - \frac{1}{z^2}\frac{3(L-1)^2-6(L-1)+1}{L^2} + \\ &\quad + \frac{\phi_1}{3z^2}\frac{(L-1)^2[10(L-1)-12]}{L^3} + \frac{2\phi_2}{3z^2}\frac{(L-1)^2[10(L-1)-12]}{L^3} \\ &\quad - \frac{6\phi_1\phi_2}{z^2}\Big(\frac{L-1}{L}\Big)^4 - \frac{2\phi_1^2}{z^2}\Big(\frac{L-1}{L}\Big)^4 - \frac{6\phi_1^2}{z^2}\Big(\frac{L-1}{L}\Big)^4 + O(z^{-3}) \qquad (2.31) \end{aligned}$$

We can consider the presentation of the Bawendi-Freed model concluded at this point for what our needs are. The essence of the Flory-Huggins theory, together with the corrections produced by the Bawendi-Freed model, represents the base of our calculations. We will start from the environment they form to proceed in our analysis of sorption and diffusion phenomena of small molecules in polymeric media. In particular we will consider the same lattice representation used by Bawendi and Freed and will move our steps from their expression of the free energy of mixing. We will also retain the second assumption of the Flory-Huggins theory relating to the polymerization index L which will be considered to be the same for all polymer molecules.

2.2. Effective Medium Theory

The analogy between electric conduction and diffusion phenomena is well known and formally established. Both are forms of transport of matter trying to relax a non equilibrium situation: in one case the non equilibrium is given by a potential difference and the particles moving to eliminate it are electrically charged, in the other one, the imbalance is given by a concentration difference and electrical charge of the particles is not considered.

Moreover, equations describing the two processes have the same form and related quantities can easily be mapped among each other.

As a consequence, results and procedures adopted in one context can be directly translated and used in the other one. The results shown in this book are a clear example of such a possibility and in chapter 4 we are going to use an effective medium approach, first outlined by Bruggeman (Bruggeman, 1935) and Landauer (Landauer, 1952) to analyze conduction in mixtures, to obtain an effective medium diffusion constant of our lattice sample.

We introduce now the main features of the Effective Medium Approximation as given in the works by Kirkpatrick (Kirkpatrick, 1971, 1973), where this technique is used to solve a random resistor network and will show later a correction proposed by Yuge in (Yuge, 1977) to take in to account some particular kind of correlations affecting the system.

2.2.1. Kirkpatrick model

The work by Kirkpatrick analyzes a two phase mixture made of conducting and insulating (or less conducting) elements in order to observe the connection between percolation and the main conductivity of the system.
Both bond and site percolation approaches are used in two and there dimensions and an effective medium conductivity is obtained and compared to Monte Carlo simulations.
Let us start our introduction with the bond case where each vertex of a cubic regular lattice may be connected with fixed probability p to each of its nearest neighbors by a conducting link. The probability factor p is therefore directly translated into the volume fraction of conducting bonds while the size of the lattice can be denoted as N and be considered to grow to infinite during the calculations.
Let us focus for a moment only at the percolation problem. Exploring the domain of p it is easy to understand that in the $p \simeq 0$ region, bonds are very sparse and form at most small groups of few bonds. Increasing a little bit the value of p, these small clusters start to grow and may merge together forming bigger clusters but still they are not able to cross the whole lattice. This happens as soon as p reaches the percolation threshold p_c. An infinite cluster appears and particles that may travel along the bonds have now the possibility to walk from an extreme of the system to the opposite one. In the

$p \to 1$ limit the lattice gets fully connected and every point is linked to all of its neighbors.

Introducing the percolation probability $P(p)$ as the probability for a bond to belong to the infinite cluster, it is possible to estimate a general behavior for $P(p)$, remaining zero below the percolation threshold, rising from zero at p_c and approaching the bisector $P(p) = p$ in the limit of p going to 1. A simple qualitative representation of such a shape is given in figure 2.2, while real experimental and simulated data are reported in Kirkpatrick (1971, 1973).

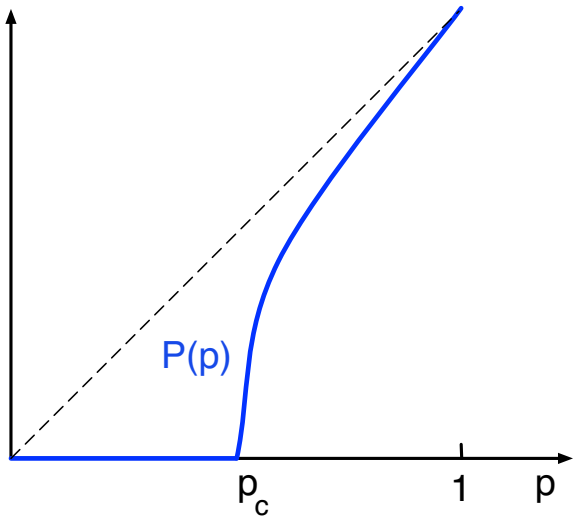

Figure 2.2.: Qualitative example of the functional behavior of the probabilty $P(p)$.

The conductance of the system is calculated by considering a finite cubic lattice and assigning a difference of potential to two opposite faces of the system. Ciclic boundary conditions are then imposed at the remaining opposite faces. In this way the lattice becomes essentially infinite in the directions perpendicular to the applied voltage. The current flowing through the bonds is then calculated by solving through a finite differences method the Kirchhoff´s equations

$$\sum_i g_{ij}(V_i - V_j) = 0 \tag{2.32}$$

where V_i is the potential at vertex i, g_{ij} is the conductance of the bond between points i and j.

Plotting both $P(p)$ and the global conductance $G(p)$, the functions show the same threshold at $p_c = 0.5$ in the bi-dimensional case and $p_c = 0.25$ in the three-dimensional one, but present severely different rising slops at $p = p_c$. The percolation probability rises abruptly from zero with infinite slope while the conductance has a slow growth with zero derivative at p_c. Therefore, even if the two quantities are obviously related to each other by topological arguments, they are not directly proportional to each other. Again, we show a pure qualitative comparison of the ways the two functions behave in figure 2.3, while corresponding data cane found in Kirkpatrick (1971, 1973).

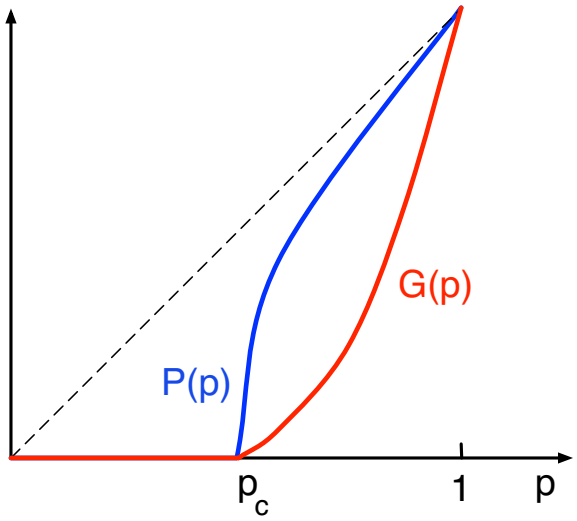

Figure 2.3.: Qualitative example of the functional behavior of the probabilty $P(p)$ and the main conductance $G(p)$.

An analytical result is obtained in the effective medium approximation context. The distribution of voltages in the random resistor network is considered to be given by the superposition of two contributions: an external field due to the voltage difference applied which increases the node potentials by a constant amount V_m along the applied voltage direction, and a local fluctuating field.
The philosophy at the base of the Effective Medium Approximation may be roughly summarized as follows: a representative element of the system is considered to be surrounded by an effective medium that has to be self-consistently determined. This is done solving for the exact field around this element and requiring that the fluctuations of the local one average to zero.
As a representative element we take a link between points A and B of conductance $g_{AB} = g$, oriented along the external field and embedded in the homogeneous effective

medium where all conductances are set to g_m (see figure (2.4)). As already said, the constant voltage V_m between the two extremes of the bond A and B due to the external field, is added to the fluctuating potential considered to be due to a fictitious current I_0, inserted in A and extracted in B and whose intensity is chosen to satisfy the current conservation at A and B

$$I_0 = V_m(g_m - g) \tag{2.33}$$

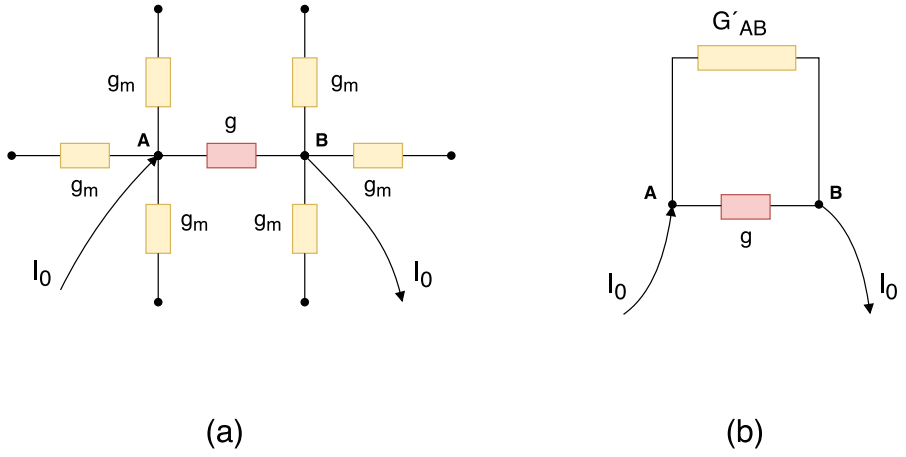

Figure 2.4.: Scheme adopted by the Effective Medium Approximation.

If we consider G'_{AB} to be the conductance of the whole network measured between points A and B once the link g_{AB} is removed, the extra voltage V_0 induced between the two points is given by

$$V_0 = \frac{I_0}{G_{AB}} = \frac{I_0}{G'_{AB} + g} \tag{2.34}$$

The value of G'_{AB} can be calculated and is given by $G'_{AB} = (z/2 - 1)g_m$ where z is the number of links departing from each point equal to $2d$ for regular networks like the one under examination. Therefore, collecting all things together we have

$$V_0 = V_m \frac{g_m - g}{g + (d-1)g_m} \tag{2.35}$$

Assuming that g is distributed according to a probability distribution $F(g)$, the condition

of the vanishing average of V_0 returns the effective medium value of g_m

$$\int dg F(g) \frac{g_m - g}{g + (d-1)g_m} = 0 \tag{2.36}$$

Let us consider the simplest binary conducting-insulating case where all bonds have the same value $g = g_1$ but a fraction $(1-p)$ of them is removed. The distribution $F(g)$ will be therefore given by

$$F(g) = p\delta(g - g_1) + (1-p)\delta(g) \tag{2.37}$$

and equation (2.36) gives

$$\int dg \Big(p\delta(g - g_1) + (1-p)\delta(g)\Big) \frac{g_m - g}{g + (d-1)g_m} = \frac{p(g_m - g_1)}{g_1 + (d-1)g_m} + \frac{1-p}{d-1} \tag{2.38}$$

solving for g_m we obtain a second degree equation whose positive root is

$$g_m = \frac{pd - 1}{d - 1} g_1 \tag{2.39}$$

which diverges for $d = 1$, revealing the fact that the theory as developed so far does not work for unidimensional systems, and goes to zero at the critical value

$$p_c = 1/d \tag{2.40}$$

showing an excellent agreement with the values found from the simulations. The same excellent agreement is found with the bond percolation simulations (we won't report here the plots shown in the original paper).

2.2.2. Yuge adaptation

In his paper Kirkpatrick has considered three different situations. The bond percolation model, which is the one we have just shown, a correlated bond percolation model and a site percolation model.

In the correlated bond percolation model each site is randomly assigned a value E_i belonging to the real interval $[-1, 1]$ and a value

$$E_{ij} = \frac{1}{2}\Big(|E_i| + |E_j| + |E_i - E_j|\Big) \tag{2.41}$$

is calculated for the bond between points i and j. Finally, all bonds having a value E_{ij} larger than a selected threshold E_0 are cut off the system.
In the easiest version of the site percolation model, a fraction $(1-p)$ of the total number of sites is removed creating an insulating vacancy.

The effective medium approximation works surprisingly well for the bond percolation case, but is not able to reproduce the profile of the simulated conductance in the region close to the threshold for the latter two cases. The reason of this misalignment stems from the correlations which inevitably arise among neighbor links in the correlated bond and site model but do not appear in the first simple bond situation. The contribution of these correlations is relevant in the critical region $p \simeq p_c$ while it decreases with increasing p. This makes the effective medium prediction overlap in any case to the simulations in the high concentration region.

The way correlations appear is pretty easy to understand. Let us consider first the correlated bond model. In this situation a bond is present only of its E_{ij} value is lower than the selected bound E_0. This means that taken a point i with a certain value E_i, the link with neighbor j will exist only if E_j is sufficiently small to obtain $E_{ij} < E_0$. Therefore, if the link E_{ij} exist, it is likely that also neighboring links will while whenever there is a vacant link, probably this is due to the fact that a certain E_i is too large and bonds starting from it are expected to be cut off.
In the site percolation case something similar happens. Once we remove a site, all its links are automatically removed, therefore every missing bond is never alone but belongs to a group of at least z missing links.
It is interesting to see the way correlations arise in the site approach, considering a slightly different model where sites can belong to two different species with different conductivities but both different from zero.
Let us assume therefore that our infinite regular cubic lattice is filled with cubes of species A and B and that the conductance of a link between two sites is dependent on the nature of the cubes it connects. We will have therefore three different categories of bonds, AA, BB and AB. Correlations come from the fact that if a certain cube is of type A, there's no possibility to have a BB link from it, and the same of course if we choose a B site. In other words, in a chain of consecutive bonds, the presence of an AA bond, excludes the possibility to have a BB one right after or before it; if we want to find a BB bond it is necessary to walk over an AB one before.

Many theories have been advanced to introduce correlation effects in the Effective Medium Approximation. We will focus our attention to the paper written by Yuge (Yuge, 1977) where the site approach is used to model a random resistor network and the contribution of the correlations is easily accounted for.

Let us therefore consider again a two phase mixture and the usual regular cubic lattice to model it. As before, cubes belong to either the A or B family. A resistor is assigned to each of the bonds between neighboring cells and a unit voltage is applied in a certain direction. If p is the volume fraction of A cubes, bond conductances will have the three values g_1 for AA bonds with probability

$$q_1 = p^2 \tag{2.42}$$

g_2 for BB bonds with probability

$$q_2 = (1-p)^2 \tag{2.43}$$

and

$$g_3 = 2\frac{g_1 g_2}{g_1 + g_2} \tag{2.44}$$

for AB bonds with probability

$$q_3 = 2p(1-p) \tag{2.45}$$

The average conductance value g_A for a bound starting from an A site is therefore given by

$$g_A = pg_1 + (1-p)g_3 \tag{2.46}$$

and similarly for a B site

$$g_B = (1-p)g_2 + pg_3 \tag{2.47}$$

In the spirit of the Effective Medium Approximation, the average effect of the g_A and g_B values can be considered equal to that of a single value g_m opportunely choosen in order to cancel out on the average the effects of restoring a conductance from g_m back to its true value.
If we take a conductance of value g_m, parallel to the potential gradient and surrounded by an homogeneous network of conductances g_m, and if we change its value to its original value g, we produce an additional voltage V_0 between the extremities of the bond. As we have seen in the previous section, V_0 is given by equation (2.35)

$$V_0 = V_m \frac{g_m - g}{g + (d-1)g_m} \tag{2.48}$$

As already said, following the guidelines of the Effective Medium Theory, the average value of V_0 has to vanish bringing to equation (2.36)

$$\int dg F(g) \frac{g_m - g}{g + (d-1)g_m} = 0 \tag{2.49}$$

Hence, in the Yuge procedure still a binary mixture is given, but it is an effective one, originated from the original lattice through rescaling equations (2.46) and (2.47), where conductances have a value equal to g_A with probability p and to g_B with probability $(1-p)$. being subjected to the binary distribution

$$F(g) = p\delta(g - g_A) + (1-p)\delta(g - g_B). \tag{2.50}$$

If we now turn to the percolation problem and let g_b go to zero, then set the average of V_0 to zero and solve for g_m, we recover the case examined in the previous section and obtain the effective medium conductance value as

$$g_m = \frac{pd-1}{d-1} g_A \tag{2.51}$$

having the same form of the expression found by Kirkpatrick and showing the same percolation threshold, but g_1 is substituted by the rescaled conductance g_A.

The new expression of g_m shows a perfect comparison with experimental data for glass particle-silicon rubber and glass fiber-plastic systems when plotted against the volume fraction parameter p. We refer to the original paper for plots and figures.

3. Sorption of small molecules in polymeric media

In this chapter we show that a consequent implementation of the "dual-mode" sorption model, including parallel mechanisms of filling of the preexisting holes in the polymeric matrix by the penetrant molecules and the dissolution of the matrix in the penetrant, leads at small pressures to a universal form of the sorption isotherm, similar to the one proposed by Sefcik and Raucher. The corresponding part of the isotherm is represented by a Lambert W-function, where $W(x)$ is the solution of the transcendental equation $We^W = x$. No additional assumptions done in formulation of the phenomenological Gas-Polymer Matrix Model are necessary to obtain the result.

Let us remind for the moment the expressions of the sorption laws we mentioned in the first introduction section, hence, the dual mode, given by

$$C = k_D P + \frac{C_H b P}{1 + bP}, \tag{3.1}$$

with K_D being the Henry's solubility coefficient, C_H the Langmuir's sorption capacity parameter and b the affinity parameter, the Gas-Polymer Matrix Model of Sefcik and Raucher expressed by

$$C = S_0 e^{-\alpha^* C} P \tag{3.2}$$

where α^* is a constant and S_0 the solubility coefficient at zero concentration and the solution of which is provided via a Lambert function by

$$C = \frac{1}{\alpha^*} W\left(\alpha^* S_0 P\right). \tag{3.3}$$

and the Flory-Huggins mode

$$v \cdot \exp\left[(1-v) + \chi(1-v)^2\right] = a \tag{3.4}$$

with v representing the penetrant volume fraction, χ the Flory-Huggins parameter and a is the penetrant activity in the gas phase.

We note that common for most of the models of the absorption in glassy polymers is the assumption of the preexisting free volume, i.e. "holes" frozen due to quenching into the glassy state. This is also an explicit assumption done in the dual sorption

mode model. The model however does not take into account that populations of sorbent molecules dissolving the polymer and absorbed in holes do essentially coexist in the same piece of a polymeric medium.

The universality of the Lambert-like isotherm originates from the particular shape of the free energy in the gas phase, and from the fact that the internal energy in a polymer-penetrant-void ternary mixture is (in the lowest order) a bilinear form in the concentrations of the three components of the system. The Lambert form appears then as a universal approximation for the sorption isotherm at low gas pressures and follows immediately from the conditions of chemical and mechanical (quasi)equilibria in the system.

Although in general the transcendental W-function representing the result of the gas-polymer matrix model and of our discussion, and a rational function as following from the dual sorption mode model differ considerably and cannot be fitted to each other over a large domain of argument values for arbitrary values of parameters, we show that the two-parametric *fits to experimental data* via the Lambert function are not inferior to the three-parametric dual-mode fits in almost all situations where the dual mode sorption model applies, so that the two-parametric fit by a Lambert function represents a quite universal behavior and has to be preferred to the three-parametric dual-mode one.

We do not intend to go far beyond this statement and to provide a quantitative theory of gas sorption in glassy polymers. Important steps on this way have been done by the extensive work of Sarti and his collaborators (Doghieri and Sarti, 1996; Sarti and Doghieri, 1998; Doghieri et al., 2006; De Angelis and Sarti, 2011). In their works the thermodynamics of the Lattice Fluid theory of Sanchez and Lacombe and of the Perturbed Hard Sphere Chain theory of Prausnitz are applied and extended to the non equilibrium glassy phase. Parallel to our simple quasi-equilibrium approach they assume the polymer density to be an additional internal state variable and a specific bulk rheology equation, describing its relaxation to a non equilibrium value, is invoked since the process is essentially a non-equilibrium one.

3.1. The model

Now we turn to the lattice model of the situation, corresponding to using a simple lattice gas model for a gas phase and a ternary variant of a Flory-Huggins model for the polymeric medium. At the beginning we will assume the chains to be flexible, so that the standard variant of the model appears, and no properties of the glass state are essentially respected. After the discussion of the results for this simplified case we will show that they essentially do not strongly depend on this assumption, rising a hope that the behavior is generic. To show that this is indeed the case we reanalyze some available experimental data.

Let us therefore consider a polymeric slab of volume V placed in a box of fixed volume Ω and surrounded by a gas of a pure substance. The whole systems is closed and kept at temperature T. A regular three dimensional cubic lattice is used to model the box. The elementary units of this lattice are cubes of volume ω and their total number is $K = \Omega/\omega$. According to the usual prescriptions of the Flory-Huggins model, the size of ω is chosen to be equal to the size of a gas molecule.

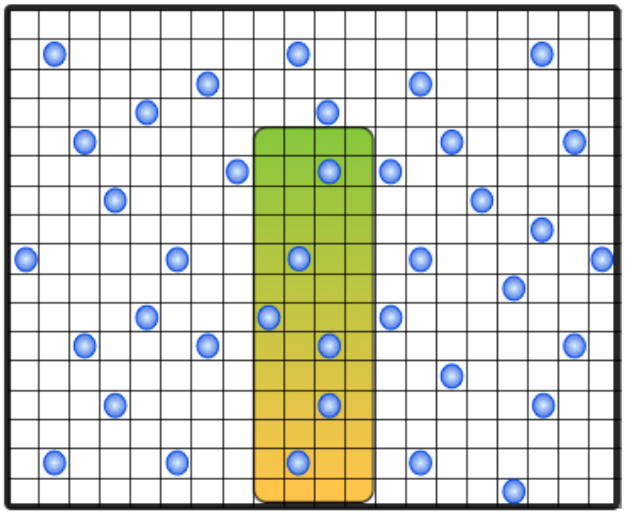

Figure 3.1.: Closed box containing the solid and the gas phase.

For the sake of clarity let us start our discussion by reminding the standard binary mixture (Bragg-Williams) model for small molecules of types A and B at number concentrations x and $y = 1 - x$ in a box with M sites. The interaction energies within the pairs of molecules will be taken $-\epsilon_{AA}$, $-\epsilon_{BB}$ and $-\epsilon_{AB}$, respectively (with ϵ_{ij} being the energy necessary to break the corresponding bond, measured in units of k_BT). The free energy is given by

$$\Delta F = U + k_BT(x \ln x + y \ln y) \tag{3.5}$$

with the entropic part given by the sum of translational entropies of the particles. The internal energy U is given by

$$\begin{aligned} \frac{U}{k_BT} &= \frac{z}{2}(-\epsilon_{AA}N_A - \epsilon_{BB}N_B) + \\ &+ \frac{1}{2}(\epsilon_{AA} + \epsilon_{BB} - 2\epsilon_{AB})N_{AB} \end{aligned} \tag{3.6}$$

where z is the coordination number of the lattice, N_A is the total number of A molecules, N_B is the total number of B molecules, and N_{AB} is the number of neighboring AB-pairs. Note that the first term in this expression is the energy of the reference state of separated A and B. Assuming well-mixedness, we get $N_{AB} = M(z/2)xy$, and obtain the standard form

$$\Delta F = k_B T\Big[x \ln x + y \ln y + \frac{z}{2}(\epsilon_{AA} + \epsilon_{BB} - 2\epsilon_{AB})xy\Big] \tag{3.7}$$

of the free energy change with respect to this reference state. The same structure of expression holds for the mixture of more then two components. Note that no "diagonal" contributions do appear in the model, and the free energy change with respect to the reference state always has the form

$$\Delta F = k_B T\Big[\sum_i x_i \ln x_i + \sum_{i<j} g_{ij} x_i x_j\Big] \tag{3.8}$$

with x_i being the corresponding concentrations. The Flory-Huggins model for polymer mixture differs from the model above only by the fact that the expressions for the translational entropies of polymers take the form $x_i \ln x_i/L_i$ where L_i is the length of the corresponding molecule (see e.g.Witte et al. (1996)). The model neglects the rest entropies corresponding to internal motion of the chains and the higher-order (e.g. triple) interactions.

The simple model considered below is essentially the one of polymer-solvent-non-solvent (i.e. poor solvent) mixture. In the absence of penetrant the gas (i.e. vacuum) phase is modeled by empty sites (voids), and the solid phase is a mixture of voids and polymer chains. The interaction energy between voids themselves and of voids with any other species is clearly zero, which sets the origin of the energy scale. Note that this to no extent means that voids are athermal solvent for the polymer, since the disruption of a monomer-monomer contact raises the total energy of the system: vacuum is essentially a poor solvent for the polymer, and voids would not be present at high concentration in an equilibrium configuration of a solid phase. For the case of polymer glass this system is quenched from the equilibrium state at higher temperature, so that the concentration of voids ϕ_0 is quenched at the equilibrium level corresponding to the higher temperature and the translational entropy of the chains is suppressed.

Parallel to the standard description of a ternary Flory-Huggins model, the sum of internal energies of separated penetrant molecules, polymer, and voids (zero) is considered as a reference state, and therefore only the changes in the corresponding interaction energies (e.g. under detaching a monomer-monomer contact and changing it for a monomer-void one) appear in the theoretical description. At the beginning we will assume that the voids and the polymer segments are well-mixed (i.e. that the system was quenched from a state with higher volume but without any perceivable local structure), but this assump-

tion is secondary. The whole system is essentially a void-penetrant phase in contact with the void-penetrant-polymer one. The existence of the (meta)stable population of voids inside the solid phase, and absence of polymers in the gas one (as fixed at formulating the model) are the only assumptions which make the model different from a fluid ternary mixture one.

The penetrant's sorption in the solid phase is assumed to be reversible, as it is the case in most of experiments. The penetrant molecules may mix with voids and with the polymer molecules: in the case they were not able to penetrate the polymer's bulk, no considerable deviations from the Langmuir's law, evident in experiment, could be observed. We consider the situation when the amount of the penetrant molecules both in the gas phase and in the solid is small, i.e. the gas can to a good approximation still be considered as ideal, and the total amount of penetrant in the solid is much smaller than the total amount of monomers. In all our examples these assumptions can be considered as fulfilled. Penetration of these small molecules could change the volume of the solid phase. The system consisting of the gas and of solid phase is in mechanical equilibrium, and in chemical equilibrium with respect to exchange of the penetrant molecules and the voids between the two phases. Moreover, when minimizing the total free energy of the system we look only for its local minimum closest to the frozen state of the system without penetrant.

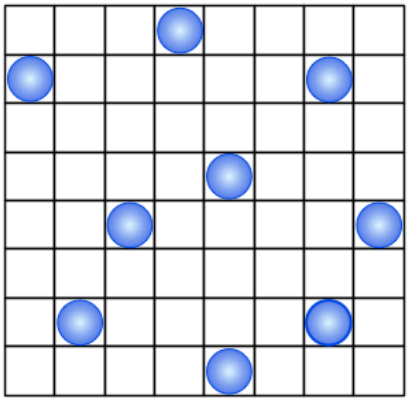

Figure 3.2.: Regular Lattice representation for the gas phase.

In the gas phase of our model we have to deal with this binary model in its pure form, with molecule-molecule interaction energy denoted by ϵ_{11}, and with void-void and void-molecule interaction energies $\epsilon_{00} = \epsilon_{01} = 0$. The number of sites available in the gas phase is M, and M_1 of these are occupied by a single gas molecule each, so that

$x = M_1/M$, while $M_0 = M - M_1$ is the number of voids (see figure 3.2 for a schematic view of the gas phase lattice). Thus, the free energy of the gas phase is

$$\Delta F_g = MK_BT\left[x\ln x + (1-x)\ln(1-x) + \frac{z}{2}\epsilon_{11}x(1-x)\right]. \tag{3.9}$$

where again z indicates the lattice coordination number.
The gas number concentration x is considered equivalent to the ratio P/P_{sat} between the pressure P and the saturated vapor pressure P_{sat} of the gas at temperature T.

The polymeric medium occupies a total of $N = K - M$ sites and every site can be occupied by one sorbed gas molecule, by a polymer segment or be empty.
Polymers are organized in chains of L segments. The total number of lattice sites in the medium corresponds then to $N = N_0 + N_1 + N_2$ where N_0 is the number of empty sites, N_1 is the number of sites occupied by penetrant molecules, and N_2 is the number of polymer segments (see figure 3.3). The number N_2 is therefore fixed. A change in the volume of the polymeric slab due to swelling involves the change of the number of penetrant molecules and empty sites.

The volume fractions ϕ_i of the corresponding sites are given by

$$\begin{aligned}
\phi_0 &= \frac{N_0}{N} \quad \text{empty sites volume fraction} \\
\phi_1 &= \frac{N_1}{N} \quad \text{penetrant molecules volume fraction} \\
\phi_2 &= \frac{N_2}{N} \quad \text{polymer segments volume fraction}
\end{aligned}$$

and satisfy the relation $\phi_0 + \phi_1 + \phi_2 = 1$.

The free energy of the polymeric compound is (Bawendi and Freed, 1988)

$$\begin{aligned}
\Delta F_s &= NK_BT\Big[\phi_0\ln\phi_0 + \phi_1\ln\phi_1 + S_{pol} + \\
&\quad + g_{01}\phi_0\phi_1 + g_{02}\phi_0\phi_2 + g_{12}\phi_1\phi_2\Big]
\end{aligned} \tag{3.10}$$

where the terms containing the logarithms account for the entropic contributions, $S_{pol} = \frac{\phi_2}{L}\ln\phi_2$ for the case of a polymer solution. The entropic contribution of the chains is small for $L \gg 1$ and essentially does not play the major role in the system's behavior at the relevant values of parameters, but will be retained for the time being. The corresponding discussion will be given at the end of the next section.

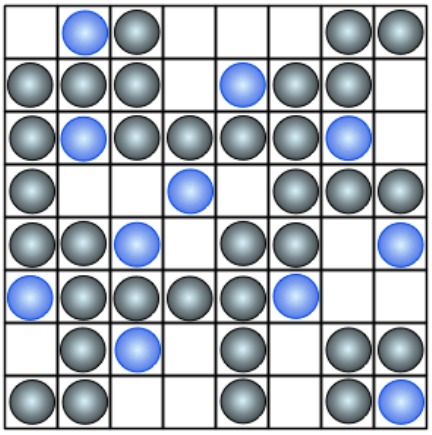

Figure 3.3.: Regular Lattice representation for the solid phase.

The energetic contributions are entirely enclosed in the last term coupling the volume fractions through the interaction functions g_{ij}. In a simple Flory-Huggins approach the entries g_{ij} are given by (Bawendi et al., 1986)

$$g_{01}^{FH} = \frac{z}{2}\epsilon_{11} \tag{3.11}$$

$$g_{02}^{FH} = \frac{z}{2}\epsilon_{22} \tag{3.12}$$

$$g_{12}^{FH} = \frac{z}{2}(\epsilon_{11} + \epsilon_{22} - 2\epsilon_{12}) \tag{3.13}$$

Here ϵ_{11} is therefore the energy necessary to remove the penetrant-penetrant molecular bond, as above, ϵ_{22} is the same for the "non-chemical" monomer-monomer bond, and ϵ_{12} is the monomer-penetrant interaction energy. The diagonal entries g_{ii} do not appear in the theory, like in the binary case above. Note that the energies of the reference states for the gas and for the solid phase do depend on M and N but sum up to a constant on the total, since the total amounts of all three components is fixed.
In the binary case ($\phi_0 = 0$) the model reduces to the classical Flory-Huggins one, with g_{12}^{FH} giving the Flory-Huggins parameter χ in equation (3.4).

For what already explained, we are using the lowest order corrections given by Bawendi

and Freed that lead to the following expressions for the g_{ij} coefficients:

$$g_{01} = z\Big[\frac{\epsilon_{11}}{2} - \frac{\epsilon_{11}^2}{4}\phi(1-\phi) + O(\epsilon_{11}^3)\Big] \tag{3.14}$$

$$g_{02} = z\Big[\frac{\epsilon_{22}}{2} - \frac{\epsilon_{22}^2}{4}\phi(1-\phi) + O(\epsilon_{22}^3)\Big] \tag{3.15}$$

$$\begin{aligned} g_{12} = z\Big[&\frac{\epsilon}{2} + \frac{\epsilon_{11}^2}{4} + \frac{\epsilon_{22}^2}{4} + \frac{\epsilon_{12}^2}{2} + \\ &+\Big(-\epsilon_{11}^2 - \frac{\epsilon_{22}^2}{2} + \epsilon_{11}\epsilon_{12} + \frac{\epsilon_{12}^2}{2}\Big)\,\phi_1 + \\ &+\Big(-\epsilon_{22}^2 - \frac{\epsilon_{11}^2}{2} + \epsilon_{22}\epsilon_{12} + \frac{\epsilon_{12}^2}{2}\Big)\,\phi_2 + \\ &+\Big(\frac{3}{4}\epsilon_{11}^2 - \frac{1}{4}\epsilon_{22}^2 - \epsilon_{11}\epsilon_{12}\Big)\,\phi_1^2 + \\ &+\Big(\frac{3}{4}\epsilon_{22}^2 - \frac{1}{4}\epsilon_{11}^2 - \epsilon_{22}\epsilon_{12}\Big)\,\phi_2^2 + \\ &+\Big(\frac{3}{4}\epsilon_{11}^2 - \frac{3}{4}\epsilon_{22}^2 - \frac{1}{2}\epsilon_{11}\epsilon_{22} - \epsilon_{12}^2\Big)\,\phi_1\phi_2 + O(\epsilon_{ij}^3)\Big] \end{aligned} \tag{3.16}$$

where $\phi = \phi_1 + \phi_2$ and $\epsilon = \epsilon_{11} + \epsilon_{22} - 2\epsilon_{12}$.

It is important to consider these corrections since they impact the free energy expansion already at the zero order in ϕ_1. In what follows we do not perform quantitative evaluation of equations, and we will not need the exact forms of g_{ij}, but we will only concentrate on the overall polynomial structure of the expansions.

3.2. The free energy

Assuming the model described above we can put down the total free energy of the system $\Delta F = \Delta F_g + \Delta F_s$:

$$\begin{aligned} \Delta F = K_B T\Big[&M\Big(x\ln x + (1-x)\ln(1-x) + \frac{z}{2}\epsilon_{11}x(1-x)\Big) + \\ &+N\Big(\phi_0\ln\phi_0 + \phi_1\ln\phi_1 + \frac{\phi_2}{L}\ln\phi_2 + \sum_{i<j} g_{ij}\phi_i\phi_j\Big)\Big] \end{aligned} \tag{3.17}$$

which depends, besides on temperature, on variables M, M_0, M_1, N, N_0, N_1, and N_2. Not all of them are independent. Thus, the volume of the box is fixed, this means that the total number of sites $K = N + M$ is constant; the total number of gas molecules in both phases is conserved, hence, the sum $M_1 + N_1$ is constant; finally, the number of polymer

segments N_2 is fixed:

$$N + M = K = const. \tag{3.18}$$
$$N_1 + M_1 = K_1 = const. \tag{3.19}$$
$$N_2 = K_2 = const. \tag{3.20}$$

This, together with the relations $M = M_0 + M_1$ and $N = N_0 + N_1 + N_2$, gives a set of five conditions for seven quantities, leaving two independent variables.

We choose them to be M and M_1, and express the remaining quantities as follows

$$M_0 = M - M_1 \tag{3.21}$$
$$N = K - M \tag{3.22}$$
$$N_0 = K - K_1 - K_2 - M + M_1 = K_0 - M + M_1 \tag{3.23}$$
$$N_1 = K_1 - M_1 \tag{3.24}$$
$$N_2 = K_2 \tag{3.25}$$

so that

$$\Delta F(M, M_1, T) = \Delta F_g(M, M_1, T) + \Delta F_s(M, M_1, T). \tag{3.26}$$

The final state is given by minimization of the free energy with respect to M and M_1:

$$\Big(\frac{\partial \Delta F}{\partial M}\Big)_{M_1,T} = \Big(\frac{\partial \Delta F_g}{\partial M}\Big)_{M_1,T} + \Big(\frac{\partial \Delta F_s}{\partial M}\Big)_{M_1,T} = 0 \tag{3.27}$$
$$\Big(\frac{\partial \Delta F}{\partial M_1}\Big)_{M,T} = \Big(\frac{\partial \Delta F_g}{\partial M_1}\Big)_{M,T} + \Big(\frac{\partial \Delta F_s}{\partial M_1}\Big)_{M,T} = 0 \tag{3.28}$$

corresponding respectively to the balance between the pressure P in the gas phase and the force per unit area exerted by the solid during its volume relaxation, and to the equality of chemical potentials of penetrant in the gas and in the solid phase.

According to Eqs. (3.21)-(3.25), the volume fractions are given by

$$x = \frac{M_1}{M} \tag{3.29}$$
$$\phi_0 = \frac{K_0 - M + M_1}{K - M} \tag{3.30}$$
$$\phi_1 = \frac{K_1 - M_1}{K - M} \tag{3.31}$$
$$\phi_2 = \frac{K_2}{K - M} \tag{3.32}$$

and the derivatives with respect to M and M_1 can be expressed as:

$$\Big(\frac{\partial \Delta F_g}{\partial M}\Big)_{M_1,T} = K_B T\Big[\ln\Big(1-x\Big) + \frac{z}{2}\epsilon_{11}x^2\Big] \tag{3.33}$$

$$\Big(\frac{\partial \Delta F_g}{\partial M_1}\Big)_{M,T} = K_B T\Big[\ln\Big(\frac{x}{1-x}\Big) + \frac{z}{2}\epsilon_{11}(1-2x)\Big] \tag{3.34}$$

$$\begin{aligned}\Big(\frac{\partial \Delta F_s}{\partial M}\Big)_{M_1,T} &= K_B T\Big[-\ln\Big(1-\phi_1-\phi_2\Big) + \\ &- \Big(1-\frac{1}{L}\Big)\phi_2 + G_0(\phi_1,\phi_2,\epsilon_{ij})\Big]\end{aligned} \tag{3.35}$$

$$\Big(\frac{\partial \Delta F_s}{\partial M_1}\Big)_{M,T} = K_B T\Big[\ln\Big(\frac{1-\phi_1-\phi_2}{\phi_1}\Big) + G_1(\phi_1,\phi_2,\epsilon_{ij})\Big] \tag{3.36}$$

where $G_0(\phi_1,\phi_2,\epsilon_{ij})$ and $G_1(\phi_1,\phi_2,\epsilon_{ij})$ are two polynomial functions of their arguments originating from the derivatives of the internal energy term:

$$\begin{aligned}G_0(\phi_1,\phi_2,\epsilon_{ij}) &= \sum_{i<j}^{0,2}\Big[\phi_i\phi_j g_{ij} - N\frac{\partial}{\partial M}\Big(\phi_i\phi_j g_{ij}\Big)\Big] = \\ &= z\Big[\frac{\epsilon_{11}}{2}\phi_1^2 + \frac{\epsilon_{22}}{2}\phi_2^2 + \epsilon_{12}\phi_1\phi_2\Big] + \\ &\quad + z\frac{\epsilon_{22}^2}{4}\Big[\phi_2^2 - 4\phi_2^3 + 3\phi_2^4\Big] + \\ &\quad + z\Big[\frac{\epsilon_{12}^2}{2}\phi_2 - \Big(2\epsilon_{22}\epsilon_{12} + \epsilon_{12}^2\Big)\phi_2^2 + 3\epsilon_{22}\epsilon_{12}\phi_2^3\Big]\phi_1 + \\ &\quad + z\Big[\frac{\epsilon_{11}^2}{4} - \Big(2\epsilon_{11}\epsilon_{12} + \epsilon_{12}^2\Big)\phi_2 + \Big(\frac{3}{2}\epsilon_{11}\epsilon_{12} + 3\epsilon_{12}^2\Big)\phi_2^2\Big]\phi_1^2 + \\ &\quad + z\Big[-\epsilon_{11}^2 + 3\epsilon_{11}\epsilon_{12}\phi_2\Big]\phi_1^3 + z\frac{3}{4}\epsilon_{11}^2\phi_1^4 + O(z\epsilon_{ij}^3)\end{aligned} \tag{3.37}$$

and

$$
\begin{aligned}
&G_1(\phi_1,\phi_2,\epsilon_{ij}) = \sum_{i<j}^{0,2} N\frac{\partial}{\partial M_1}\Big(\phi_i\phi_j g_{ij}\Big) = \\
&= z\Big[-\frac{\epsilon_{11}}{2}+\epsilon_{11}\phi_1+\epsilon_{12}\phi_2\Big] + z\Big[\frac{\epsilon_{12}^2}{2}\phi_2 - \Big(\epsilon_{22}\epsilon_{12}+\frac{\epsilon_{12}^2}{2}\Big)\phi_2^2+\epsilon_{22}\epsilon_{12}\phi_2^3\Big] + \\
&+ z\Big[\frac{\epsilon_{11}^2}{2}+\Big(\epsilon_{12}^2-\frac{3}{2}\epsilon_{11}^2-\frac{3}{2}\epsilon_{22}^2-2\epsilon_{11}\epsilon_{12}+\epsilon_{11}\epsilon_{22}\Big)\phi_2+\frac{3}{2}\Big(\epsilon_{11}^2+\epsilon_{22}^2\Big)\phi_2^2\Big]\phi_1 + \\
&+ z\Big[-\frac{3}{2}\epsilon_{11}^2+3\epsilon_{11}\epsilon_{12}\phi_2\Big]\phi_1^2 + z\epsilon_{11}^2\phi_1^3 + O(z\epsilon_{ij}^3)
\end{aligned}
\tag{3.38}
$$

Applying now equations (3.27) and (3.28) we obtain the following system of equations

$$
\begin{cases}
(1-\phi_1-\phi_2)e^{(1-\frac{1}{L})\phi_2-G_0(\phi_1,\phi_2,\epsilon_{ij})} &= (1-x)\,e^{-z\epsilon_{11}x^2/2} \\
\dfrac{\phi_1}{(1-\phi_1-\phi_2)}e^{-G_1(\phi_1,\phi_2,\epsilon_{ij})} &= \dfrac{x}{1-x}\,e^{z\epsilon_{11}(1-2x)/2}
\end{cases}
\tag{3.39}
$$

the solution of which gives

$$
\phi_1\cdot e^{(1-\frac{1}{L})\phi_2-G(\phi_1,\phi_2,\epsilon_{ij})} = x\cdot e^{H(x,\epsilon_{11})} \tag{3.40}
$$

where

$$
G(\phi_1,\phi_2,\epsilon_{ij}) = G_0(\phi_1,\phi_2,\epsilon_{ij}) + G_1(\phi_1,\phi_2,\epsilon_{ij}) \tag{3.41}
$$

and

$$
H(x,\epsilon_{11}) = \frac{z}{2}\,\epsilon_{11}\Big(1-2x+x^2\Big). \tag{3.42}
$$

The function G can be separated into two parts, one independent on ϕ_1 and one depending on it:

$$
\begin{aligned}
G(\phi_1,\phi_2,\epsilon_{ij}) &= Q(\phi_2,\epsilon_{ij}) + R(\phi_1,\phi_2,\epsilon_{ij}) = \\
&= Q(\phi_2,\epsilon_{ij}) + \sum_k r_k(\phi_2,\epsilon_{ij})\cdot\phi_1^k
\end{aligned}
\tag{3.43}
$$

where the entire dependence on penetrant concentration ϕ_1 is enclosed in the function R, which is a polynomial

$$
R(\phi_1,\phi_2,\epsilon_{ij}) = \sum_k r_k(\phi_2,\epsilon_{ij})\cdot\phi_1^k \tag{3.44}
$$

starting with the linear term in ϕ_1, while the Q part depends exclusively on segment con-

centration ϕ_2. We refrain from writing down explicit results for both models discussed, since only this polynomial form is of importance for what follows. To proceed, we note that at relatively low pressures ($x \ll 1$) ϕ_1, the number concentration of the penetrant is low, and ϕ_2 is close to its value ϕ_2^0 in the absence of the penetrant. Expansions around these values provide the results desired.

We rewrite equation (3.40) separating the Q and R contributions and leaving only the contributions of the lowest order in ϕ_1 in the corresponding exponentials:

$$\phi_1 e^{-r_1(\phi_2,\epsilon_{ij})\phi_1} = x e^{H(x,\epsilon_{11})-(1-\frac{1}{L})\phi_2+Q(\phi_2,\epsilon_{ij})} \tag{3.45}$$

In the moderate pressure regime the solution of (3.45) is given by

$$\phi_1 = -\frac{1}{r_1} W\Big(- r_1 \, e^{H(x)-(1-\frac{1}{L})\phi_2^0+Q} \, x\Big) \tag{3.46}$$

where W is the Lambert W-function.

If the empty sites concentration ϕ_0 was low from the very beginning or when it goes to zero as it happens in the high pressure limit $x \to 1$ (as can be easily shown by solving equation (3.27)), $\phi_2^0 \approx 1$, the solid compound turns to a binary solution, and our model reduces to the Flory-Huggins theory of sorption, once the variable x is identified as the activity of the gas a and the quantity $z\epsilon/2$ is recognized as the Flory-Huggins parameter. Setting $\phi_0 = 0$ and $\phi_1 = 1 - \phi_2$ we have

$$G(\phi_1, \epsilon_{ij}) = -\frac{z}{2}\epsilon \, (1-\phi_1)^2 + O(z\epsilon_{ij}^2) \tag{3.47}$$

and equation (3.40) goes to

$$\phi_1 \cdot \exp\Big[\Big(1-\frac{1}{L}\Big)(1-\phi_1) + \chi(1-\phi_1)^2\Big] = x \tag{3.48}$$

corresponding to equation (3.4) when L goes to infinity and when the ideal gas case with $H(x, \epsilon_{11}) = 0$ is considered. Note that if in this regime ϕ_1 is still small compared to unity, the previous equation turns to

$$\phi_1 e^{1+\chi} e^{-(1+2\chi)\phi_1} = x,$$

and its solution is again given by the Lambert function.

In the very low pressure limit we can assume $x \ll 1$, and ϕ_1 small. In this case ϕ_2 equals its value ϕ_2^0 without the penetrant, and $H(x)$ can be neglected if compared to the constant terms in the argument of the exponential. Thereby, Eq.(3.45) gives a linear

relation between penetrant concentration and pressure (Henry's law)

$$\phi_1 \simeq e^{-(1-\frac{1}{L})\phi_2^0+Q(\phi_2^0,\epsilon_{ij})}\ x \tag{3.49}$$

with the term $\exp\left[-(1-\frac{1}{L})\phi_2^0+Q(\phi_2^0,\epsilon_{ij})\right]$ proportional to the Henry's solubility constant. Note that setting $H=0$ corresponds essentially to taking the activity of penetrant in gas phase to be equal to the particle's concentration, i.e. to the ideal gas assumption. This approximation is quite accurate for all gases and in the whole domain of pressures for which our fits in the next section are performed.

The model as discussed above is essentially a model of a ternary polymer-penetrant-void mixture in a contact with the lattice gas (binary mixture of the penetrant molecules and voids) in which the polymer chains are considered as flexible, which might seem to be quite a deficient model for the glassy polymer matrix. The alternative interpretation could correspond to considering the polymer entropic term as a "frozen entropy" pertinent to the ensemble of different realizations of chain's conformations in the matrix, in which case the model discussed can be considered as a kind of a mean field approximation (of uncontrolled quality) to the realistic situation. In both cases however, one has to note that the chains' entropic contribution is small, of the order of $\phi_2^0 L^{-1}$, i.e. can be neglected altogether for longer chains. Another variant of the model leading to the same result corresponds to fully suppressing the chains' entropic contribution and considering the contribution of a matrix as an additional term in the internal energy due to elastic deformation of the matrix, proportional to its volume change compared to its value in the absence of penetrant, giving an additional linear contribution to the free energy of the solid phase. Since the polynomial structure of G stays unperturbed, all these models lead to the same qualitative predictions, and their applicability is mostly bounded by the requirement that the gas phase is still close to the ideal gas. We moreover might suppress the mobility of some populations of holes, change the details of interactions etc. The overall functional form stays the same as long as the penetrant molecules are assumed mobile within the whole volume of the polymeric phase and their interactions with the surroundings can be reduced to bilinear forms. All these changes influence only the parameters but not the form of the solution. This leads to a hope, that the main effect of the glassiness lays in the supporting a quasi-equilibrium population of voids which can be filled by penetrants, and is not connected with the particular properties of the one of the chains. To see whether our hope is fulfilled, we proceed with reanalyzing experimental data typically fitted using the dual mode model for the pressures under which the gas phase can still be considered as ideal.

3.3. Fits

We use the results reported in "*IUPAC-NIST Solubility Data Series 70. Solubility of gases in glassy polymers*" (Paterson et al., 1999), where the data for several gas-polymer systems at temperatures below the glass transition are provided as a function of pressure.

The dimensionless volume concentration ϕ_1 is converted by a proportionality factor to the measured concentration C which is usually given in cubic centimeters of penetrant at standard temperature and pressure per cubic centimeter of polymer, $[cm^3(STP)/cm^3(pol)]$

$$\phi_1 = \gamma C \tag{3.50}$$

and equation (3.45) becomes

$$\gamma C e^{-r_1 \gamma C} \simeq \frac{P}{P_{sat}} e^{-(1-\frac{1}{L})\phi_2^0 + Q}. \tag{3.51}$$

Setting $\sigma = \gamma e^{(1-\frac{1}{L})\phi_2^0 - Q} P_{sat}$ and $\tau = -\gamma r_1$ we get

$$\sigma C e^{\tau C} \simeq P. \tag{3.52}$$

The parameter σ corresponds to the inverse of the infinite dilution solubility S_0, as can be seen by performing a limiting transition

$$S_0 = \lim_{P \to 0} \frac{C}{P} = \lim_{P \to 0} \frac{1}{\sigma} e^{-\tau C} = \frac{1}{\sigma}. \tag{3.53}$$

or by direct comparison with equation (3.2). We first obtain the values of σ and τ by fitting the inverted sorption data, i.e. pressure vs. concentration, given in Paterson et al. (1999), and then plot equation (3.46) in its rescaled form

$$C = \frac{1}{\tau} W\left(\frac{\tau}{\sigma} P\right). \tag{3.54}$$

The agreement of the corresponding fit to the experimental data is excellent and our two-parametric fits are not inferior to the three-parametric ones of the dual mode model, as it is possible to see in the following pictures where both modes are plotted. The likelihood of each fit has also been considered and the dual mode gives a definitely larger one only for argon in EC (fig.3.4(f)), carbon dioxide in unoriented PS at $298K$ (fig.3.4(d)) and carbon dioxide in PETP $\alpha = 0.57$ (fig.3.4(e)). In all the other cases examined, the Lambert mode results to have a considerably larger or comparable likelihood.
Moreover, Eq.(3.54) easily fits both concave isotherms (which can also be reproduced by the the dual sorption mode model) and the convex ones (for which the interpretation of the dual mode parameters is problematic).

3.3.1. Concave isotherms

In figure 3.4 we show the plots resulted by fitting equation (3.54) to experimental data. We used the Nonlinearmodelfit procedure of MATHEMATICA. This method returns a nonlinear least squares fit with a default 95% confidence level assuming normally distributed errors in the data. These plots are given for different systems in a low-average pressure regime and are characterized by a downward concavity to the pressure axis. Dual mode isotherms of equation (3.1) are also shown for a direct comparison.

Fit	**Dual mode**			**Lambert mode**	
	$\mathbf{k_d}$	$\mathbf{C_H}$	**b**	σ	τ
Fig.3.4(a) blue solid line*	3.972	28.533	0.662	0.043	0.027
Fig.3.4(a) red dashed line	1.036	2.170	0.485	0.507	0.074
Fig.3.4(b) blue solid line	9.040	12.590	2.329	0.026	0.045
Fig.3.4(b) red dashed line	5.241	7.090	2.556	0.045	0.075
Fig.3.4(c) blue solid line	4.3975	9.832	2.136	0.046	0.058
Fig.3.4(c) magenta dashed line	5.625	6.050	3.948	0.050	0.054
Fig.3.4(c) red dotted line*	3.913	18.747	0.136	0.157	0.006
Fig.3.4(c) green dash-dotted line*	4.135	0.025	0.001	0.264	-0.009
Fig.3.4(d) magenta dash-dotted line	1.806	2.870	0.668	0.301	0.039
Fig.3.4(d) blue solid line*	0.928	4.780	0.231	0.517	0.041
Fig.3.4(d) red dashed line	0.890	1.20	0.400	0.797	0.030
Fig.3.4(d) green dotted line*	0.903	2.480	0.241	0.702	0.033
Fig.3.4(e) blue dotted line	$0.022^{\dagger}$	1.150	$0.018^{\dagger}$	$24.77^{\dagger}$	0.116
Fig.3.4(e) green dashed line*	$0.010^{\dagger}$	0.640	$0.026^{\dagger}$	$50.144^{\dagger}$	0.201
Fig.3.4(e) red solid line*	$0.009^{\dagger}$	2.289	$0.0085^{\dagger}$	$36.696^{\dagger}$	0.169
Fig.3.4(f) blue solid line	$0.171^{\dagger}$	3.718	$0.2345^{\dagger}$	$1.431^{\dagger}$	0.117
Fig.3.4(f) red dashed line*	$0.125^{\dagger}$	1.456	$0.193^{\dagger}$	$3.412^{\dagger}$	0.124
Fig.3.4(f) green dotted line	$0.089^{\dagger}$	0.303	$0.319^{\dagger}$	$7.862^{\dagger}$	0.103

Table 3.1.: Lambert and dual mode parameters for the fits in figure 3.4. Dual mode parameters are taken from (Paterson et al., 1999), except for fits signed with a star (*) where parameters have been obtained by the authors through a fitting procedure.
Units of k_d values are $cm^3(STP)/(cm^3(pol)MPa)$ except for values signed with a cross (†) expressed in $cm^3(STP)/(cm^3(pol)kPa)$. Units of C_H values are $cm^3(STP)/cm^3(pol)$. Units of b values are MPa^{-1} except for values signed with a cross (†) expressed in kPa^{-1}. Units of σ values are $cm^3(pol)MPa/cm^3(STP)$ except for values signed with a cross (†) expressed in $cm^3(pol)kPa/cm^3(STP)$. Units of τ values are $cm^3(pol)/cm^3(STP)$.

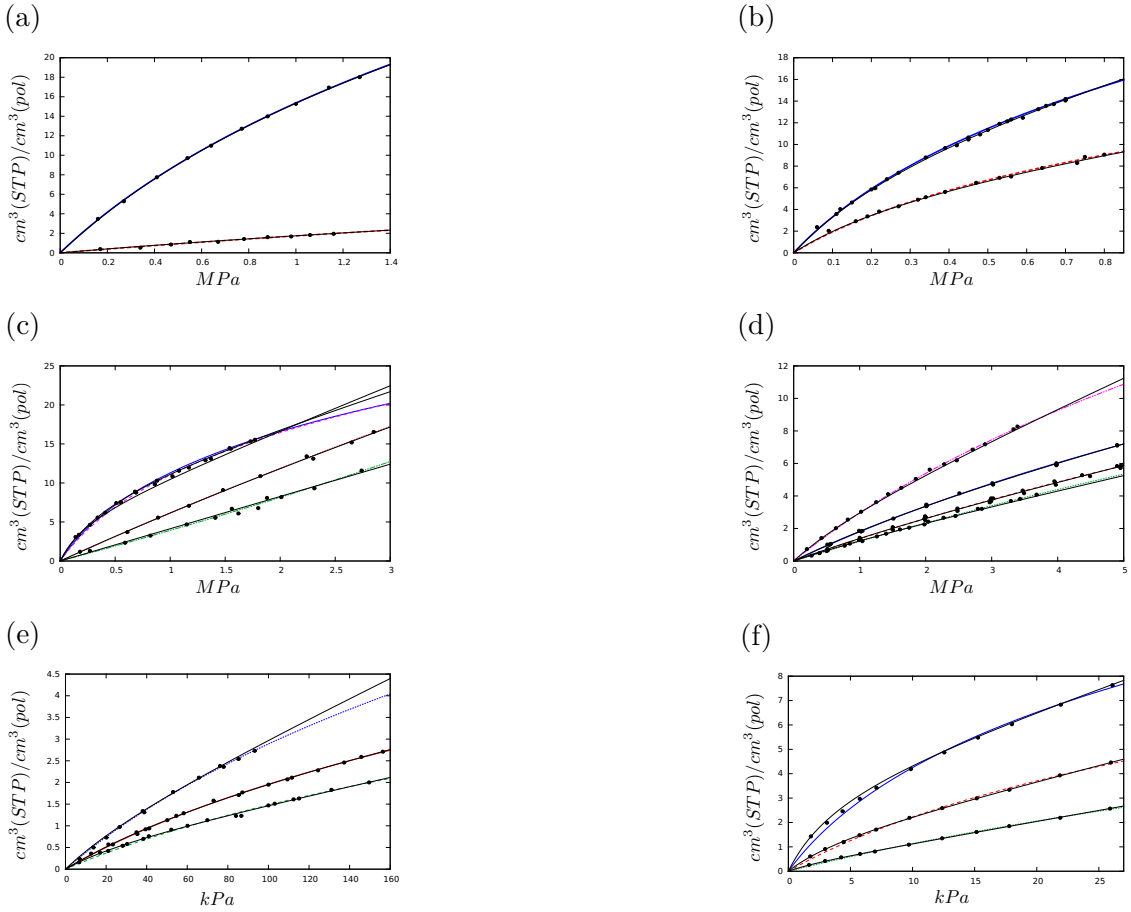

Figure 3.4.: Lambert and dual mode sorption isotherms for different gas-polymer systems;
Lambert lines are given by eq.(3.54) and are represented by colored lines in different styles. Dual mode lines are given by eq.(3.1) and are represented by a thinner black solid line. In some cases this is not distinguishable from the Lambert line.
Respective Lambert and dual mode parameters are reported in table 3.1. Black dots represent data from (Paterson et al., 1999).
(a): Carbon dioxide (blue solid line) and Methane (red dashed line) in PVC at $T = 298K$;
(b): Carbon dioxide (blue solid line) and Ethylene (red dashed line) in PMMA at $T = 308K$
(c): Carbon dioxide in: unoriented PS at $T = 298K$ (blue solid line); oriented PS at $T = 298K$ (magenta dashed line);
unoriented PS at $T = 353K$ (red dotted line); oriented PS at $T = 353K$ (green dashed-dotted line)
(d): Methane sorption isotherm in PEMA at $T = 298K$ (magenta dashed-dotted line) and Argon sorption isotherms in PEMA at $T = 278.4K$ (blue solid line), $T = 358K$ (red dashed line) and $T = 308K$ (green dotted line).
(e): Carbon dioxide in PETP with $\alpha = 1$ (red solid line), $\alpha = 0.57$ (green dashed line) at $T = 298K$
(α is the amorphous volume fraction) and Carbon dioxide in PVCH at $278K$ (blue dotted line).
(f): n-Butane in EC at $T = 303K$ (blue solid line), $T = 323K$ (red dashed line) and $T = 343K$ (green dotted line).

3.3.2. Convex isotherms

At higher pressures, voids tend to be completely filled by penetrant molecules and the solid compound turns to a binary mixture; as previously said, this corresponds to the situation considered in the Flory-Huggins theory. In this case the interaction between penetrants becomes prevalent and sorption is strongly accelerated by the already sorbed molecules. When penetrants are bad solvents, the χ parameter is negative and isotherms take the typical convex shape. This behavior is easily reproduced by the Lambert mode. In figure 3.5 the Lambert isotherms are plotted together with the experimental data in some of such cases.

3.4. List of abbreviations

- EC: Ethyl Cellulose
- PEMA: Poly(Ethyl Methacrylate)
- PETP: Poly(Ethylene Terephthalate)
- PMMA: Poly(Methyl Methacrylate)
- PS: Polystyrenes
- PVA: Poly(Vinyl Acetate)
- PVC: Poly(Vinyl Chloride)
- PVCH: Poly(Vinyl Cyclohexane Carboxylate)

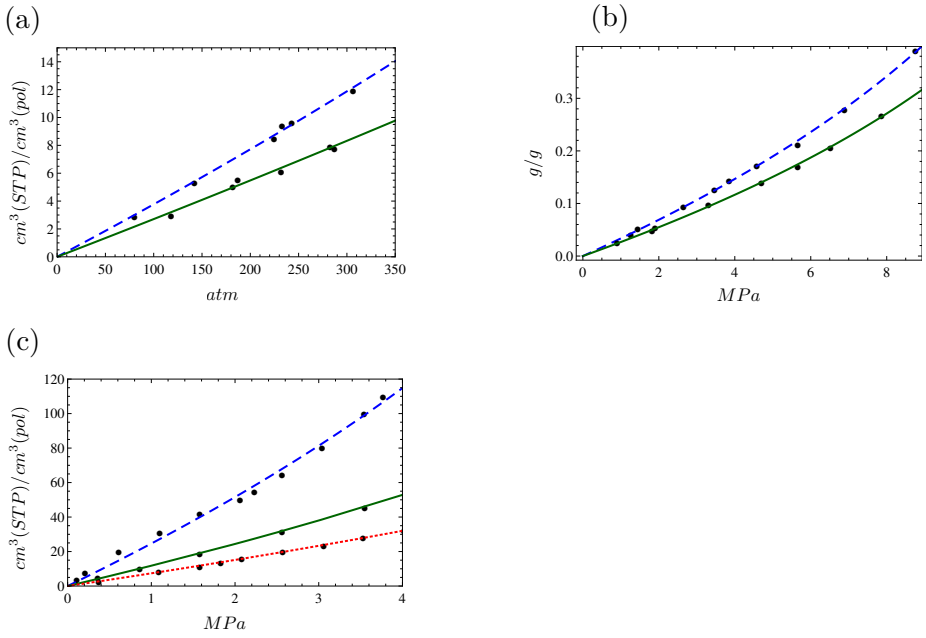

Figure 3.5.: Convex Lambert sorption isotherms; lines are given by eq.(3.54), black dots represent data from (Paterson et al., 1999).
(a): Hydrogen H_2 (blue dashed line) and nitrogen N_2 (green solid line) in PS at $T = 443K$.
Hydrogen: $\sigma = 27.166\ atm/cm^3(STP)/cm^3(pol)$;
$\tau = -0.006\ (cm^3(STP)/cm^3(pol))^{-1}$.
Nitrogen: $\sigma = 37.370\ atm/cm^3(STP)/cm^3(pol)$;
$\tau = -0.004\ (cm^3(STP)/cm^3(pol))^{-1}$.
(b): Carbon dioxide sorption in PVA at $T = 313.2K$ (blue dashed line) and $T = 323.2K$ (green solid line).
The concentration is expressed as a weight fraction, grams of penetrant per gram of polymer (g/g).
Blue dashed line: $\sigma = 30.618\ MPa/g/g$; $\tau = -0.786\ (g/g)^{-1}$.
Green solid line: $\sigma = 38.466\ MPa/g/g$; $\tau = -0.977\ (g/g)^{-1}$.
(c): Carbon dioxide sorption isotherms in PEMA at $T = 288K$ (blue dashed line),
$T = 318K$ (green solid line), $T = 348K$ (red dotted line).
Blue dashed line: $\sigma = 0.042\ MPa/cm^3(STP)/cm^3(pol)$;
$\tau = -0.002\ (cm^3(STP)/cm^3(pol))^{-1}$.
Green solid line: $\sigma = 0.088\ MPa/cm^3(STP)/cm^3(pol)$;
$\tau = -0.003\ (cm^3(STP)/cm^3(pol))^{-1}$.
Red dotted line: $\sigma = 0.139\ MPa/cm^3(STP)/cm^3(pol)$;
$\tau = -0.003\ (cm^3(STP)/cm^3(pol))^{-1}$.

4. Diffusion of small molecules in polymeric media

4.1. Normal and anomalous diffusion in random potential landscapes

We open this section proposing a general remark about the nature of diffusion of independent non interacting classical particles in a random energy landscape.
In usual conditions this results to be a normal diffusion process but can become subdiffusive in some particular cases that coincide with the vanishing of the diffusion constant. On the other hand, a superdiffusive process has never been observed in such systems. In what follows we will therefore describe the conditions that bring to subdiffusion and explain why superdiffusion is not possible by showing that the diffusion constant can never diverge.

Let us start by considering the probability p_i to find a particle at a particular site i of a d-dimensional lattice. The behavior of each p_i is governed by the master equation

$$\dot{p}_i = \sum_j (w_{ij} p_j - w_{ji} p_i) \tag{4.1}$$

where w_{ij} are transition rates from site j to site i, different from zero only for nearest neighbors and the indices i and j belong to the interval of naturals $[1, M]$ where $M \gg 1$ is the total number of sites. Eq. (4.1) can either be considered as following from some microscopic scheme or obtained by a discretization of the diffusion (Fokker-Planck) equation for the overdamped motion in a continuous potential. The details of the latter procedure are given in the Appendix.
The distribution of the transition rates is considered homogeneous and isotropic. This requirement excludes underdamped cases for which the velocities and coordinates enter differently, thus leading to anisotropy of the state (phase) space with respect to rotations mixing coordinates and velocities. This can be formulated as a demand that the state space of the system is its configuration space.
An energy value E_i is assigned to each site. These are independent identically distributed random variables and some of them may be infinite corresponding to blocking sites and giving rise to percolation questions.

We assume that the system is isothermic and possesses true thermodynamical equilibrium, i.e. that the transition rates fulfill the condition

$$w_{ij}p_j^0 = w_{ji}p_i^0 \tag{4.2}$$

where $p_i^0 \propto \exp(-\beta E_i)$ is the probability to find a particle at site i at equilibrium, where $\beta = 1/K_B T$ is the usual inverse temperature factor and T is the temperature. This further requirement follows from the detailed balance condition, being the microscopic consequence of the Second Law of Thermodynamics (Ebeling and Sokolov, 2005).
In what follows we only concentrate on the effective diffusion coefficient describing the particles' transport in the system at long times or large scales, where, as we proceed to show, thermodynamics helps a lot in clarifying the relations between different properties of the system neglecting the discussion of time-dependent problems.
Our discussion maps the initial problem onto the one for random resistor-capacitor networks. We then rely on the general theory of electric circuits and on percolation theory and assume that we are (in principle) able to evaluate the mean conductivity of a corresponding disordered resistor network in the static regime. From this we obtain a general formal expression for the diffusion coefficient, evaluated within the effective medium approximation. This allows us to investigate some peculiarities of the behavior of this effective diffusion coefficient, as illustrated by approximate and exact results for binary continua and for systems with site energies following a rectangular distribution.

We show that the diffusion coefficient is always finite, hence no superdiffusion can be observed in such random potential models, and discuss the conditions under which the diffusion coefficient may vanish, possibly giving rise to subdiffusion. Namely we demonstrate that there are two and only two reasons why this can happen. Independently on the particular distribution of *nonzero* transition rates and *finite* site energies, this is possible either if the percolation threshold in the corresponding network is one (e.g. in one dimension, on finitely ramified fractals, or when we are already at percolation threshold) or if the mean Boltzmann factor $\langle \exp(-\beta E_i) \rangle$ diverges. We therefore obtain necessary conditions under which subdiffusion in a random potential model can be observed. We note that, according to the Arrhenius law, the situation with diverging mean Boltzmann factor corresponds to the divergence of the mean sojourn time at a site, and is pertinent to trap models. The situation when both possibilities are realized simultaneously gives rise to the subdiffusion of mixed origins (Meroz et al., 2010).

4.1.1. General considerations

Let us first generalize some known results about random potential models and random resistor-capacitor networks as discussed in Bouchaud and Georges (1990b), using how-

ever a different approach. Eq.(4.1) can be rewritten as a one for mean numbers or concentrations of particles on the corresponding sites

$$\dot{n}_i = \sum_j \left(w_{ij} n_j - w_{ji} n_i \right). \tag{4.3}$$

by simply multiplying both members by the total number of particles N and defining the concentration $n_i = N p_i$. The corresponding transition rates $0 \leq w_{ij} < \infty$ are not necessarily bounded from above or below, and some of them may actually be put to zero to mimic percolation situations or diffusion on a fractal structure. They are furthermore connected by the detailed balance condition

$$w_{ij} n_j^0 = w_{ji} n_i^0 \tag{4.4}$$

corresponding to a vanishing flux through each bond in the equilibrium stable state. At equilibrium the concentrations n_i^0 are proportional to the Boltzmann factors $b_i = \exp(-\beta E_i)$ as well, and we can therefore write

$$n_i^0 = C b_i \tag{4.5}$$

with the constant prefactor C depending on the number of particles N, on the size of the system M and on the particular distribution of the Boltzmann factors b_i. The detailed balance condition states that the quantity

$$g_{ij} = w_{ij} n_j^0 \tag{4.6}$$

is a symmetric function of the indices $g_{ij} = g_{ji}$ and is a specific property of the bond.[1] Using this notation we rewrite Eq.(4.3) as

$$\dot{n}_i = \sum_j g_{ij} \left[\frac{n_j}{n_j^0} - \frac{n_i}{n_i^0} \right]. \tag{4.7}$$

Adding a weak external potential, for example an electric field giving rise to an additional potential energy V_j at site j, changes the equilibrium concentrations and hence the corresponding equation to

$$\dot{n}_i = \sum_j g_{ij} \left[\frac{n_j}{n_j^0} e^{\beta V_j} - \frac{n_i}{n_i^0} e^{\beta V_i} \right]. \tag{4.8}$$

[1] In the simplest case when the sites correspond to the minima of a continuous random potential (energies E_i) and the bonds connecting them pass through the transition states (energies $E_{ij}^{\ddagger}$), $w_{ij} \propto \exp[-\beta(E_{ij}^{\ddagger} - E_i)]$, $g_{ij} \propto \exp[-(\beta E_{ij}^{\ddagger})]$ describes the property of the transition state (barrier) alone (Bouchaud and Georges, 1990b). In more complex cases g_{ij} may depend on both energies E_i and E_j in a nontrivial way.

This equation can be interpreted as a combination of the local continuity $\dot{n}_i = \sum_j J_{ij}$ and local response equation $J_{ij} = g_{ij}(\zeta_j - \zeta_i)$ with

$$\zeta_j = \frac{n_j}{n_j^0} e^{\beta V_j} \tag{4.9}$$

which will be called the activity of the sites since the quantity

$$\mu_i = K_B T \ln \zeta_i = K_B T \ln \frac{n_i}{n_i^0} + V_i \tag{4.10}$$

can be interpreted as chemical potentials on the sites. Close to the equilibrium and for very small potentials V the values of ζ are close to unity, so that deviations of the chemical potentials from their zero equilibrium values are small. Therefore, close to equilibrium we have

$$\dot{n}_i = \sum_j J_{ij} \qquad \text{and} \qquad J_{ij} = \frac{g_{ij}}{K_B T}(\mu_j - \mu_i). \tag{4.11}$$

The master equation for concentrations Eq.(4.3) can be rewritten as the equation for the temporal evolution of activities ζ_i proportional to them. Assuming the external potential V_i to vanish we obtain the following equation

$$\dot{\zeta}_i = \frac{1}{n_i^0} \sum_j g_{ij} \left(\zeta_j - \zeta_i\right) \tag{4.12}$$

which is formally equivalent to the evolution equation of voltages in a random resistor-capacitor model (Bouchaud and Georges, 1990b), with conductivities given by g_{ij} and capacitances given by n_i^0. It is interesting to note that not the chemical potentials but the activities at the sites play the role of the electric potentials. This leads to differences in the behavior of the random resistor-capacitor model and the random potential model far from equilibrium, i.e. for large concentration gradients.

4.1.2. Effective diffusion coefficient close to equilibrium

Let us now concentrate on the calculation of the effective diffusion coefficient provided it exists, i.e. provided the system homogenizes at large scales, and each part of it, macroscopic but small compared to the overall dimension of the system, is characterized by the same effective parameters. To do this we invest some time in the description of our "experimental" procedure close to equilibrium and its theoretical implementation.

In our approach we mimic the stationary experiment on measuring the diffusion coefficient via the first Fick's law. A membrane of thickness L and transversal dimension W

separates two reservoirs, the left one with a well-stirred solution (or gas) of the corresponding particles at concentration ν_l, and the right one with the concentration slightly below ν_r, so that $\nu_l - \nu_r \ll (\nu_l + \nu_r)/2$. Both concentrations are kept constant during the experiment. In the case of the solution the membrane is considered as impermeable for the solvent. Then the particles flow I through the membrane is measured and connected with the mean diffusion coefficient inside of it.

Since in general a jump of the (free) energy per particle can form on a contact between the membrane and the solution (e.g. in the case when the fluid is a good solvent for diffusing particles and the membrane is, on the average, a bad one, or the other way around) this has either to be explicitly taken into account or the effective diffusion coefficient *inside* the membrane can be defined through

$$D^* = \frac{IL}{W^{d-1}(\langle n_l \rangle - \langle n_r \rangle)} \tag{4.13}$$

where $\langle n_l \rangle$ and $\langle n_r \rangle$ are the mean particle concentrations in the layers of the membrane in immediate contact with the solution, see figure 4.1.

We note that in the thermodynamical limit $L \to \infty$ the permeability of the membrane tends to zero, and all local currents in it as well, and therefore the corresponding D^* is measured in a very large system under the condition of vanishing currents. For the rest of this section, this situation will be denoted as "quasi-equilibrium". We note that this condition corresponds to a stationary state, $\dot{\zeta}_i = 0$, so that

$$\sum_j g_{ij}\zeta_j - \Big(\sum_j g_{ij}\Big)\zeta_i = 0, \tag{4.14}$$

where the sum runs over the nearest neighbors of the site i, and

$$J_{ij} = g_{ij}(\zeta_j - \zeta_i) \to 0. \tag{4.15}$$

In the continuous limit (applicable in the case when all parameters are slowly changing functions of coordinates) we can identify this equation as a continuity equation in combination with the linear response one:

$$\dot{n}(\mathbf{x}) = -\mathrm{div}\mathbf{J}(\mathbf{x}); \tag{4.16}$$

$$\mathbf{J}(\mathbf{x}) = -\frac{g(\mathbf{x})}{K_B T}\,\mathrm{grad}\mu(\mathbf{x}), \tag{4.17}$$

or

$$\dot{n}(\mathbf{x}) = \mathrm{div}\frac{g(\mathbf{x})}{K_B T}\,\mathrm{grad}\mu(\mathbf{x}) \tag{4.18}$$

and identify $\tilde{\mu}(\mathbf{x}) = g(\mathbf{x})/K_B T$ with the local particle's mobility and therefore $g(\mathbf{x})$ with

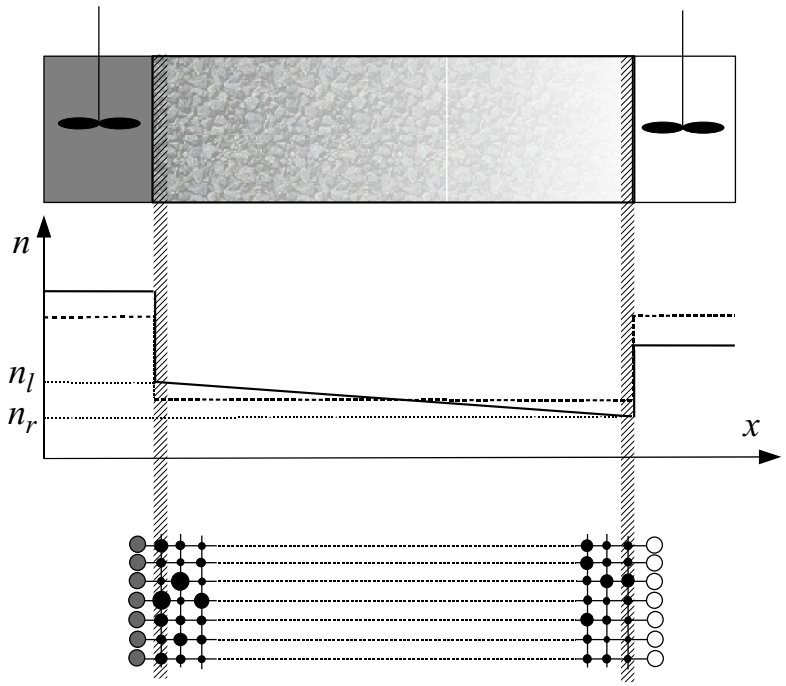

Figure 4.1.: A schematic illustration of the system considered: the disordered medium in contact with two reservoirs, the mean concentration at different positions and the lattice model applied.

the local diffusion coefficient of the particle.

The contact with the solution can be modeled by additional arrays of sites to the left and to the right from the membrane's boundary, with constant concentrations of particles and fixed energies E_0 which can be chosen arbitrarily (this E_0 defines the "quality of the solvent" discussed above and governs the redistribution of the particles between the solvent and the membrane at equilibrium). These additional sites are connected to the ones on the corresponding membrane's sides via extremely high transition rates fulfilling the detailed-balance condition. In this case a local equilibrium between the surface sites and the solutions immediately establishes and persists independently on the particles' distribution inside the bulk.

Due to this local equilibrium the concentrations at the surface sites are proportional to the corresponding Boltzmann factors, and the activities of the corresponding surface sites are all the same and proportional to ν_l or ν_r. Since all these sites are in equilibrium with the ones at the additional layer, they are also in equilibrium between themselves, and the currents between them vanish, which means that their activities are equal to each other and to $\zeta_l = A\nu_l$ and $\zeta_r = A\nu_r$ respectively at the left and right boundary of the membrane, where the prefactor A depends on the corresponding E_0.
Thus, all n_i in the leftmost layer are proportional to $\zeta_l n_i^0 = A\nu_l n_i^0$ and in the right layer to $\zeta_r n_i^0 = A\nu_r n_i^0$ so that the mean concentrations in the layers are

$$\langle n_l \rangle = A\nu_l \langle b_i^0 \rangle \tag{4.19}$$

$$\langle n_r \rangle = A\nu_r \langle b_i^0 \rangle \tag{4.20}$$

where we assume that the distribution of the site energies in the surface layers is the same as in the bulk, and therefore the mean Boltzmann factors $\langle b_i^0 \rangle$ are the same.

We then calculate the corresponding total current I in our system, which is a standard task since the equations for the currents and activities in a stationary states are the same as the ones given by the Kirchhoff's laws for an electric circuit, where g_{ij} stands for the corresponding conductivity and ζ_i for the electric potential of the node. Making such a reinterpretation we see that

$$I = g^* \frac{W^{d-1}}{L} (\zeta_l - \zeta_r) \tag{4.21}$$

where g^* is the effective conductance of the bond in the electric system, i.e. the conductivity of the bond in the *effective ordered medium* with the same total conductivity as our heterogeneous one. Comparing equation 4.21 with equation 4.13 it is easy to obtain

$$D^* = \frac{g^*}{\langle b_i^0 \rangle}. \tag{4.22}$$

and returning to the initial notation we see that

$$D^* = a^2 \frac{\langle w_{ji} \exp(-E_i/K_B T) \rangle_{EM}}{\langle \exp(-E_i/K_B T) \rangle}. \tag{4.23}$$

The squared lattice constant a^2 is introduced to restore the correct dimension as following from equation 4.13, when passing from the distances L measured in number of sites to the distances measured in centimeters, and the subscript EM denotes the effective medium mean, the averaging procedure connecting g^* with the distribution of g_{ij} for $g_{ij} = w_{ij} b_j^0$ i.e. the EM mean of the leaving rates from a site through the bond times the equilibrium probability that the site is occupied by a particle.

Equation 4.23 generalizes the corresponding equation 2.15 of reference Bouchaud and Georges (1990b) for the symmetric barrier model to a general case of random potential. We note that this result reproduces the exact one-dimensional result by Kutner and collaborators, and differs from the one in Maass and Rinn (2001), due to a different interpretation of the equilibrium dynamics in dispersive systems. Thus, if one is able to calculate the effective conductivity of a random resistor network, one can also calculate the effective diffusion coefficient in an energetically disordered network by simple renormalization, and vice versa. The physical content of equation 4.23 is rather transparent and can be elucidated by assuming that we are able to measure the effective electric conductivity of the system, and connect this conductivity with the effective mobility μ^* and thus with the diffusion coefficient via Nernts-Einstein equation

$$\sigma^* = n_0 q \mu^* = n_0 q D^* / kT \tag{4.24}$$

with q being the particle's charge. Reverting this expression we get $D^* \propto \sigma^*/n_0$, which is essentially the meaning of 4.23.

For random resistor networks the homogenization can be proved provided the local conductances are bounded from above and from below. The boundness of the conductances from above (boundness of the transition rates) is not a problem, while the boundness from below excludes percolation cases (see Chayes and Chayes (1986) and references therein). This condition can be relaxed (Mathieu, 2008) *provided* the system percolates.

One may argue that the correct way of measuring D^* were to keep the concentrations (and not the activities) of the sites of the first layer the same, and one has to prove that both procedures lead to the same result. Moreover, one may ask what happens if we define the effective diffusion coefficient through the gradient of the coarse-grained concentration, and not via the total concentration difference. The answer is quite simple since the local concentrations and the local activities decouple under the condition of quasi-equilibrium.
To show this let us assume that at large scales the corresponding electric system homogenizes, which means that its effective conductance per bond really exists as a well-defined quantity, and can be (in principle) measured or calculated. In this case the total voltage profile obtained by the coarse graining of the voltages (activities) over macroscopic domains of the system which are large enough compared to the lattice spacing but small compared to L follows a linear behavior (similar to those of the effective concentration in figure 4.1) with the total potential difference is fixed and the potential gradient vanishing at quasi-equilibrium.

Now we show that in quasi-equilibrium the local concentrations and the local activities

("potentials") tend to be independent from each other (although the local transition rates are correlated with the Boltzmann factors and thus to local concentrations). To see this we note that according to equation 4.14 the activity (potential) at a site i acts like the weight in the arithmetic mean of the activities of the neighbors it is connected to, and equation 4.15 states that the difference between the activities of the connected sites under quasi-equilibrium tends arbitrarily small. To give a better view of this we rewrite the equations as follows

$$\zeta_i = \frac{\sum_j g_{ij}\zeta_j}{\sum_j g_{ij}} \tag{4.25}$$

$$J_{ij} = g_{ij}(\zeta_j - \zeta_i) \overset{L\to 0}{\longrightarrow} 0 \tag{4.26}$$

Therefore our system can be considered as composed of large, practically equipotential regions whose potential hardly fluctuates around its mean ζ^* depending on the region's position. In these regions the concentrations $n_i = \zeta_i n_i^0$ can be averaged over the physically small volume still containing a large number of sites, so that

$$\langle n \rangle = \zeta^* \langle n_i^0 \rangle. \tag{4.27}$$

We note that this last property does not rely on homogenization or on the isotropy and will hold even if our system is built of independent parallel or interwoven wires! If then the coarse-grained activity is a linear function of the coordinate (i.e. the corresponding random resistor network shows homogenization), so is also the coarse grained concentration, with the proportionality factor $\langle n_i^0 \rangle$ between the both.

Equation 4.23 gives the possibility to obtain the universal bounds on the effective diffusion coefficient based on those for the effective conductance, i.e. the universal Wiener bounds (Wiener, 1912) and the tighter Hashin-Shtrikman bounds for isotropic systems (Hashin and Shtrikman, 1962). The universal Wiener bounds for the conductance are given by $\langle g_{ij}^{-1} \rangle^{-1} \leq \langle g_{ij} \rangle_{EM} \leq \langle g_{ij} \rangle$, which in our case corresponds to

$$\frac{a^2 w_0}{\langle \exp(\beta E_i) \rangle \langle \exp(-\beta E_i) \rangle} \leq D^* \leq a^2 w_0. \tag{4.28}$$

Note that the lower bound reproduces the exact result for the one-dimensional system with random potential and constant diffusion coefficient.
In next figures 4.2 and 4.3 we plot the comparison between an opportunely rescaled expression of D^* and corresponding Hashin-Shtrikman bounds in the two and three dimensional cases for two specific situations: the case of binary disorder where the site energy E_i can take only two values E_a and E_b with given probabilities, and the case of

E_i possessing an exponential distribution with cutoffs

$$P(E_i) = \frac{\beta\, e^{-\beta E_i}}{e^{-\beta E_a} - e^{-\beta E_b}} \tag{4.29}$$

in the interval $[E_a, E_b]$ and vanishing outside. The results are plotted against the contrast

$$x = \exp\left[(E_b - E_a)/K_B T\right] \tag{4.30}$$

being the ratio between the largest and smallest values of g_{ij}. Details of the calculations leading to these plots are given in the Appendix.

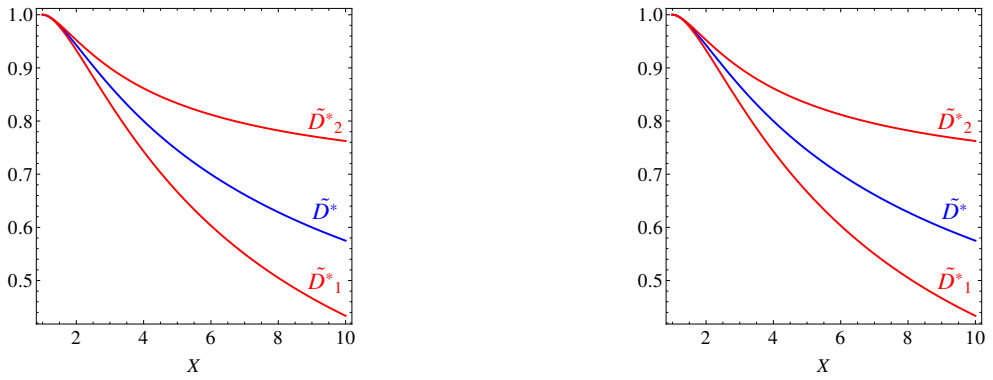

Figure 4.2.: Effective Diffusivity D^* and Hashin-Shtrikman Bounds D_1^* and D_2^* in the binary case vs $x = g_2/g_1$ ratio for: $p = 1/2$ and (a) $d = 2$; (b) $d = 3$.

4.1.3. Two and only two sources of anomalous diffusion

In the limit of a very strongly disordered system D^* may vanish or diverge. In the first case $D = 0$ the system either does not show any transport (does not percolate) or shows anomalous transport slower than diffusion (i.e. shows *subdiffusion*). In the second case it might show superdiffusion.
If D^* vanishes, it can do so either because the enumerator $\langle w_{ji} \exp(-E_i/kT)\rangle_{EM}$ vanishes or because the denominator $\langle \exp(-E_i/kT)\rangle$ diverges, as well as in the cases when both of these possibilities are realized simultaneously. If D^* diverges, it can do so because the enumerator diverges, or because the denominator vanishes, or both.

For further discussion we first recapitulate the following properties of percolation systems:
(i) The mixture of resistors with given finite conductivity (at concentration p) with in-

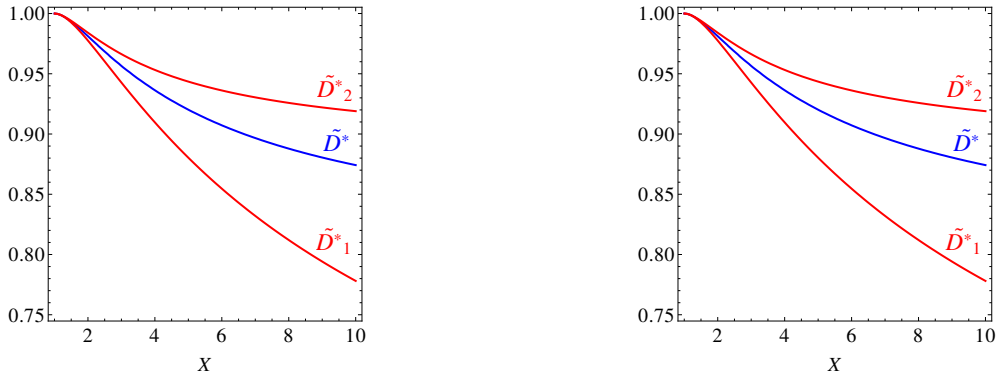

Figure 4.3.: Effective diffusivity D^* and Hashin-Shtrikman Bounds D_1^* and D_2^* in the uniform case vs $x = g_2/g_1$ ratio for: (a) $d = 2$; (b) $d = 3$.

sulating bonds (of zero conductivity) at concentration $1 - p$ possesses zero conductance below the percolation threshold p_c and finite conductance above it. The corresponding system homogenizes at scales above the correlation length (Bouchaud and Georges, 1990b). This homogenization also takes place for arbitrary distributions of the conductivities of the resistors (Mathieu, 2008).
(ii) The mixture of resistors with given finite conductivity (at concentration p) with superconducting bonds (at concentration $1 - p$) possesses finite conductance below the percolation threshold p_c^s for superconducting bonds, with $1 - p_c^s = p_c$, and infinite conductance above it.

These properties do hold not only for the Bernoulli percolation model but also in the case when the short-range correlations in the occupation probabilities of the bond by the corresponding resistors / insulators / superconductors are present (e.g. in the site model). This statement is a (silently assumed) basis of all renormalization group approaches in percolation. In $d = 1$ the corresponding percolation concentrations are $p_c = 0$ and $p_c^s = 1$.

Moreover, the total conductivity of any passive circuit is a non-decaying function of the conductivity of each particular bond. To see this we use the results of the theory of electric circuits (see e.g. Newstead (1959)). Let us consider our system as placed between two "superconducting" bars and look at its conductivity (impedance). The bars are considered as a terminal 1 of the system. Let us moreover consider the points i and j, at which the conductivity g_{ij} is switched, as the two other poles of a system constituting its terminal 2. We now use the theory of two-terminal circuits and calculate the input impedance (conductivity) z_{in}, as a function of load g_{ij}. This input impedance

is given by

$$z_{\text{in}} = z_{11} - \frac{z_{12}z_{21}}{z_{22} + g_{ij}}$$

where $z_{\alpha\beta}$ are the elements of the impedance matrix characterizing the system. For a system of reciprocal passive elements (i.e. no batteries, no diodes) this matrix is non-negatively definite (as a consequence of non-negative heat production), so that

$$\begin{aligned} z_{11} &\geq 0 \\ z_{22} &\geq 0 \\ z_{11}z_{22} - z_{12}z_{21} &\geq 0 \end{aligned}$$

and symmetric, $z_{12} = z_{21}$ (as a consequence of the reciprocity theorem). In the case of pure resistor network the matrix is real. The last means that

$$z_{12}z_{21} = (z_{12})^2 \geq 0$$

and thus that z_{in} is a non-decaying function of g_{ij}. The only case when the function is a non-growing one is when there is no dependence on g_{ij} at all, i.e. when $z_{12} = z_{21} = 0$ and the corresponding conductance is totally decoupled from the rest of the circuit, i.e. belongs to a finite cluster.

Let us now first concentrate on the situation when the denominator in equation 4.23 diverges. Since $b_i = \exp(-E_i/kT)$ is proportional to the sojourn time at a site i in equilibrium, this last situation corresponds to diverging mean sojourn time at a site, i.e. to a trap model, which in high dimensions is equivalent to CTRW with a broad distribution of waiting times.

Now we show that the enumerator never actually diverges, even if the denominator does. To see this we fix some $q < 1 - p_c^s = p_c$ and declare the fraction q of all bonds (starting from the ones with largest conductivities) to be superconductive. The lowest conductivity of such a changed bond is $\sigma_{\min}$. The superconducting bonds are non-percolating by construction, and the conductivity of the remaining system is finite, being smaller than a conductance of the resistor-superconductor mixture where all conductivities of single resistors are put to $\sigma_{\min}$. Thus, the enumerator can only diverge if $p_c^s = 1$, and $p_c = 0$, i.e. never in finite dimension.

Let us now turn to the case when the enumerator vanishes. It is easy to show, that the total conductance z_{in} does not vanish in a system with finite percolation concentration $p_c > 0$ unless the distribution of conductivities of remaining resistors possesses an atom in zero (i.e. unless some other bonds are totally removed). To see this let us remove a

finite portion $p < p_c$ of bonds with smallest conductances without destroying percolation and let us denote the largest removed conductivity as g_c. The rest of the system percolates and has a conductance which is *larger* then the conductance of a two-phase system constructed of resistors with $g_{ij} > g_c$ and $g_{ij} = 0$, which is nonzero since we are above percolation concentration. It can only vanish if the percolation concentration is zero and no finite portion of resistors can be removed without destroying this percolation.

There are no other situations in which subdiffusion in a system is possible except for these two.

Although superdiffusion is never observed in standard simple models of random potentials (random barrier and trap model) it is interesting to show that it is essentially ruled out by our consideration. Since we already showed that the enumerator never diverges, the only thing to do is to show that the denominator never vanishes. Let $p(E)$ be the probability density of the site energy distribution, and E_M the median value of this distribution defined by

$$\int_{-\infty}^{E_M} p(E)dE = 1/2. \tag{4.31}$$

Then

$$\begin{aligned} \langle \exp(-E_i/K_BT) \rangle &= \int_{-\infty}^{\infty} e^{-E/K_BT} p(E)dE & (4.32) \\ &= \int_{-\infty}^{E_M} e^{-E/K_BT} p(E)dE + \int_{E_M}^{\infty} e^{-E/K_BT} p(E)dE. & (4.33) \end{aligned}$$

Now we can use the fact that e^{-E/K_BT} is a non-negative and monotonously decaying function, and that $p(E)$ is non-negative. Thus, the first integral in the second line is larger or equal to

$$e^{-E_M/K_BT} \int_{-\infty}^{E_M} p(E)dE = \frac{1}{2} e^{-E_M/K_BT} \tag{4.34}$$

(where we changed the Boltzmann factor for its lower bound on the interval of integration), and the second integral is definitely non-negative, so that

$$\langle \exp(-E_i/K_BT) \rangle \geq \frac{1}{2} \exp\left(-\frac{E_M}{K_BT}\right)$$

and can vanish only if $E_M \to \infty$ (i.e. only if infinite energies are considered).

To summarize our findings we state that we found a general correspondence between the effective diffusion coefficient in a random potential landscape and the macroscopic

conductance of a corresponding random resistor model. This simple relation allows us to obtain exact bounds on the effective diffusion coefficient as well as the effective medium approximations for it. The very same relation allows for elucidating possible sources of anomalous diffusion in such model. Thus, we show that subdiffusion in the system is possible either if the mean Boltzmann factor of the corresponding potential diverges (energetic disorder, the situation leading to a trap model in some special case) or if the percolation concentration in a system is equal to zero, i.e. if the system is already at the percolation threshold, in one dimension or on finitely ramified fractals (structural disorder) and that superdiffusion is impossible in our system under any condition.

4.2. Diffusion in a random energy landscape.

We now proceed to analyze the diffusion of a set of independent small particles in an amorphous solid polymeric medium, from the perspective of a model being a close relative of a classical Flory-Huggins model of polymer solutions. Together with an analytical treatment, Monte Carlo simulations will be performed and the comparison between the two will be shown.

The polymer matrix is modeled by a three-dimensional ternary lattice similar in spirit but slightly different from those previously shown. In this new case the ternary nature of the lattice will not be given by a solute-segment-void mixture but by a different triplet of elements: each site can indeed be a polymer segment, be empty or be an interaction site where the polymer-solute energy exchange takes place. We keep the requirement that the size of each site has to be taken equal to the size of the diffusing particle. Such a lattice is outlined in Figure 4.4.
Polymers are modeled as phantom random walks of length L. This chain conformation corresponds to the Gaussian nature of chains in melts from which our solid matrix is obtained by quenching. The whole matrix is considered as static: no chain motion is taken into account. Once the system is created, the sites of the lattice occupied by chains are considered impenetrable for small solute molecules. This hard-core repulsion is represented by assigning them an infinite energy value. The number concentration of these sites is denoted as $\phi_2 = M_2/M$ where M_2 is their total number and M is the total number of sites composing the lattice. These segments sites are represented as black boxes in figure 4.4.
The particle-polymer interaction is considered to take place only if the particle occupies a nearest neighboring site of a polymer segment. An energy value $U = \varepsilon$ is therefore assigned to all the nearest neighbors of the sites occupied by segments. The sign of this energy parameter fixes the nature of the force experienced by the particles: if ε is negative polymer tend to attract penetrant particles while in the case ε is positive, the interaction is repulsive. These site are denoted as interaction sites. Their total number is M_1, their number concentration is $\phi_1 = M_1/M$ and they are represented as red boxes in figure 4.4.
Sites not belonging to either of these two categories, represented by white boxes in figure 4.4, are considered as places where penetrants perform a free motion not being subjected to any force. These sites are assigned an energy value $U = 0$ and their number concentration is $\phi_0 = M_0/M = 1 - \phi_1 - \phi_2$, where again M_0 is their total number.
Our system is thus represented by a random but correlated ternary energy landscape with site assigned energies $0, \varepsilon$, or ∞ for the white, red and black sites respectively.

Computer simulations are pertinent to this lattice. Penetrants can diffuse along empty or interactions sites, their concentration is considered low, and their mutual interaction

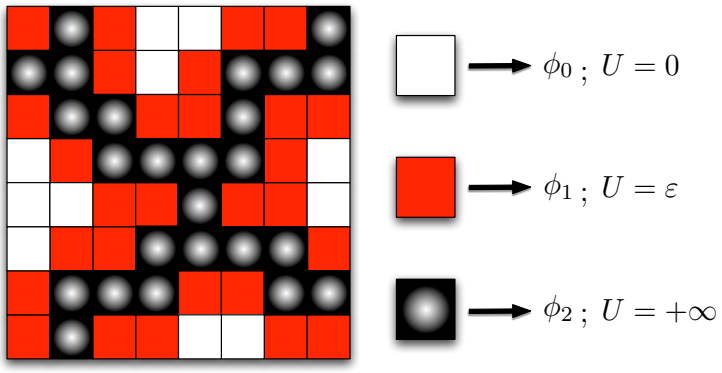

Figure 4.4.: The ternary lattice of the initial model and different kinds of cells with corresponding number concentrations and energy values.

is neglected. We note that finite concentrations, giving rise to non linear effects, could be easily included in the system, but here we want to concentrate on the simpler situation in which particles interact only with the host medium.
In this environment the small molecule diffusion is numerically simulated as a nearest-neighbor random walk with transition rates between the sites given by the corresponding energy differences:

$$w_{ij} = w_0 e^{-\frac{\beta}{2}(U_i - U_j)}. \tag{4.35}$$

The constant rate w_0 defining the time unit of the process is set to unity in all simulations and β is the usual $1/K_BT$ term.
Details about simulations are readily given: Simple random walks of L steps are let run independently in a lattice of 400^3 sites with periodic boundary conditions. This operation is stopped when the total concentration of segments (sites visited at least once) is within 0.01 from the desired value of ϕ_2. Proper energy values are then assigned to white and red sites and their concentration is calculated. Once the environment is created, 10^6 random walks of 10^3 to 10^4 steps, depending on the speed of homogenization of the system, are launched from a free site chosen at random in a cube of 50^3 sites placed in the center of the medium. With this choice, the probability for a diffusing particle to reach the borders of the lattice is extremely low and does not spoil the statistics. The algorithm used is the Monte Carlo Blind Ant one. The whole procedure is then repeated for 10 different lattice realizations and averages are taken. We have observed a normal diffusion process $\langle r^2(t)\rangle \propto t$ from which the proportionality constant has been extracted.

Analytical calculations refer to a simpler mean field version of the previous lattice built by disassembling the chains and letting segments, interaction and empty sites fill the space in a completely random fashion at given concentrations. This model strongly resembles the classical Flory-Huggins model (Flory, 1942; Huggins, 1942; Bawendi and Freed, 1988; Bawendi et al., 1986) used for the description of the thermodynamical properties of polymeric solutions, in which the number concentrations of the sites occupied by polymer segments is kept, but the correlations between their positions (necessarily introduced by the existence of chains) are fully neglected. Each lattice site is assigned an energy value U_i which can take one of the three values $0, \varepsilon$, or ∞ at random, with probabilities ϕ_k. The existence of an infinite cluster of black sites, which we need to preserve the solidness of the system, is guaranteed by maintaining the concentration ϕ_2 above the percolation threshold which is known to be approximately 0.32 for the three-dimensional simple cubic lattice. We denote this construction as mean field lattice and represent it in Figure 4.5. Again, no chain motion is taken into account.
The diffusion on this mean field lattice is then treated using the effective medium approximation for a diffusion in a random potential landscape. The mean field medium results are compared with the results of direct numerical simulations discussed above, and show qualitatively similar behavior.

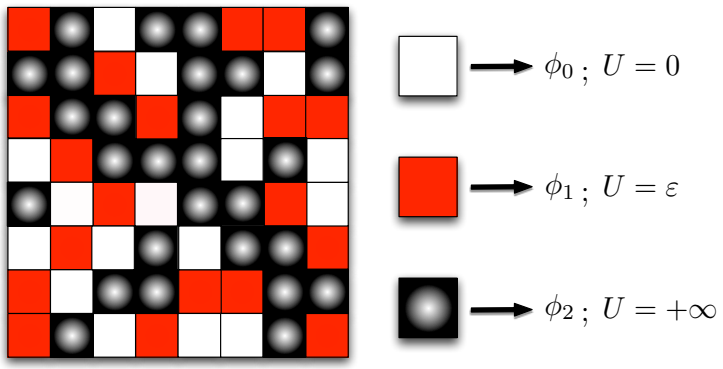

Figure 4.5.: Mean field ternary lattice and different kinds of cells with corresponding probabilities and energy values.

4.2.1. Effective medium approximation for diffusivity

The particles' motion in such an energy landscape is described via the master equation we have previously introduced

$$\dot{p}_i = \sum_j \left(w_{ij} p_j - w_{ji} p_i \right), \tag{4.36}$$

where p_i is the probability for a particle to be at a site i at time t. The transition rate from site j to site i w_{ij} is given by equation (4.35) for j and i nearest neighbors and is equal to zero otherwise. For the sake of generality calculations will be referring to the d-dimensional case.

In order to have the possibility to use the parallelism between conduction and diffusion models, we reconsider the procedure adopted in the previous chapter and multiply both sides of equation (4.36) by the number of particles N. In this way we obtain the master equation for the site mean number or "concentration" function $n_i = Np_i$.

$$\dot{n}_i = \sum_j \left(w_{ij} n_j - w_{ji} n_i \right). \tag{4.37}$$

As already shown, if we assume the existence of an equilibrium state, the transition rates are naturally linked to each other through the detailed balance condition at equilibrium

$$w_{ij} n_j^0 = w_{ji} n_i^0 \tag{4.38}$$

where $n_i^0 = Np_i^0$ and $p_i^0 \propto \exp\left(-\beta U_i\right)$ is the equilibrium probability to find the particle at site i. Thus one can introduce the simmetrized rates g_{ij} being the properties of a bond of the lattice,

$$g_{ij} = w_{ij} n_j^0 = w_{ji} n_i^0 = g_{ji} = g_0 e^{-\frac{\beta}{2}(U_i + U_j)} \tag{4.39}$$

with

$$g_0 = \frac{N w_0}{Z(\vec{\phi}, \varepsilon)} \tag{4.40}$$

where $Z(\vec{\phi}, \varepsilon)$ is the normalization factor of p_i^0, namely the partition function for the small particles equilibrium distribution and $\vec{\phi}$ is the triplet (ϕ_0, ϕ_1, ϕ_2). Then, the analogy between the diffusion and the electric conduction in a random medium can be used (Bouchaud and Georges, 1990a; Doyle and Snell, 1984; Camboni and Sokolov, 2012): the corresponding diffusion coefficient is connected with the macroscopic conductivity $\langle g \rangle_{em}$ of a disordered lattice with bond conductivities g_{ij} via (Camboni and Sokolov,

2012; Dean et al., 2007; Maass et al., 1999; Rinn et al., 2000)

$$D_{em} = a^2 \frac{\langle g \rangle_{em}}{\langle n_i^0 \rangle} = a^2 \frac{\langle w_{ji} \exp(-\beta U_i) \rangle_{em}}{\langle \exp(-\beta U_i) \rangle}. \tag{4.41}$$

with a the lattice spacing set to unity in all simulations.

Our system exhibits four different bond conductivity values depending on the color of the sites involved. These are

$$g_1 = g_0; \quad g_2 = g_0 e^{-\beta\varepsilon}; \quad g_3 = g_0 e^{-\beta\varepsilon/2}; \quad g_4 = 0. \tag{4.42}$$

Figure 4.6 gives an overall view of this situation.

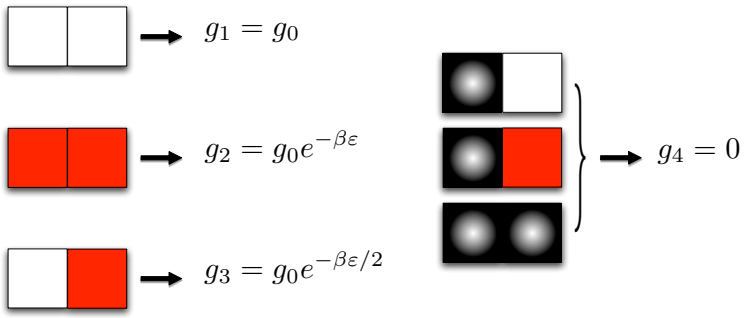

Figure 4.6.: Bond conductivities for the corresponding site couples.

The effective conductivity $\langle g \rangle_{em}$ can then be calculated within the effective medium approximation EMA. However, the application of the effective medium approximation to site models like ours, requires the considerations on correlations we shown in the previous sections and the Effective Medium Approximation technique adopted will be therefore the Yuge one.
Calculations start by considering for any site of the lattice possessing a color index $\alpha = 0, 1, 2$, corresponding to white, red and black, respectively, the mathematical expectation of the conductivity $\bar{g}_\alpha$ of a bond originating from it:

$$\begin{aligned} \bar{g}_0 &= \phi_0 g_1 + \phi_1 g_3 \\ \bar{g}_1 &= \phi_0 g_3 + \phi_1 g_2 \\ \bar{g}_2 &= 0 \end{aligned} \tag{4.43}$$

These values appear in the system according to the the probabilities of their respective

sites

$$P(\bar{g}) = \sum_{\alpha=0}^{2} \phi_\alpha \delta(\bar{g} - \bar{g}_\alpha). \tag{4.44}$$

The effective conductivity is then obtained through the usual self-consistency condition (Kirkpatrick, 1973)

$$\left\langle \frac{g_{em} - \bar{g}}{(d-1)g_{em} + \bar{g}} \right\rangle_P = 0. \tag{4.45}$$

where d is the dimension and $\langle\cdot\rangle_P$ is the average with respect to the distribution P above. If we now define a rescaled effective conductivity

$$f_{em} = (d-1)\frac{g_{em}}{g_0} \tag{4.46}$$

and introduce the arithmetic mean and the ϕ_α-weighted average of the quantity $E_i = e^{-\beta U_i/2}$

$$\overline{E} = \frac{1}{3}(1 + e^{-\beta\varepsilon/2}) \qquad \text{and} \qquad \langle E\rangle = \phi_0 + \phi_1 e^{-\beta\varepsilon/2} \tag{4.47}$$

equation (4.45) reduces to a quadratic equation for f_{em},

$$f_{em}^2 + \; b(\vec{\phi},\varepsilon)\; f_{em} + \; c(\vec{\phi},\varepsilon) = 0 \tag{4.48}$$

with

$$\begin{aligned} b(\vec{\phi},\varepsilon) &= \langle E\rangle\Big(3\overline{E} - d\langle E\rangle\Big) \\ c(\vec{\phi},\varepsilon) &= \langle E\rangle^2\Big(1 - d(1-\phi_2)\Big)e^{-\beta\varepsilon/2}. \end{aligned}$$

The value of D_{em} follows from the solution of this equation via

$$\begin{aligned} D_{em} &= \frac{a^2 g_{em}}{\langle n_i^0\rangle} = a^2 w_0 \cdot \frac{f_{em}}{(d-1)(\phi_0 + \phi_1 e^{-\beta\varepsilon})} = \\ &= D_0 \cdot \tilde{D}_d(\vec{\phi},\varepsilon) \end{aligned} \tag{4.49}$$

where $D_0 = a^2 w_0$ is the diffusivity of a completely white lattice where the energy landscape has been substituted by a flat surface (in few words D_0 is the diffusivity associated to a simple d-dimensional random walk with fixed jumping rates w_0) and

$$\tilde{D}_d(\vec{\phi},\varepsilon) = \frac{f_{em}}{(d-1)(\phi_0 + \phi_1 e^{-\beta\varepsilon})} = \frac{D_{em}}{D_0} \tag{4.50}$$

is a normalized effective diffusivity which originates from the presence of the energy landscape and goes to 1 whenever this is removed.

The critical threshold at which D_{em} vanishes can be easily obtained by setting $c(\vec{\phi}, \varepsilon) = 0$

$$\phi_2^c = 1 - 1/d. \tag{4.51}$$

At variance with a classical binary Flory-Huggins situation, where the connectedness of the molecules could be disregarded to a large extent, the presence of the molecules does matter here, since it leads to a redistribution of empty sites between the red and white classes. The problem of distribution of the sites between these two classes (i.e. the one of finding ϕ_0 and ϕ_1 as functions of a given parameter ϕ_2, the polymer density) in systems with chains is a complex problem of statistical geometry, which, up to our knowledge, was never approached. We can however separate this geometrical problem (which we leave for further investigation) from the problem of the diffusion. Thus we first simulate our polymer model and extract the numerical values of ϕ_0 and ϕ_1 from these simulations. These numerical values are then used in the corresponding EMA calculations, whose predictions (for example, with respect to temperature dependence of the diffusion coefficient), in their turn, are (favorably) compared with the results of simulations of diffusion.

To get a flavor of the problem, let us first consider the situation in which the black sites are not connected into chains, but randomly distributed in the system (simple Bernoulli percolation, but now with interactions between the solute and the black matrix) on a cubic lattice with connectivity $\lambda = 6$. This case leads to a relatively simple behavior. Black sites are randomly distributed on the lattice, and the probability that a given site is black is exactly ϕ_2; this ϕ_2 is the control parameter of the model. The site is white if it itself and none of its nearest neighbors is black, so that the concentration of the white sites is

$$\phi_0 = (1 - \phi_2)^{\lambda+1}. \tag{4.52}$$

The sites which are not black or white are red, so that the concentration of red sites is

$$\phi_1 = (1 - \phi_2) - (1 - \phi_2)^{\lambda+1}. \tag{4.53}$$

Thus, ϕ_0 is a monotonously decaying function of ϕ_2, and ϕ_1 shows a pronounced maximum at

$$\phi_1 = 1 - (\lambda + 1)^{-1/\lambda}. \tag{4.54}$$

The parameter $\gamma = \phi_0/(1 - \phi_2)$ which will be repeatedly used in what follows (see equations 4.58 and 4.59) is thus given by $\gamma = (1 - \phi_2)^{\lambda}$ and is a monotonously decaying function of ϕ_2.

The presence of the chains reduces the total number of available sites being neighbors of

the black ones. If the molecules would follow parallel straight lines, the effective number of potentially available neighbors of a black sites will be reduced to 4, so that $\lambda = 4$ would have to be taken in the previous equation.
The numerical simulations show that the existence of the chains does matter even more. The fact that the molecules are wiggled, and the possibility of their intersection reduces the effective values of λ almost down to 2. This is made evident in figure 4.7 where the results from equations 4.52 and 4.53 are plotted versus the black concentration ϕ_2 together with the values of ϕ_0 and ϕ_1 measured in simulations.

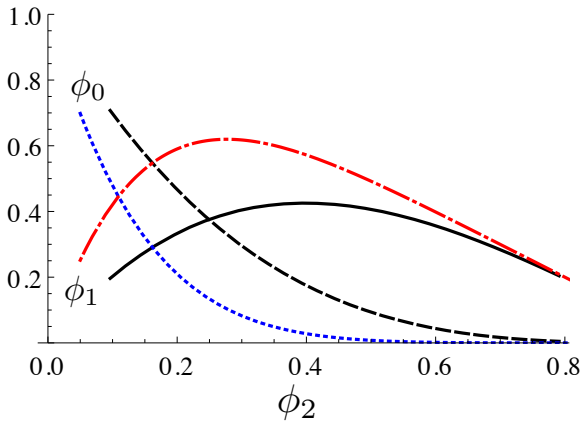

Figure 4.7.: Red and white sites' concentrations in the system of chains and in the uncorrelated model. Results obtained in the simulations for ϕ_0 (black dashed line) and for ϕ_1 (black solid line). Results for the uncorrelated site model: ϕ_0 as given by Eq.(4.52) (blue dotted line) and ϕ_1 from Eq.(4.53) (red dash-dotted line).

It is furthermore possible to estimate an approximate value for the effective exponent λ as following from simulations. The theoretical value of the black concentration $\bar{\phi}_2$ at which white and red sites are equally distributed can be easily found by equating equations 4.52 and 4.53. This gives

$$\bar{\phi}_2 = 1 - \frac{1}{2^{1/\lambda}} \qquad (\simeq 0.11 \quad \text{for a cubic lattice}). \tag{4.55}$$

The simulation results in figure 4.7 lead to a larger value of $\bar{\phi}_2 \simeq 0.25$. Therefore the value of λ as obtained by inverting equation 4.55 is as low as

$$\lambda = -\frac{\ln 2}{\ln(1 - \bar{\phi}_2)} \simeq 2.41. \tag{4.56}$$

4.2.2. Pure percolation (binary) model

It would be nice to know, how large is the typical error arising from disregarding the chain structure of black sites, and what is the role the chain length plays in the simplest case, namely in a percolation model with correlated black sites given by the chains. In this section we consider therefore a pure binary black and white lattice and neglect the red sites. Our previous considerations reduce then to the original Yuge's result for site percolation.
Thus, we consider a pure percolation situation in which the only interactions are the excluded volume ones. The results of simulations for the systems of chains of different lengths are shown in Fig. 4.8(a). The figure representing the dependence of the diffusion coefficient on the concentration of sites occupied by segments of the chain shows this for the chain lengths from $L = 1$ (usual Bernoulli site percolation problem) to $L = 10$. The simulations were performed also for longer chains, but for L larger than 10 the corresponding graphs are indistinguishable from that for $L = 10$ within the statistical accuracy. Thus, a result for $L = 100$, (not shown) is indistinguishable from the one for $L = 10$ on the scales of Fig 4.8(a).

Simulations are performed along the same lines previously given. Again a normal diffusion process $\langle r^2(t)\rangle \propto t$ is observed and the corresponding diffusion factor $\tilde{D}_3$ is reported in Fig. 4.8(a). We stress the fact that the homogenization of $\langle r^2(t)\rangle$ slows down in the proximity of the critical point. For this reason 10^4 time steps become insufficient and the diffusivity is systematically overestimated. Our attention however is focused on a range of values of ϕ_2 which are above the percolation threshold.
The curves do not differ drastically, but definitely show different percolation thresholds $\phi_0^c(l)$ depending on L. For the Bernoulli case the total behavior of diffusivity is reproduced sufficiently well by EMA for ϕ_2 close to unity but departures from the EMA line for concentrations close to a critical one. For longer chains the critical concentration gets lower, and the diffusion coefficient at given ϕ_0 gets larger than for the Bernoulli case. Although different, the curves however show a large amount of universality which is unveiled when rescaling the concentration and diffusivity according to

$$\phi_0^{'} = \frac{\phi_0}{\phi_0^c} - 1 \qquad \text{and} \qquad \tilde{D}_3^{'} = \tilde{D}_3 \frac{(1-\phi_0^c)}{\phi_0^c}, \tag{4.57}$$

so that the critical concentration is mapped onto the point $\phi_0^{'} = 0$, see 4.8(b). In this case all the curves fall onto the same master curve, and the mean-field result, accordingly rescaled, gives a straight line (of slope 1) which reproduces the results of simulations astonishingly well up to the critical domain. This high degree of universality shows that the correlations introduced by the existence of the chains are not of high importance and can be fully accounted for by rescaling the results of EMA according

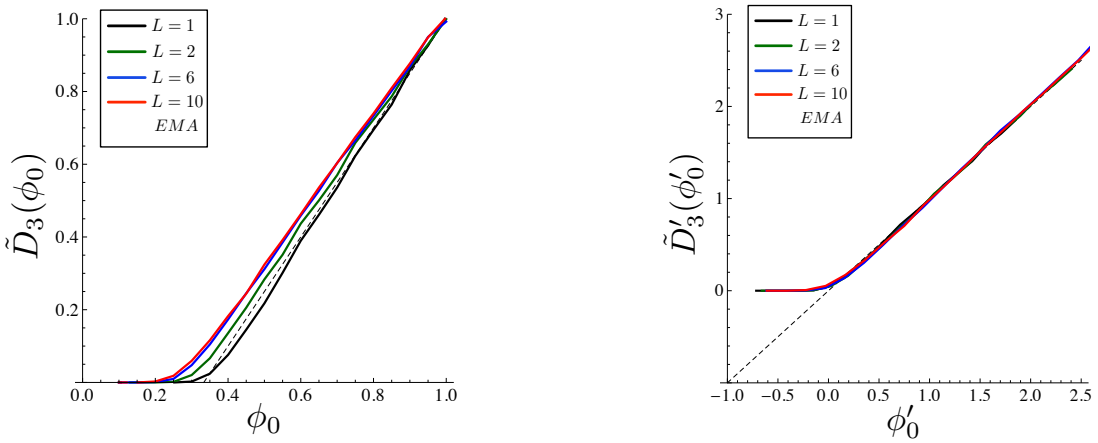

(a) (b)

Figure 4.8.: (a) Normalized diffusivities $\tilde{D}_3$ in the purely percolation case vs. the concentration ϕ_0 of white sites; (b) Rescaled normalized diffusivities $\tilde{D}_3'$ vs. rescaled white concentration ϕ_0'. The dotted line represents in both figures the effective medium approximation.

to the equations above. The corresponding critical concentration has however to be obtained numerically. Alternatively, it can be extrapolated from the slope of diffusion coefficient for concentrations close to unity.

4.2.3. Results for ternary model

In this section we discuss results for the normalized effective diffusivity $\tilde{D}_3(\vec{\phi}, \varepsilon)$ and concentrate on the role of interaction energy ε between the diffusing particles and the polymer matrix. All the figures refer to the three-dimensional case. The reduced interaction energy $\beta\varepsilon = \bar{\varepsilon}$ is chosen to span in the interval $[-5, 5]$ according to the following reasoning: typical absolute values of ε_{XX}/K_B, the coupling strength of a Lennard-Jones potential describing the interaction between two atoms of the same kind X, can be roughly enclosed in the interval corresponding to temperatures $[0, 500K]$ (Putintsev and Putintsev, 2004; Bernardes, 1958; Kittel, 2005). In order to consider the interaction between two different atoms X and Y, the Lorentz-Berthelot mixing rule is used to obtain $\varepsilon_{XY} = \sqrt{\varepsilon_{XX}\varepsilon_{YY}}$ which, being an average, belongs to the same interval. Using ε in place of ε_{XY}, considering both positive and negative values and taking the temperature not too far from the ambient one, it is straightforward to see that the choice $\bar{\varepsilon} \in [-5, 5]$ is a reasonable one. For the discussion of the Arrhenius or non-Arrhenius temperature dependencies in next section 4.2.3 broader bounds are anyway used, $\bar{\varepsilon} \in [-10, 10]$

Effective diffusivity vs interaction energy

Let us first discuss general features of the dependence of the diffusion coefficient on number concentrations and on interaction energy ε. The EMA results for $\tilde{D}_3(\vec{\phi}, \varepsilon)$ in the three different cases corresponding to different relations between ϕ_0 and ϕ_1 at ϕ_2 fixed are shown in Fig. 4.9. These plots show the behavior for the attractive and repulsive interaction and the way the diffusivity approaches zero when the black sites concentration approaches its critical value $\phi_2^c = 2/3$ (see Eq.(4.51)). At this value in fact, particles remain confined in finite subregions of the system, due to the overwhelming predominance of polymer segments.

Plots are given for three different sets of the ϕ_k values in order to consider symmetrically the situations in which red sites are in minority, equally probable or predominant with respect to the white ones, at given ϕ_2. For this purpose we introduce the real parameter $\gamma \in [0, 1]$ we previously mentioned, and define the number concentrations of white and red sites as

$$\phi_0 = \gamma(1 - \phi_2) \tag{4.58}$$

$$\phi_1 = (1 - \gamma)(1 - \phi_2). \tag{4.59}$$

Graphs are then taken for three different values of γ: $\gamma = 1/4$ (red dashed lines, $\phi_1 > \phi_0$), $\gamma = 1/2$ (green dotted lines, $\phi_1 = \phi_0$) and $\gamma = 3/4$ (blue dash-dotted lines, $\phi_1 < \phi_0$). This imbalance will deeply influence the behavior of the effective diffusivity when ε crosses the zero value. In the symmetric case $\phi_1 = \phi_0$, $\tilde{D}_3$ is invariant under the change of the sign of the interaction energy $\bar{\varepsilon} \to -\bar{\varepsilon}$. On the contrary, when the white-red balance is broken, the effective diffusivity decreases or increases depending on the sign of the energy parameter and on the value of γ.
To better explain, let us consider the situation in which $\phi_1 > \phi_0$ (e.g. $\gamma = 1/4$, Fig. 4.9(b), red dashed lines) and restrict our attention on the attractive $\bar{\varepsilon} < 0$ region; with this choice of the parameters, we have increased the number of the red-red g_2 bonds (showing larger conductivity) with respect to the number of the white-white g_0 ones which have the lowest conductivity. This results in a global increasing of the effective diffusion constant. If we now invert the sign of ε, i.e. consider the repulsive interaction, the g_2 bonds are still the most numerous, but now they bring the lowest conductivity value, decreasing in this way the whole diffusivity of the system. The opposite happens if we consider $\phi_1 < \phi_0$ and the corresponding graph in Fig.4.9(c) results in a mirror image of the one in Fig.4.9(b).

The comparison between the mean field calculations and the Monte Carlo simulations performed in the original ternary lattice with the chain length $L = 100$ is quite satisfac-

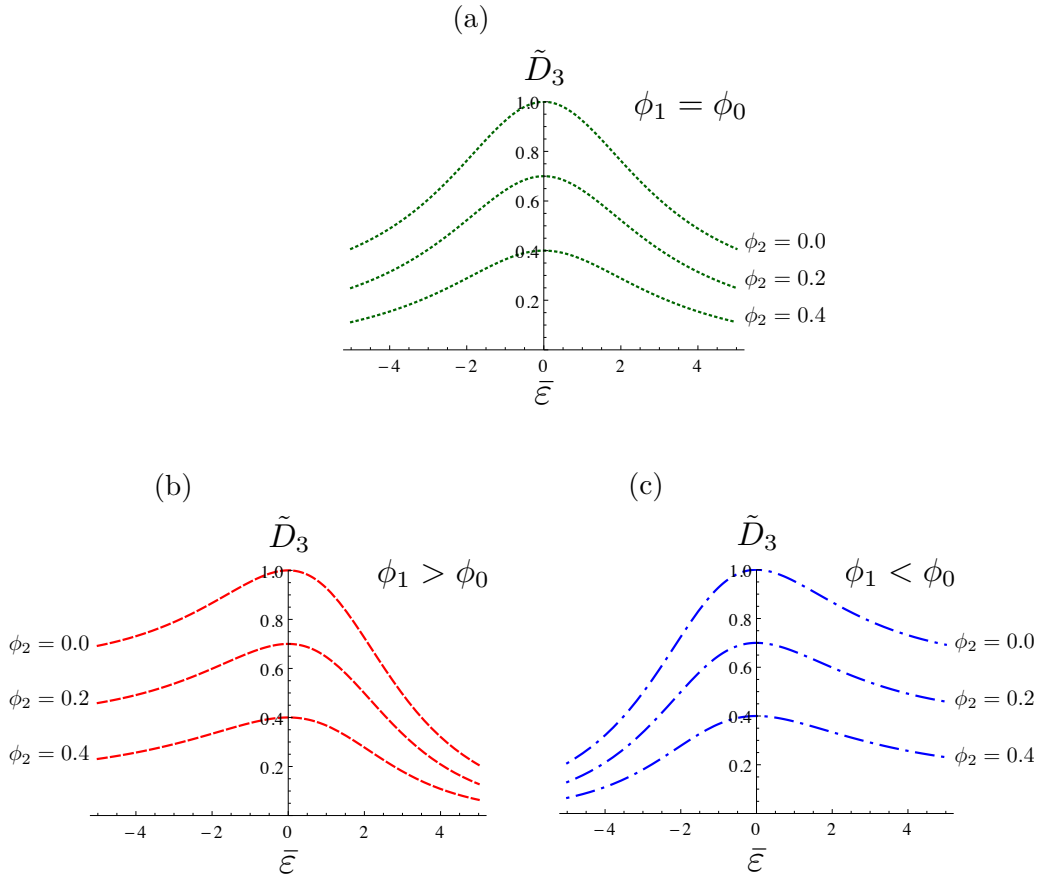

Figure 4.9.: EMA normalized effective diffusivity $\tilde{D}_3$ vs $\bar{\varepsilon}$ in the cases $\phi_2 = 0; 0.2; 0.4$ and: (a) $\gamma = 1/2$; (b) $\gamma = 1/4$; (c) $\gamma = 3/4$.

tory (Fig.4.10). Representative samples corresponding to the the cases $\phi_1 > \phi_0$, $\phi_1 \simeq \phi_0$ and $\phi_1 < \phi_0$, namely, the red, green and blue ones, were found according to the suggestions of Fig.4.7 giving the concentration values reported in Fig.4.10. The numerical result is plotted together with the mean field calculations in which the same values are used. We note that the value of the polymer concentration is close to the critical domain in Fig. 4.10(b) corresponding to $\varepsilon = 0$, so that the total accuracy of EMA is not too high in this domain. However, the EMA-results reproduce the dependence qualitatively well, and, moreover, the accuracy of EMA improves for higher interaction strengths.

Arrhenius vs. non-Arrhenius behavior

A non-trivial aspect of the dependence of diffusivity on the interaction strength is revealed by the Arrhenius plots shown in Fig.4.11 where the logarithm of $\tilde{D}_3$ is plotted as a function of $\bar{\varepsilon} = \varepsilon/K_BT$ in the wider interval $[-10, 10]$ to investigate the role played by activation in the diffusion process; the segment concentration is set here to $\phi_2 = 0.4$. The three curves correspond to the values of $\gamma = 1/4$ (red dashed line), $\gamma = 1/2$ (green dotted line) and $\gamma = 3/4$ (blue dash-dotted line). As in the previous figures, the curve for $\gamma = 1/2$ represents an even function of $\bar{\varepsilon}$, and the curves for $\gamma = 1/4$ and $\gamma = 3/4$ are mirror images of each other. For $\bar{\varepsilon}$ close to zero, the activation process is not relevant, the curves fall together and reproduce the diffusion constant in the black-and-white lattice of section 4.2.2. When one moves away from the $\bar{\varepsilon} = 0$ value, the activation acquires importance. For $\gamma = 1/2$ this behavior becomes Arrhenius-like and the curve shows a linear decay for both signs of $\bar{\varepsilon}$ provided the interaction is strong enough. For asymmetric cases $\gamma \neq 1/2$ the Arrhenius behavior is seen only for interaction energy of the corresponding sign (attractive interaction for $\gamma < 1/2$ and repulsive interaction for $\gamma > 1/2$). For the opposite sign of interaction, at low temperatures, or high absolute values of ε, the lines become horizontal, quitting the Arrhenius regime.

This non-Arrhenius behavior can be explained as follows. Let us focus our attention again on the red (dashed) line in the negative $\bar{\varepsilon}$ half-plane. Under segment concentration $\phi_2 = 0.4$ the black infinite cluster exists but is not dense enough to prevent the existence of infinite white or red ones. The concentration of red sites is $\phi_1 = 0.45$ ($\gamma = 1/4$) and thus lays above the percolation threshold for a cubic lattice. This means that red sites form an infinite cluster crossing the whole system, and once a particle finds it, it becomes more probable to travel along it than escape from it by activation. As a consequence diffusivity saturates and the system never freezes. In the repulsive region, the same behavior is shown by the blue (dash-dotted) line, indicating the existence of a white infinite cluster.
The green (dotted) line, the one for symmetric situation $\phi_2 = 0.4$, $\phi_1 = \phi_0 = 0.3$, doesn't show any saturation. This suggests that in such a case white and red concentrations are below the percolation threshold, and the activation processes are necessary to traverse the system.
Figure 4.12 shows the comparison between theory and simulation Arrhenius plots in the original interval $\bar{\varepsilon} \in [-5, 5]$ and for the same concentration values of Fig.4.10.

On the total the following regimes of behavior can be qualitatively distinguished:

(1) If the concentration of black sites is so high that percolation on red and white sites is not possible, the diffusion coefficient vanishes. In the case when percolation over the

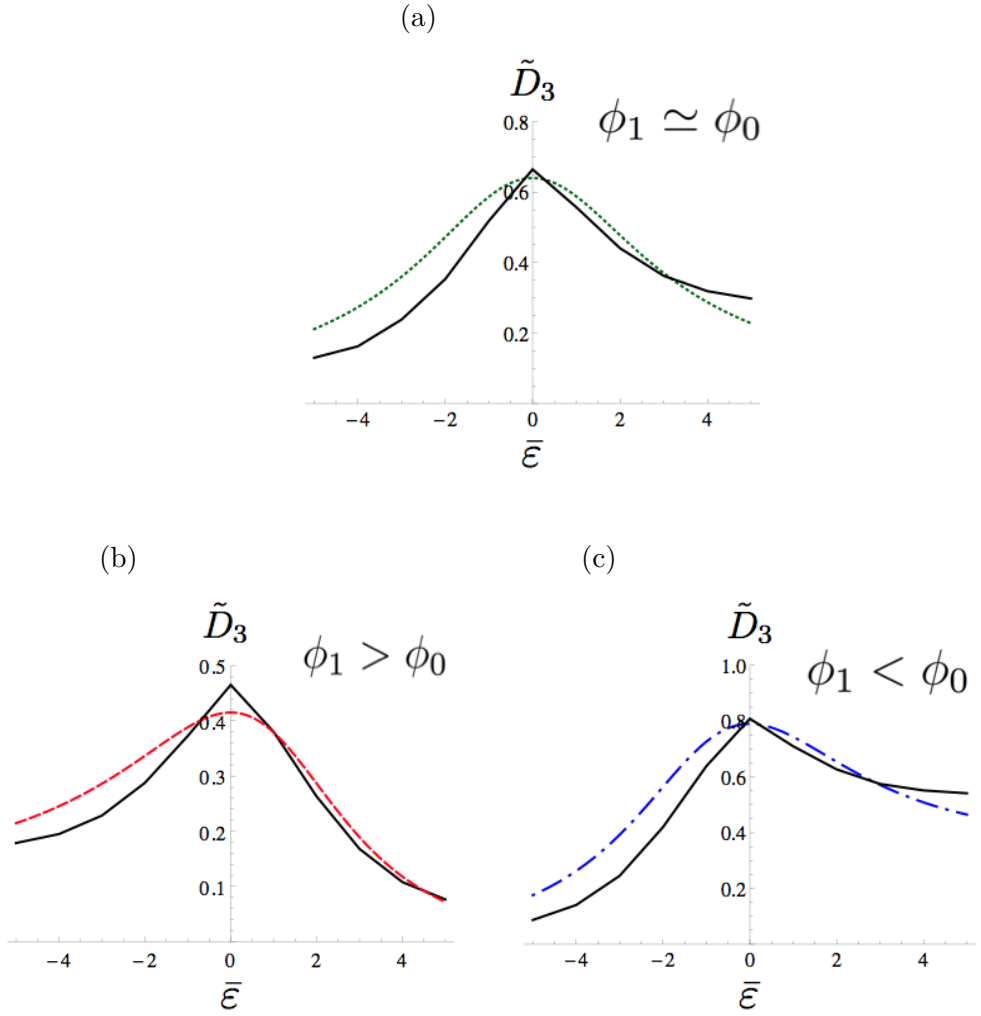

Figure 4.10.: Comparison between theory and simulations (black solid line) in the cases:
(a) $\phi_0 = 0.39$, $\phi_1 = 0.37$, $\phi_2 = 0.24$, $(\gamma = 0.513,\ \phi_1 \simeq \phi_0)$;
(b) $\phi_0 = 0.18$, $\phi_1 = 0.43$, $\phi_2 = 0.39$, $(\gamma = 0.295,\ \phi_1 > \phi_0)$;
(c) $\phi_0 = 0.59$, $\phi_1 = 0.27$, $\phi_2 = 0.14$, $(\gamma = 0.686,\ \phi_1 < \phi_0)$.

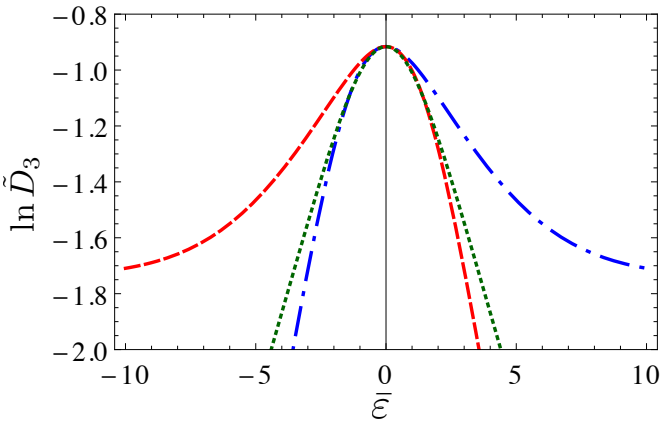

Figure 4.11.: Arrhenius plots of the different EMA normalized effective diffusivities vs. $\bar{\varepsilon}$ at $\phi_2 = 0.4$ and $\gamma = 1/4$ (red dashed line), $\gamma = 1/2$ (green dotted line), $\gamma = 3/4$ (blue dash-dotted line).

red-and-white domains is possible, the diffusion coefficient is nonzero, and its behavior as a function of temperature depends on the percolation properties of red and white clusters, and on the sign of interaction energy.

If the interaction is repulsive, two regimes appear:
(2) If white sites percolate, the diffusion over the white cluster is always possible and does not need activation. The temperature dependence saturates.
(3) If white clusters do not percolate, the diffusion is only possible over red sites, and involves an activation process; its temperature dependence shows the Arrhenius behavior.

In the case of attractive interaction the roles of white and red sites interchange, and percolation over red sites is what determines the temperature dependence of the diffusion coefficient:
(4) If red sites do percolate, the diffusion over the red cluster is possible and does not need activation. The temperature dependence saturates.
(5) If red clusters do not percolate, the diffusion has to go via white sites, and therefore involves an activation process; its temperature dependence shows the Arrhenius behavior.

These features, predicted by EMA, have also been found in simulations of a genuine ternary lattice in which red clusters run clung on the black chains by construction. Fig-

ure 4.13 shows the behavior of Arrhenius plots for low polymer concentrations in the case of attractive interaction. It shows the logarithm of the normalized effective diffusivity for different values of ϕ_2. For $\phi_2 < 0.06$, polymers remain sparse and isolated, their red perimeter sites do not percolate, no infinite red cluster exists and the system is in an Arrhenius regime (5). When the number of chains is increased, the transition from the Arrhenius to the saturation behavior (4) is observed at the critical value $\phi_2 = 0.06$, revealing the emergence of an infinite red cluster. This critical value is far below the usual percolation threshold of a cubic lattice due to the fact that red sites are arranged in connected groups on the perimeters of black chains. This number can not be predicted by simple EMA and can be translated into an estimate of the percolation threshold of perimeter sites of chains.

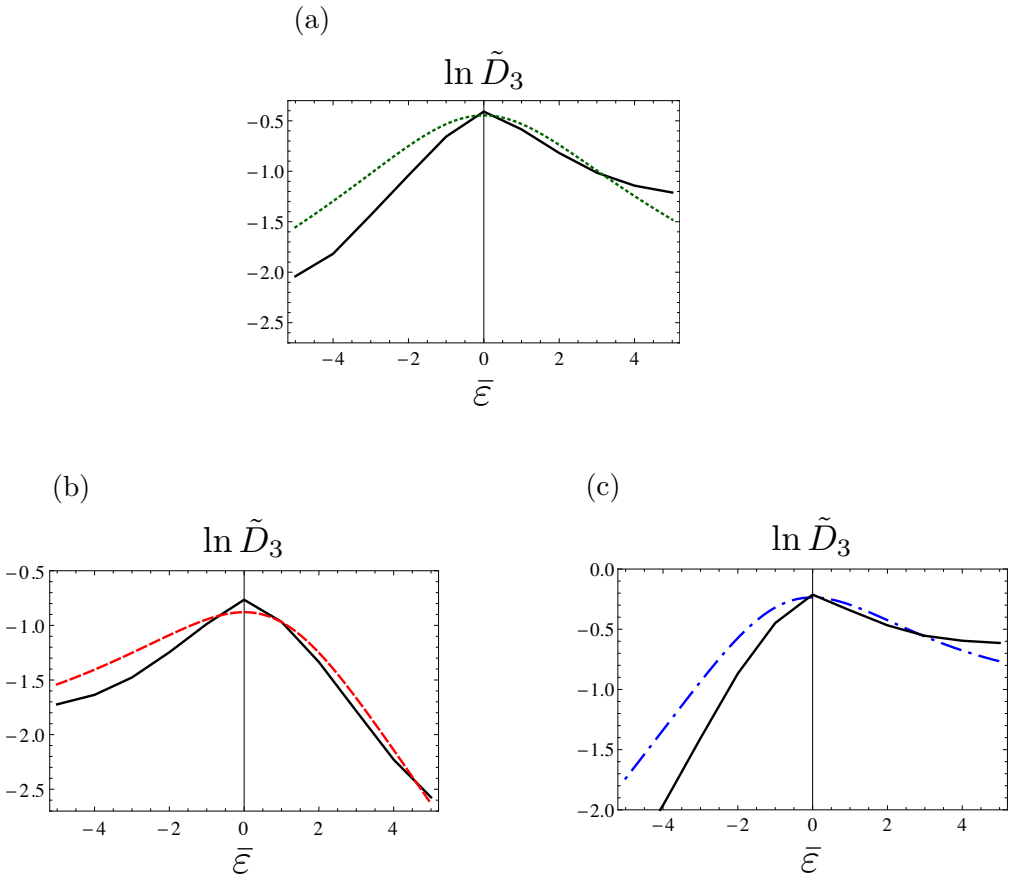

Figure 4.12.: Comparison between theory and simulation (black solid lines) Arrhenius plots at:
(a) $\phi_0 = 0.39$, $\phi_1 = 0.37$, $\phi_2 = 0.24$, ($\gamma = 0.513$, $\phi_1 \simeq \phi_0$);
(b) $\phi_0 = 0.18$, $\phi_1 = 0.43$, $\phi_2 = 0.39$, ($\gamma = 0.295$, $\phi_1 > \phi_0$);
(c) $\phi_0 = 0.59$, $\phi_1 = 0.27$, $\phi_2 = 0.14$, ($\gamma = 0.686$, $\phi_1 < \phi_0$).

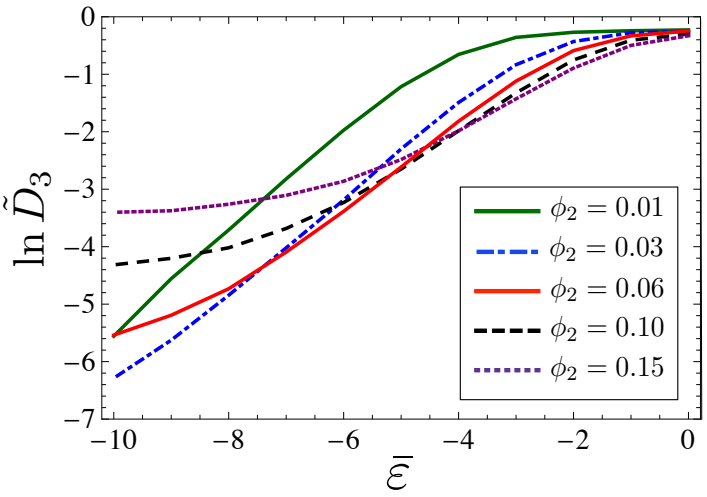

Figure 4.13.: Simulation graph: Arrhenius plots of the normalized diffusivity in the attractive case vs. $\bar{\varepsilon}$ for different segment concentrations.

5. Summary and conclusion

A simple model has been considered to analyze the interaction between a polymeric material and a gaseous substance. In our *gedankenexperiment* two main processes arise once these two systems are put in contact: a first sorption of gas molecules in the polymeric slab, and a consequent diffusion of the same sorbed molecules within the polymeric medium.

We adopted a model of penetrant molecules sorption in a polymeric medium based essentially on the same ideas as the dual mode model of sorption: the sorption is partly due to dissolution of the molecules in the polymer matrix and partly due to filling the preexisting holes. Applying basic thermodynamic principles we obtained a relation linking the penetrant concentration to the external pressure. The ensuing formula is however not of the dual mode kind. The solution (in the domain of pressures where the gas can be considered as ideal) is given by a transcendental equation similar in form to the one obtained in the Gas-Polymer matrix model of Sefcik and Raucher, in spite of the fact that none of the hypothesis specifying the matrix model has been assumed. The corresponding sorption isotherms is represented by a Lambert W-function, and corresponding two-parametric fits show an excellent agreement with the experimental data typically fitted within the dual sorption mode model; our fits are not inferior to the corresponding three-parametric fits. The Lambert-like isotherms appear universally at low and moderate pressures and originate from the assumption that the internal energy in a polymer-penetrant-void ternary mixture is (in the lowest order) a bilinear form in the concentrations of the three components. This analysis is shown in chapter 3.

We then started to analyze the diffusive properties of this population of gas particles that entered the polymeric medium.
We started with a general remark considering the possible sources of anomalous diffusion and which kind of anomalous diffusion may occur in such a system. We found out that for dimensions larger than 1, no superdiffusion could be ever observed while the process may go subdiffusive either due to the energetic disorder, making the mean Boltzmann factor diverge, or to topological disorder as for example in finitely ramified fractals. These statements have been derived in the scenario of the equivalence between diffusive and conductive phenomena, where the Effective Medium Approximation has been extensively used. These results are derived in the first section of chapter 4.
Finally, we considered a lattice model to obtain an expression for the diffusion con-

stant taking into account the interaction between polymers and diffusing particles which can be both attractive or repulsive. The diffusivity has been analyzed from different perspectives both analytically, using a modified effective medium approximation, and numerically by performing direct Monte Carlo simulations. While the diffusivity is only slightly affected by the chain's length, its temperature dependence crucially depends on the kind of interaction. This behavior depends on the sign of the interaction energy and is related to the existence of a percolating cluster of interaction sites surrounding polymer segments and/or a percolating cluster of voids on which particles are free to travel without activation. This is shown in the second section of chapter 4.

A. Appendix

Just to complete the overview presented in the introduction on the analysis of diffusion problems and Brownian Motion, we reserve the following sections to illustrate some of the most important moments that signed the history and the development of this extraordinarily rich field.
Moreover, we will show the steps of a procedure that maps the Fokker-Planck equation form a continuous space to a discrete one, being this strictly related to the master equation used to obtain the results of section 4. We give at last the details of the Hashin-Shtrikman expressions demonstrating that these effectively provide two bounding limits.

A.1. Smoluchowsky Equation

In the same period when Einstein was working on Brownian motion, the Polish physicist Marian Smoluchowski was developing an alternative description of the same physical phenomenon, arriving to a different but equivalent representation of the Brownian Motion.
Calculations start from adding an external potential contribution $U(x)$ to the second Fick´s law, contribution which is directly related to a force through a gradient term

$$F = -\frac{\partial U}{\partial x} \tag{A.1}$$

Being F applied to each diffusing particle, it causes a drift velocity v to appear, that in the limit of a weak force can be taken to be linearly dependent on F

$$v = \nu F = -\nu \frac{\partial U}{\partial x} \tag{A.2}$$

The proportionality factor ν is defined as the mobility constant and its inverse

$$\zeta = \frac{1}{\nu} \tag{A.3}$$

is the friction constant already encountered during the exposure of the Einstein relation. The drift velocity v has therefore to be added to the first Fick's law giving rise to a second flux term Cv where C is the concentration

$$J = -D\frac{\partial C}{\partial x} + Cv = -D\frac{\partial C}{\partial x} - C\nu\frac{\partial U}{\partial x} \tag{A.4}$$

An equilibrium situation is reached when the flux is stopped and J vanishes

$$D\frac{\partial C}{\partial x} = -C\nu\frac{\partial U}{\partial x} \tag{A.5}$$

Assuming a Boltzmann distribution for the concentration at equilibrium

$$C(x) \simeq \exp\left[-U(x)/K_BT\right] \tag{A.6}$$

the Einstein relation for the diffusion coefficient is obtained by solving equation (A.5)

$$D = \nu K_BT = \frac{K_BT}{\zeta} \tag{A.7}$$

Doing a step back and putting together equations (A.4) and (A.7) we can rewrite the formula for the flux J

$$J = -\nu\Big(K_BT\frac{\partial C}{\partial x} + C\frac{\partial U}{\partial x}\Big) \tag{A.8}$$

and the diffusion equation gets slightly changed in shape, giving raise to the relation that has been denoted since then on as the Smoluchowski equation

$$\frac{\partial C}{\partial t} = \frac{\partial}{\partial x}\nu\Big(K_BT\frac{\partial C}{\partial x} + C\frac{\partial U}{\partial x}\Big). \tag{A.9}$$

The Smoluchowski equation can be obtained in a different way where its thermodynamic content is clearly revealed. Let us reformulate the flux J of equation (A.8) extracting the two x-derivatives

$$J = -\nu C\frac{\partial}{\partial x}\Big(K_BT\ln C + U\Big) \tag{A.10}$$

The quantity in round brackets is the expression of the chemical potential of a set of noninteracting particles having concentration C, and the last equation states a proportionality between the flux and the spatial gradient of the chemical potential. It is possible

therefore to define a flux velocity v_f as

$$v_f = J/C = -\nu \frac{\partial}{\partial x}\Big(K_B T \ln C + U\Big) \tag{A.11}$$

which generalizes previous equation (A.2) by replacing the external potential with the chemical potential. If we now apply the usual continuity equation

$$\frac{\partial C}{\partial t} = -\frac{\partial J}{\partial x} = -\frac{\partial C v_f}{\partial x} \tag{A.12}$$

equation (A.9) is easily obtained by direct substitution. Therefore, the Smoluchowski equation results in a generalization of the Fick's law, where the equilibrium state is defined by the homogeneity of the chemical potential in place of the particle concentration.

The concentration C in the Smoluchowski approach can be easily replaced by a probability distribution $P(x,t)$ defining the probability for a particle to stay at place x at time t, being the two functions simply related by a constant normalization factor in the case of non interacting particles. This replacement then, allows for an increase in the application domain of the Smoluchowski equation that becomes a more general tool for describing the fluctuations of thermodynamic quantities. Therefore let us consider

$$\begin{aligned} \frac{\partial P}{\partial t} &= \frac{\partial}{\partial x}\nu\Big(K_B T \frac{\partial P}{\partial x} + P\frac{\partial U}{\partial x}\Big) \\ &= D\frac{\partial^2 P}{\partial x^2} + \nu\frac{\partial}{\partial x}\Big(\frac{\partial U}{\partial x}P\Big) \end{aligned} \tag{A.13}$$

and let us for a moment expand our dimensional space and consider $x_1, x_2, ..., x_n = X$ as the set of the n degrees of freedom of the system. The Smoluchowski equation is obtained by considering the relation between the average velocity v_n and the external force $F_n = -\partial U/\partial x_n$ generally taken as

$$v_n = \sum_m L_{nm}(X) F_m \tag{A.14}$$

where the sum runs obviously along the number of degrees and the coefficients L_{nm} are the n, m elements of the mobility matrix L. It is possible to demonstrate that L is symmetric and positive definite

$$L_{nm} = L_{mn} \qquad \sum_{n,m} L_{nm}(X) F_m F_n \geq 0 \tag{A.15}$$

Defining the flux velocity as

$$v_{fn} = \sum_m L_{nm}(X) \frac{\partial}{\partial x_m} \Big(K_B T \ln P + U \Big) \tag{A.16}$$

and considering the usual continuity equation

$$\frac{\partial P}{\partial t} = - \sum_n \frac{\partial}{\partial x_n} \Big(v_{fn} P \Big) \tag{A.17}$$

the Smoluchowski equation reads

$$\frac{\partial P}{\partial t} = \sum_{n,m} \frac{\partial}{\partial x_n} L_{nm} \Big(K_B T \frac{\partial P}{\partial x_m} + P \frac{\partial U}{\partial x_m} \Big). \tag{A.18}$$

The previous reasoning allows to demonstrate a crucial property of the Smoluchowski equation. In the case of a potential not depending on time and when there is a zero flux at the boundary of the system, a solution P of the equation always converges at equilibrium to the function P_{eq}

$$P_{eq}(x) = \frac{e^{-U(x)/K_B T}}{\int dx e^{-U(x)/K_B T}} \tag{A.19}$$

Let us start from the functional

$$A[\Psi] = \int d\{x\} \Psi (K_B T \ln \Psi + U) \tag{A.20}$$

whose argument is a general solution of the Smoluchowski equation, and consider its time derivative

$$\frac{d}{dt} A[\Psi] = \int d\{x\} \Big[\frac{\partial \Psi}{\partial t} (K_B T \ln \Psi + U) + K_B T \frac{\partial \Psi}{\partial t} \Big] \tag{A.21}$$

Integrating by parts with the help of equation (A.18) and considering the boundary assumptions, we have

$$\frac{d}{dt} A[\Psi] = - \int d\{x\} \Psi \sum_{n,m} L_{nm} \Big[K_B T \frac{\partial \Psi}{\partial x_n} \ln \Big(\frac{\Psi}{\Psi_{eq}} \Big) \Big] \Big[K_B T \frac{\partial \Psi}{\partial x_m} \ln \Big(\frac{\Psi}{\Psi_{eq}} \Big) \Big] \tag{A.22}$$

Last expression is non positive definite being always negative except for the equilibrium case when the $\Psi = \Psi_{eq}$ condition makes it vanish and poses A to its minimum. Therefore the functional always decreases until its minimum is reached where $\Psi = \Psi_{eq}$. At equilibrium, A results to be the free energy of the system

$$A[\Psi_{eq}] = -K_B T \ln \Big[\int d\{x\} \exp \Big(-U/K_B T \Big) \Big] \tag{A.23}$$

A.2. The Langevin equation

The perspective adopted to describe a Brownian motion is usually a collective one. The system is taken as a whole and calculations are considered for global functions as concentration, flux, potential and chemical potential.
Another approach is possible if the attention is focused on one single Brownian particle, taken as representative of all the others, and its equation of motion is considered. The randomness of the process is entirely represented by a time dependent stochastic term $f(t)$ added to the usual deterministic external force term $-\partial U/\partial x$,

$$\zeta \frac{dx}{dt} = -\frac{\partial U}{\partial x} + f(t) \tag{A.24}$$

$f(t)$ represents therefore a random force, describing the continuous collisions of the particle with the surrounding molecules giving raise to the unpredictable trajectories of the Brownian motion. This kind of approach has been introduced in 1908 by the French physicist Paul Langevin and previous equation (A.24) representing its mathematical translation is known as the Langevin equation.
The model is strongly characterized by the nature of the distribution $\Psi[f(t)]$ followed by the random force and by the values of tis moments. The most usual and reasonable step to take is to assume the distribution to be Gaussian

$$\Psi[f(t)] \propto \exp \Big(-\frac{1}{4\zeta K_B T} \int dt f^2(t) \Big) \tag{A.25}$$

and the first two moments of $f(t)$ to be as follows

$$\langle f(t) \rangle = 0 \qquad \langle f(t) f(t') \rangle = 2\zeta K_B T \delta(t - t'). \tag{A.26}$$

The solution for the displacement ξ of the x-position in the limit of a small time interval Δt, can be easily obtained by direct integration.

$$\xi(t) = V(x)\Delta t + \frac{1}{\zeta} \int_t^{t+\Delta t} dt' f(t') \tag{A.27}$$

where the velocity term

$$V(x) = \frac{1}{\zeta}\frac{\partial U}{\partial t} \tag{A.28}$$

has been supposed to be constant on the scale of the small displacement ξ. With the assumptions made on the $f(t)$ term, the displacement results in a sum of Gaussian terms and therefore a Gaussian variable it self with moments

$$\langle \xi(t) \rangle = V(x)\Delta t \tag{A.29}$$

and

$$\begin{aligned}
\langle (\xi - \langle \xi(t) \rangle)^2 \rangle &= \Big\langle \Big(\frac{1}{\zeta} \int_t^{t+\Delta t} dt' f(t') \Big) \cdot \Big(\frac{1}{\zeta} \int_t^{t+\Delta t} dt'' f(t'') \Big) \Big\rangle = \\
&= \frac{1}{\zeta^2} \int_t^{t+\Delta t} dt' \int_t^{t+\Delta t} dt'' \langle f(t') \cdot f(t'') \rangle = \\
&= \frac{2K_B T}{\zeta} \int_t^{t+\Delta t} dt' \int_t^{t+\Delta t} dt'' \delta(t' - t'') = \\
&= \frac{2K_B T}{\zeta} \Delta t \\
&= 2D\Delta t
\end{aligned} \tag{A.30}$$

The distribution of the displacement is

$$\Phi(\xi, \Delta t; x) = \frac{1}{\sqrt{4\pi D \Delta t}} \exp\Big(- \frac{(\xi - V(x)\Delta t)^2}{4D\Delta t} \Big). \tag{A.31}$$

Therefore, the probability $\Psi(x,t)$ for a particle to stay at position x at time t is given by the probability to stay at position x' at a certain previous moment t' times the probability to travel exactly the distance $x - x'$ in the time interval $t - t'$ and summed up over all the possible positions and moments

$$\begin{aligned}
\Psi(x, t + \Delta t) &= \int d\xi \int dx' \delta(x - x' - \xi) \Phi(\xi, \Delta t; x') \Psi(x - xi, t) \\
&= \frac{1}{\sqrt{4\pi D \Delta t}} \int d\xi \exp\Big(- \frac{(\xi - V(x)\Delta t)^2}{4D\Delta t} \Big) \Psi(x - \xi, t)
\end{aligned} \tag{A.32}$$

Being the function strongly centered around the null displacement, it is reasonable to expand the integrand function around $\xi = 0$. At the first order in Δt and relaxing the notation this gives

$$\Psi(x, t + \Delta t) = \Big(1 - \frac{dV}{dx}\Delta t \Big) \Psi - V \frac{\partial \Psi}{\partial x} \Delta t + D \frac{\partial^2 \Psi}{\partial x^2} \Delta t. \tag{A.33}$$

If we collect together the terms coupled to the time interval Δt, we obtain the Smoluchowski equation (A.13)

$$\begin{aligned} \frac{\partial \Psi}{\partial t} &= -\frac{\partial}{\partial x}\Big(V(x)\Psi(x,t)\Big) + D\frac{\partial^2 \Psi}{\partial x^2} \\ &= D\frac{\partial^2 \Psi}{\partial x^2} + \frac{1}{\zeta}\frac{\partial}{\partial x}\Big(\frac{\partial U}{\partial x}\Psi\Big) \end{aligned} \tag{A.34}$$

It may be interesting to consider a slightly different situation. So far the friction term ζ has been assumed to be a constant, but the last analysis can be easily generalized to the case when this is depending on the position. This is reflecting those systems where the diffusion constant is space dependent.
Let us start for the moment from the non dependent case and rescale friction and random force terms, and reformulate the original equation of motion (A.24) as follows

$$\frac{dx}{dt} = V(x) + \sigma g(t) \tag{A.35}$$

where

$$\sigma = \Big(\frac{K_B T}{\zeta}\Big)^{1/2} = D^{1/2} \tag{A.36}$$

and $g(t)$ is another random variable properly introduced to correctly rescale the random force and whose moments are

$$\langle g(t)\rangle = 0 \qquad \langle g(t)g(t')\rangle = 2\delta(t-t'). \tag{A.37}$$

When one introduces the space dependency of the diffusion constant the equation of motion has to be modified with the addition of a new term

$$\frac{dx}{dt} = V(x) + \sigma(x)g(t) + \sigma(x)\frac{d\sigma}{dx} \tag{A.38}$$

Dividing both sides by σ we obtain the Langevin equation of motion of a new variable coupling the x coordinate to the rescaled friction. Writing therefore

$$\frac{1}{\sigma(x)}\frac{dx}{dt} = V(x) + \frac{d\sigma}{dx} + g(t) \tag{A.39}$$

we obtain

$$\frac{dX}{dt} = \hat{V}(X) + g(t) \tag{A.40}$$

where we have defined

$$X(t) = \int^{x(t)} \frac{dx'}{\sigma(x')} \qquad \text{and} \qquad \hat{V} = V + \frac{d\sigma}{dx} \tag{A.41}$$

that can be solved in the same way we have solved the D-constant case and giving therefore the following differential equation governing the probability distribution for the variable X

$$\frac{\partial \hat{\Psi}(X)}{\partial t} = \frac{\partial}{\partial X}\Big(\frac{\partial \hat{\Psi}}{\partial X} - \hat{V}\hat{\Psi}\Big) \tag{A.42}$$

According to the definition of X it follows that

$$\hat{\Psi}(X,t) = \sigma(x)\Psi(x,t) \tag{A.43}$$

and

$$\frac{\partial}{\partial X} = \sigma(x)\frac{\partial}{\partial x} \tag{A.44}$$

It is therefore possible to demonstrate that the probability of the x-coordinate satisfies

$$\frac{\partial \Psi}{\partial t} = \frac{\partial}{\partial x}\Big(\sigma^2 \frac{\partial \Psi}{\partial x} - V\Psi\Big) = \frac{\partial}{\partial x}\frac{1}{\zeta}\Big(K_B T \frac{\partial \Psi}{\partial x} + \frac{\partial U}{\partial x}\Psi\Big) \tag{A.45}$$

A.3. Einstein relation from the Fluctuation Dissipation theorem

As stated before, the Einstein relation can be obtained as a particular case of the Fluctuation Dissipation Theorem. This theorem states a general relationship between the response of a given system to an external disturbance and the internal fluctuation of the system in the absence of the disturbance. Such a response is characterized by a response function while the internal fluctuation is characterized by a correlation function of relevant physical quantities of the system fluctuating in thermal equilibrium.

A.3.1. Time correlation function

Let us consider a Brownian particle and let us measure the value of a physical quantity $A(t)$ at time t. The time autocorrelation function is defined as the average value calculated over many equilibrium samples of the product between two values of A taken at different times, even if usually one of them is taken at $t = 0$ and the function becomes a simple function of t. Hence

$$C_{AA}(t) = \langle A(t)A(0)\rangle \tag{A.46}$$

Normally C_{AA} displays an exponentially decaying behavior, with a typical decay time denoted as correlation time, and converges to the product of the averages

$$\langle A(t)\rangle\langle A(0)\rangle = \langle A\rangle^2. \tag{A.47}$$

Th physical content of the difference between C_{AA} and its asymptote $\langle A\rangle^2$, is the influence of the value of A at time zero on the value of A at time t, in other words it gives an idea of the typical memory of the system relative to the A quantity
It is also possible to define a correlation function between different quantities, what is called a crosscorrelation function, where the value of A at time t is coupled to the beginning value of a second quantity B

$$C_{AB}(t) = \langle A(t)B(0)\rangle \tag{A.48}$$

In what follows we won´t make any difference between auto or cross correlation functions and simply talk about correlation functions.

Let us consider now a multidimensional system and let us denote for the moment as x the whole set of coordinates $x_1, x_2, ..., x_n$. The probability $G(x, x', t)$ for the system to be in state x at time t being started at state x' at time zero, evolves according to the Smoluchowski equation

$$\frac{\partial G}{\partial t} = \sum_{n,m} \frac{\partial}{\partial x_n} L_{nm}\Big(K_B T \frac{\partial G}{\partial x_m} + G\frac{\partial U}{\partial x_m}\Big). \tag{A.49}$$

with the initial condition given by

$$G(x, x', 0) = \delta(x - x') \tag{A.50}$$

It is not that easy to find an explicit expression of the Green function G, but it is nonetheless possible to obtain in this context some expressions revealing important aspects of the system. To keep the formalism coherent and correct, it is important to distinguish now for any physical quantity A the dependence on the state coordinates that we will denote as $\tilde{A}(x)$ from the value the quantity takes at time t and that will be simply written as $A(t)$. That specification made, the correlation function reads

$$\begin{aligned} C_{AB}(t) &= \langle A(t)B(0)\rangle \\ &= \int dx \int dx' \tilde{A}(x)\tilde{B}(x')G(x, x', t)\Psi_{eq}(x') \end{aligned} \tag{A.51}$$

where the product $G \cdot \Psi_{eq}$ gives the probability for the system to be evolved from state x' to state x in a time interval going form 0 to t, remaining at equilibrium.

A useful quantity is given by the initial slope of the correlation function. The time derivative is evaluated as

$$\begin{aligned}\frac{d}{dt}C_{AB}(t) &= \frac{d}{dt}\langle A(t)B(0)\rangle \\ &= \int dx \int dx' \tilde{A}(x)\tilde{B}(x')\frac{\partial G}{\partial t}\Psi_{eq}(x') \\ = \int dx \int dx' \tilde{A}(x)\tilde{B}(x')\sum_{n,m}\frac{\partial}{\partial x_n}L_{nm}\Big(K_BT\frac{\partial G}{\partial x_m} + G\frac{\partial U}{\partial x_m}\Big)\Psi_{eq}(x')\Big) \qquad \text{(A.52)}\end{aligned}$$

At time $t = 0$ the Green function reduces to the delta $\delta(x - x')$ and this gives

$$\begin{aligned}\frac{d}{dt}C_{AB}(t)\Big|_{t=0} &= \frac{d}{dt}\langle A(t)B(0)\rangle\Big|_{t=0} \\ = \int dx\tilde{A}(x)\sum_{n,m}\frac{\partial}{\partial x_n}L_{nm}\Big[K_BT\frac{\partial}{\partial x_m}\Big(\tilde{B}(x)\Psi_{eq}(x)\Big) + \tilde{B}(x)\Psi_{eq}(x)\frac{\partial U}{\partial x_m}\Big]\end{aligned}$$

Integrating by parts and using the Boltzmann expression of the equilibrium distribution Ψ_{eq}, we have

$$\begin{aligned}\frac{d}{dt}C_{AB}(t)\Big|_{t=0} &= \frac{d}{dt}\langle A(t)B(0)\rangle\Big|_{t=0} \\ &= -K_BT\int dx\sum_{n,m}\Psi_{eq}(x)\frac{\partial\tilde{A}(x)}{\partial x_n}L_{nm}\frac{\partial\tilde{B}(x)}{\partial x_m} \\ &= -K_BT\sum_{n,m}\Big\langle\frac{\partial\tilde{A}(x)}{\partial x_n}L_{nm}\frac{\partial\tilde{B}(x)}{\partial x_m}\Big\rangle \qquad \text{(A.53)}\end{aligned}$$

Last expression is used to calculate te initial decay rate Γ_0 as

$$\begin{aligned}\Gamma_0 &= -\frac{\frac{d}{dt}\langle A(t)B(0)\rangle|_{t=0}}{\langle AB\rangle - \langle A\rangle\langle B\rangle} \\ &= \frac{K_BT}{\langle AB\rangle - \langle A\rangle\langle B\rangle}\sum_{n,m}\Big\langle\frac{\partial\tilde{A}(x)}{\partial x_n}L_{nm}\frac{\partial\tilde{B}(x)}{\partial x_m}\Big\rangle \qquad \text{(A.54)}\end{aligned}$$

A.3.2. Fluctuation Dissipation Theorem

An external field $h(t)$ is applied at time $t = 0$ to a system supposed to be at equilibrium until that moment. The average value of a physical quantity $A(t)$ responds to the perturbation given by $h(t)$ and if the field is weak enough, its change can be given by

the following expression

$$\langle A(t)\rangle_h - \langle A\rangle_0 = \int_{-\infty}^{t} dt' \mu(t-t')h(t') \tag{A.55}$$

where $\langle A(t)\rangle_h$ denotes the average of the A quantity on presence of the field and $\langle A\rangle_0$ the average before the filed was switched off. The function $\mu(t)$ is called the response function and the Fluctuation Dissipation Theorem shows that it is equal to

$$\mu(t) = -\frac{1}{K_B T}\frac{d}{dt}C_{AB}(t) \tag{A.56}$$

where the second physical quantity $B(x)$ represents a conjugate variable to the field h building the potential energy term

$$U_h(x,t) = -h(t)B(x) \tag{A.57}$$

For the sake of simplicity we assume the external field to be a step function, being zero until $t = 0$ and switched suddenly on to a constant value h for positive times.
In this case we have for a general physical quantity A

$$\langle A(t)\rangle_h - \langle A\rangle_0 = \int_{-\infty}^{t} dt' \mu(t-t')h(t') = h\int_{0}^{t} dt' \mu(t') = h\beta(t) \tag{A.58}$$

where we have introduced the function

$$\beta(t) = \int_{0}^{t} dt' \mu(t') \tag{A.59}$$

Considering the $A = B$ case and A as the x-coordinate of a particle performing a Brownian Motion, the Fluctuation Dissipation Theorem allows to solve last integral as

$$\begin{aligned}
\beta(t) &= -\frac{1}{K_B T}\Big(C_{xx}(t) - C_x(0)\Big) \\
&= \frac{1}{2K_B T}\Big(\langle x^2(t)\rangle + \langle x^2(0)\rangle - 2\langle x(t)x(0)\rangle\Big) \\
&= \frac{1}{2K_B T}\langle (x(t)-x(0))^2\rangle
\end{aligned} \tag{A.60}$$

On the other hand, when the field is applied, the particle starts to move with the constant velocity $v = F/\zeta$ and this makes the function $\beta(t)$ to be equal to t/ζ.

Hence, setting things together, we have

$$\frac{t}{\zeta} = \frac{1}{2K_BT}\langle (x(t) - x(0))^2 \rangle \tag{A.61}$$

The Einstein relation is recovered if we consider the diffusion constant to be defined as

$$2Dt = \langle (x(t) - x(0))^2 \rangle \tag{A.62}$$

and as a consequence

$$D = \frac{K_BT}{\zeta} \tag{A.63}$$

A.4. Discretization of a continuous Fokker-Planck equation with random potential

We show in this section the discretization procedure linking the Fokker-Planck equation to the master equation. The equation in a continuous d-dimensional space is discretized using a regular hypercubic lattice with lattice constant a considered sufficiently small. The sites are identified by the vectors $\mathbf{i}$, the site energies $E_{\mathbf{i}}$ are given by corresponding values of the random potential $U(\mathbf{x})$ at the position of site $\mathbf{i}$, $\mathbf{x} = \mathbf{i} = (i_1, ..., i_d) = a(n_1, ..., n_d)$ where n_k is an integer number and k runs from 1 to d . Correspondingly, the derivatives ∂_k along a certain direction k are linked to the forward differences Δ_k in the following way:

$$\begin{aligned} \partial_k p(\mathbf{x}) &\rightarrow \frac{1}{a}\Delta_k p_{\mathbf{i}} = \frac{1}{a}[p_{\mathbf{i}+a\hat{k}} - p_{\mathbf{i}}] \\ \partial_k^2 p(\mathbf{x}) &\rightarrow \frac{1}{a^2}\Delta_k^2 p_{\mathbf{i}} = \frac{1}{a^2}[p_{\mathbf{i}+a\hat{k}} - 2p_{\mathbf{i}} + p_{\mathbf{i}-a\hat{k}}] \end{aligned} \tag{A.64}$$

where $\hat{k}$ is the unit vector in the k-th direction. Hence, from

$$\begin{aligned} \dot{p}(\mathbf{x}) &= D\nabla^2 p(\mathbf{x}) + D\beta\nabla[\nabla U(\mathbf{x}) \cdot p(\mathbf{x})] = \\ &= D\sum_{k=1}^{d}\Big[\partial_k^2 p(\mathbf{x}) + \beta\partial_k[\partial_k U(\mathbf{x}) \cdot p(\mathbf{x})]\Big] \end{aligned}$$

follows

$$\begin{aligned} \dot{p}_{\mathbf{i}} &= D\sum_{k=1}^{d}\Big[\frac{1}{a^2}[p_{\mathbf{i}+a\hat{k}} - 2p_{\mathbf{i}} + p_{\mathbf{i}-a\hat{k}}] + \\ &\quad + \frac{\beta}{a}\partial_k\Big((E_{\mathbf{i}+a\hat{k}} - E_{\mathbf{i}})p_{\mathbf{i}}\Big)\Big] \end{aligned} \tag{A.65}$$

We consider the potential to be a slowly varying function of the position; this allows to substitute the remaining partial derivative with half of a double step forward difference, the consequent error being of the smaller order of magnitude $\Delta_k^2 E$.

$$\begin{aligned}\dot{p}_{\mathbf{i}} &= \frac{D}{a^2}\sum_{k=1}^{d}\Big[[p_{\mathbf{i}+a\hat{k}} - 2p_{\mathbf{i}} + p_{\mathbf{i}-a\hat{k}}] + \\ &+\frac{\beta}{2}\Big((E_{\mathbf{i}+2a\hat{k}} - E_{\mathbf{i}+a\hat{k}})p_{\mathbf{i}+a\hat{k}} - (E_{\mathbf{i}} - E_{\mathbf{i}-a\hat{k}})p_{\mathbf{i}-a\hat{k}}\Big)\Big]\end{aligned} \tag{A.66}$$

Neglecting again second order terms, we replace the quantity $(E_{\mathbf{i}+2a\hat{k}} - E_{\mathbf{i}+a\hat{k}})$ with $(E_{\mathbf{i}+a\hat{k}} - E_{\mathbf{i}})$, and add and subtract the term $(E_{\mathbf{i}+a\hat{k}} - E_{\mathbf{i}})p_{\mathbf{i}}$

$$\begin{aligned}\dot{p}_{\mathbf{i}} &= \frac{D}{a^2}\sum_{k=1}^{d}\Big[[p_{\mathbf{i}+a\hat{k}} - 2p_{\mathbf{i}} + p_{\mathbf{i}-a\hat{k}}] + \\ &+\frac{\beta}{2}\Big((E_{\mathbf{i}+a\hat{k}} - E_{\mathbf{i}})p_{\mathbf{i}+a\hat{k}} - (E_{\mathbf{i}} - E_{\mathbf{i}-a\hat{k}})p_{\mathbf{i}-a\hat{k}} + \\ &+(E_{\mathbf{i}+a\hat{k}} - E_{\mathbf{i}})p_{\mathbf{i}} - (E_{\mathbf{i}+a\hat{k}} - E_{\mathbf{i}})p_{\mathbf{i}}\Big)\Big] =\end{aligned} \tag{A.67}$$

$$\begin{aligned}&= \frac{D}{a^2}\sum_{k=1}^{d}\Big[[p_{\mathbf{i}+a\hat{k}} - 2p_{\mathbf{i}} + p_{\mathbf{i}-a\hat{k}}] + \\ &+\frac{\beta}{2}\Big((E_{\mathbf{i}+a\hat{k}} - E_{\mathbf{i}})p_{\mathbf{i}+a\hat{k}} - (E_{\mathbf{i}} - E_{\mathbf{i}-a\hat{k}})p_{\mathbf{i}-a\hat{k}} + \\ &+(E_{\mathbf{i}+a\hat{k}} - E_{\mathbf{i}})p_{\mathbf{i}} + (E_{\mathbf{i}-a\hat{k}} - E_{\mathbf{i}})p_{\mathbf{i}}\Big)\Big] =\end{aligned} \tag{A.68}$$

$$\begin{aligned}&= \frac{D}{a^2}\sum_{k=1}^{d}\Big[[p_{\mathbf{i}+a\hat{k}}\Big(1 - \frac{\beta}{2}(E_{\mathbf{i}} - E_{\mathbf{i}+a\hat{k}})\Big) + \\ &+p_{\mathbf{i}-a\hat{k}}\Big(1 - \frac{\beta}{2}(E_{\mathbf{i}} - E_{\mathbf{i}-a\hat{k}})\Big) + \\ &-p_{\mathbf{i}}\Big(2 - \frac{\beta}{2}(E_{\mathbf{i}+a\hat{k}} - E_{\mathbf{i}}) - \frac{\beta}{2}(E_{\mathbf{i}-a\hat{k}} - E_{\mathbf{i}})\Big)\Big]\end{aligned} \tag{A.69}$$

Since the difference between the energies at neighbouring sites is small, in the lowest nonvanishing order we can put

$$\begin{aligned}\dot{p}_{\mathbf{i}} &= \frac{D}{a^2}\sum_{k=1}^{d}\Big[[p_{\mathbf{i}+a\hat{k}}e^{-\frac{\beta}{2}(E_{\mathbf{i}} - E_{\mathbf{i}+a\hat{k}})} + \\ &+ p_{\mathbf{i}-a\hat{k}}e^{-\frac{\beta}{2}(E_{\mathbf{i}} - E_{\mathbf{i}-a\hat{k}})} + \\ &- p_{\mathbf{i}}\Big(e^{-\frac{\beta}{2}(E_{\mathbf{i}+a\hat{k}} - E_{\mathbf{i}})} + e^{-\frac{\beta}{2}(E_{\mathbf{i}-a\hat{k}} - E_{\mathbf{i}})}\Big)\Big]\end{aligned} \tag{A.70}$$

At this point, the discretized Fokker-Planck equation is shown to be equivalent to the master equation

$$\begin{aligned} \dot{p}_{\mathbf{i}} &= \sum_{k=1}^{d} \Big[w_{\mathbf{i},\mathbf{i}+a\hat{k}} p_{\mathbf{i}+a\hat{k}} + w_{\mathbf{i},\mathbf{i}-a\hat{k}} p_{\mathbf{i}-a\hat{k}} + \\ &- p_{\mathbf{i}} (w_{\mathbf{i}+a\hat{k},\mathbf{i}} + w_{\mathbf{i}-a\hat{k},\mathbf{i}}) \Big] \end{aligned} \tag{A.71}$$

by setting

$$w_{\mathbf{i},\mathbf{j}} = \frac{D}{a^2} e^{-\frac{\beta}{2}(E_{\mathbf{i}} - E_{\mathbf{j}})} = w_0 e^{-\frac{\beta}{2}(E_{\mathbf{i}} - E_{\mathbf{j}})}$$

implying that, up to constant factors

$$g_{\mathbf{i},\mathbf{j}} = w_{\mathbf{i},\mathbf{j}} e^{-\beta E_{\mathbf{j}}} = w_0 e^{-\frac{\beta}{2}(E_{\mathbf{i}} + E_{\mathbf{j}})}.$$

In what follows $\frac{\beta}{2}(E_{\mathbf{i}} + E_{\mathbf{j}})$ can be changed for $\beta U(\mathbf{x})$. Thus, returning to the continuous limit when calculating the macroscopic (effective medium) conductance of the continuous disordered medium we can take its local conductivity to be $g(\mathbf{x}) = g_0 \exp(-U(\mathbf{x})/kT)$ with $g_0 = D/a^2$.

A.5. Hashin - Shtrikman bounds on the effective diffusivity

In this section we show that it is possible to give stricter upper and lower bounds on the effective conductance g^* using the technique introduced by Z.Hashin and S.Shtrikman in Hashin and Shtrikman (1962). Thanks to equation 4.22 this limitation is then easily reflected on the effective diffusivity.
We will therefore focus our attention on the bond function g_{ij} considering two particular cases: one in which it can take only two values according to fixed probabilities, and one in which it is given by a random variable uniformly distributed in a finite interval.
Once calculated the effective conductance by the use of the Effective Medium Approximation, we proceed to formulate its Hashin-Shtrikman limits.

Binary case

We assume E_i to be a binary random variable

$$E_i = \begin{cases} E_a & \text{with probability} \quad p_1 = p \\ E_b & \text{with probability} \quad p_2 = 1 - p \end{cases} \tag{A.72}$$

with $E_a < E_b$. As a consequence, the local conductance g_{ij} is a binary variable as well

$$g_{ij} = \begin{cases} g_1 \propto g_0 e^{-\beta E_a} & \text{with probability} \quad p_1 = p \\ g_2 \propto g_0 e^{-\beta E_b} & \text{with probability} \quad p_2 = 1-p \end{cases} \tag{A.73}$$

or, equivalently, a random variable subject to the distribution

$$Q(g_{ij}) = p_1 \delta(g_{ij} - g_1) + p_2 \delta(g_{ij} - g_2) \tag{A.74}$$

and giving the following medium, arithmetic and geometric averages

$$\begin{aligned} \langle g \rangle_Q &= p_1 g_1 + p_2 g_2 \\ \langle g \rangle_A &= \frac{1}{2}(g_1 + g_2) \\ \langle g \rangle_G &= \sqrt{g_1 g_2} \end{aligned} \tag{A.75}$$

Obeying the Effective Medium Approximation guidelines, we find the effective conductance g^* through the use of the self-consistency condition

$$\Big\langle \frac{g^* - g}{(d-1)g^* + g} \Big\rangle_Q = 0 \tag{A.76}$$

resulting in

$$g^* = \frac{d\langle g \rangle_Q - 2\langle g \rangle_A}{2(d-1)} \left[1 + \sqrt{1 + \frac{4(d-1)\langle g \rangle_G^2}{[d\langle g \rangle_Q - 2\langle g \rangle_A]^2}} \right] \tag{A.77}$$

The percolating case is easily recovered in the limit $E_b \to +\infty$, $g_1 \to 0$, giving the wellknown results

$$g^* = \frac{dp_2 - 1}{d-1} g_2 \tag{A.78}$$

$$p_2^c = 1/d \tag{A.79}$$

while simple calculations can show that in the bidimensional symmetric case, $d = 2$, $p = 1/2$, g^* equals the geometric mean $\sqrt{g_1 g_2}$.

Equation (A.77) is finally used to calculate the effective medium diffusion constant

$$\begin{aligned} D^* &= \frac{a^2 g^*}{\langle \exp -\beta E_i \rangle} = \frac{a^2 g^*}{\langle g \rangle} \\ &= D \frac{d\langle g \rangle_Q - 2\langle g \rangle_A}{2(d-1)\langle g \rangle_Q} \left[1 + \sqrt{1 + \frac{4(d-1)\langle g \rangle_G^2}{[d\langle g \rangle_Q - 2\langle g \rangle_A]^2}} \right] \end{aligned} \tag{A.80}$$

Following the strategy outlined in (Hashin and Shtrikman, 1962), we now introduce a free parameter g_0 and define the function

$$B(g_0) = \left\langle \frac{g - g_0}{(d-1)g_0 + g} \right\rangle_Q \tag{A.81}$$

which allows to state

$$\begin{aligned} g^* &> g_0\Big(1 + \frac{dB(g_0)}{1 - B(g_0)}\Big) \quad \text{if} \quad g_0 < \min(g_{ij}) = g_1 \\ g^* &< g_0\Big(1 + \frac{dB(g_0)}{1 - B(g_0)}\Big) \quad \text{if} \quad g_0 > \max(g_{ij}) = g_2 \end{aligned}$$

Calling

$$g_1^* = g_1\Big(1 + \frac{dB(g_1)}{1 - B(g_1)}\Big) \tag{A.82}$$

$$g_2^* = g_2\Big(1 + \frac{dB(g_2)}{1 - B(g_2)}\Big) \tag{A.83}$$

it is then possible to write the following inequalities

$$g^* > g_1^* = g_1\Big[1 + \frac{d(1-p)(g_2 - g_1)}{dg_1 + p(g_2 - g_1)}\Big] \tag{A.84}$$

$$g^* < g_2^* = g_2\Big[1 - \frac{dp(g_2 - g_1)}{dg_2 - (1-p)(g_2 - g_1)}\Big] \tag{A.85}$$

and define

$$D_1^* = \frac{a^2 g_1^*}{\langle e^{-\beta E_i}\rangle} = D\frac{g_1}{\langle g\rangle}\Big[1 + \frac{d(1-p)(g_2 - g_1)}{dg_1 + p(g_2 - g_1)}\Big] \tag{A.86}$$

$$D_2^* = \frac{a^2 g_2^*}{\langle e^{-\beta E_i}\rangle} = D\frac{g_2}{\langle g\rangle}\Big[1 - \frac{dp(g_2 - g_1)}{dg_2 - (1-p)(g_2 - g_1)}\Big] \tag{A.87}$$

giving the bounds

$$D_1^* \leq D^* \leq D_2^* \tag{A.88}$$

Through a simple rescaling of the units fixing $D = g_1 = 1$ and substituting g_2 and g^* with their ratio with g_1, $g_2 \to x = g_2/g1$, $g^* \to \tilde{g}^* = g^*/g_1$, we reformulate last

expressions in order to have a better graphical view on the bounds

$$\tilde{D}^* = \frac{d[p+(1-p)x]-(x+1)}{2(d-1)[p+(1-p)x]}\left[1+\sqrt{1+\frac{4(d-1)x}{[d(p+(1-p)x)-(x+1)]^2}}\right] \quad (A.89)$$

$$\tilde{D}_1^* = \frac{1}{p+(1-p)x}\Big[1+\frac{d(1-p)(x-1)}{d+p(x-1)}\Big] \quad (A.90)$$

$$\tilde{D}_2^* = \frac{x}{p+(1-p)x}\Big[1-\frac{dp(x-1)}{dx-(1-p)(x-1)}\Big] \quad (A.91)$$

with

$$\tilde{D}_1^* \leq \tilde{D}^* \leq \tilde{D}_2^* \quad (A.92)$$

Uniform case

Let us now consider the case in which the possible values of the energy barriers E_{ij} are exponentially distributed in the interval $[E_a, E_b]$

$$P(E_i) = \frac{\beta\, e^{-\beta E_i}}{e^{-\beta E_a} - e^{-\beta E_b}} \quad (A.93)$$

Performing the change of variables, it is easy to show that the bond conductance is a random variable uniformly distributed in the interval

$$[\, g_1 = e^{-\beta E_b}\,,\; g_2 = e^{-\beta E_a}\,] \quad (A.94)$$

$$Q(g_{ij}) = \frac{1}{g_2 - g_1} \quad (A.95)$$

Eq.(A.76) then gives the following condition to be satisfied by the effective conductance

$$\Big[(d-1)g^* + g_2\Big]e^{-g_2/dg^*} = \Big[(d-1)g^* + g_1\Big]e^{-g_1/dg^*} \quad (A.96)$$

or by the effective diffusivity D^*

$$\Big[(d-1)\langle g\rangle D^* + g_2 D\Big]e^{-g_2 D/(d\langle g\rangle D^*)} = \Big[(d-1)\langle g\rangle D^* + g_1 D\Big]e^{-g_1 D/(d\langle g\rangle D^*)} \quad (A.97)$$

which can be rewritten through the previous rescaling as

$$\Big[(d-1)(x+1))\tilde{D}^* + 2x\Big]e^{-2x/(d(x+1)\tilde{D}^*} = \Big[(d-1)(x+1))\tilde{D}^* + 2\Big]e^{-2/(d(x+1)\tilde{D}^*} \quad (A.98)$$

We now consider again

$$B(g_0) = \langle \frac{g - g_0}{(d-1)g_0 + g} \rangle_Q \tag{A.99}$$

and the inequalities

$$\begin{aligned} g^* &> g_0\Big(1 + \frac{dB(g_0)}{1 - B(g_0)}\Big) \quad \text{if} \quad g_0 < \min(g_{ij}) = g_1 \\ g^* &< g_0\Big(1 + \frac{dB(g_0)}{1 - B(g_0)}\Big) \quad \text{if} \quad g_0 > \max(g_{ij}) = g_2 \end{aligned}$$

In this case we have

$$B(g_0) = 1 - \frac{dg_0}{g_2 - g_1} \ln\Big[\frac{(d-1)g_0 + g_2}{(d-1)g_0 + g_1}\Big] \tag{A.100}$$

and setting respectively $g_0 = g_1$ and $g_0 = g_2$, we can write

$$\begin{aligned} B(g_1) &= 1 - \frac{dg_1}{g_2 - g_1} \ln\Big[\frac{dg_1 + g_2 - g_1}{dg_1}\Big] \\ &= 1 - \frac{1}{y_1} \log\Big(1 + y_1\Big) \qquad \text{(A.101)} \\ B(g_2) &= 1 - \frac{dg_2}{g_2 - g_1} \ln\Big[\frac{dg_2}{dg_2 - g_2 + g_1}\Big] \\ &= 1 + \frac{1}{y_2} \log\Big(1 - y_2\Big) \qquad \text{(A.102)} \end{aligned}$$

where the couple of parameters

$$\begin{aligned} y_1 &= \frac{g_2 - g_1}{dg_1} \qquad \text{(A.103)} \\ y_2 &= \frac{g_2 - g_1}{dg_2} \qquad \text{(A.104)} \end{aligned}$$

has been introduced. At the end, the two bounds are given by

$$\begin{aligned} g^* &> g_1^* = g_1\Big[1 + d\Big(\frac{y_1}{\log(1 + y_1)} - 1\Big)\Big] \qquad \text{(A.105)} \\ g^* &< g_2^* = g_2\Big[1 - d\Big(\frac{y_2}{\log(1 - y_2)} + 1\Big)\Big] \qquad \text{(A.106)} \end{aligned}$$

from which we obtain

$$D_1^* = D\frac{g_1}{\langle g\rangle}\Big[1 + d\Big(\frac{y_1}{\log(1+y_1)} - 1\Big)\Big] \tag{A.107}$$

$$D_2^* = D\frac{g_2}{\langle g\rangle}\Big[1 - d\Big(\frac{y_2}{\log(1-y_2)} + 1\Big)\Big] \tag{A.108}$$

and the corresponding bonds

$$D_1^* \leq D^* \leq D_2^* \tag{A.109}$$

Fixing again $D = g_1 = 1$, $g_2 = x$, $g^* = \tilde{g}^* = g^*/g_1$, we can see that

$$\tilde{D}_1^* = \frac{2}{x+1}\Big[1 - d + \frac{x-1}{\log(1+\frac{x-1}{d})}\Big] \tag{A.110}$$

$$\tilde{D}_2^* = \frac{2x}{x+1}\Big[1 - d - \frac{x-1}{x\log(1-\frac{x-1}{dx})}\Big]x \tag{A.111}$$

with the usual

$$\tilde{D}_1^* \leq \tilde{D}^* \leq \tilde{D}_2^* \tag{A.112}$$

Acknowledgement

This work was produced in the framework of the “Zuverlaessigkeit von PV Modulen II" project and was financed by the Bundesministerium der Umwelt. I would like to thank all the project managers, all the people involved in the development of the project and all the people met during the several meetings.

I would like to express my sincere gratitude to Prof.Igor Sokolov for the continuous support on my Ph.D study and related research, for his patience, motivation. His guidance helped me in all the time of research and writing of this thesis.

I would like to thank first of all the person who has been the perfect mate of thousands of discussions around Physics and so many other topics, Hartmut Lentz.

I thank my family whose presence and example have always been supporting me.
At last i would like to thank Antonella for accompanying and inciting me with all the patience and strength of the world along each phase of my Ph.D.

A special thank to all the people this Ph.D gave me the enormous luck to know: Daniele, Eva, Fred, Rebecka, Cetin, Katia, Johannes, Burak, Steffi, all the guys of the THC Franziskaner, all the people at the Humboldt University, Vitaly, Galen and Pinar. Thank you so much to all of you for making those five years in Berlin that wonderful.

Bibliography

Barrer, R., Barrie, J., and Slater, J. (1958). Sorption and diffusion in ethyl cellulose. part iii. comparison between ethyl cellulose and rubber. *Journal of Polymer Science Part A: Polymer Chemistry*, 27(115):177–197.

Bawendi, M. and Freed, K. F. (1988). Systematic corrections to flory–huggins theory: Polymer–solvent–void systems and binary blend–void systems. *The Journal of Chemical Physics*, 88(4):2741–2756.

Bawendi, M., Freed, K. F., and Mohanty, U. (1986). A lattice model for self-avoiding polymers with controlled length distributions. ii. corrections to flory–huggins mean field. *The Journal of Chemical Physics*, 84(12):7036–7047.

Bernardes, N. (1958). Theory of solid ne, a, kr, and xe at 0 k. *Physical review*, 112(5):1534.

Bouchaud, J.-P. and Georges, A. (1990a). Anomalous diffusion in disordered media: statistical mechanisms, models and physical applications. *Physics reports*, 195(4-5):127–293.

Bouchaud, J.-P. and Georges, A. (1990b). Anomalous diffusion in disordered media: statistical mechanisms, models and physical applications. *Physics reports*, 195(4-5):127–293.

Bruggeman, V. D. (1935). Berechnung verschiedener physikalischer konstanten von heterogenen substanzen. i. dielektrizitätskonstanten und leitfähigkeiten der mischkörper aus isotropen substanzen. *Annalen der physik*, 416(7):636–664.

Camboni, F. and Sokolov, I. M. (2012). Normal and anomalous diffusion in random potential landscapes. *Physical Review E*, 85(5):050104.

Chayes, J. and Chayes, L. (1986). Bulk transport properties and exponent inequalities for random resistor and flow networks. *Communications in mathematical physics*, 105(1):133–152.

Chiou, J. and Paul, D. R. (1986). Sorption and transport of co2 in pvf2/pmma blends. *Journal of applied polymer science*, 32(1):2897–2918.

De Angelis, M. G. and Sarti, G. C. (2011). Solubility of gases and liquids in glassy polymers. *Annual review of chemical and biomolecular engineering*, 2:97–120.

Dean, D., Drummond, I., and Horgan, R. (2007). Effective transport properties for diffusion in random media. *Journal of Statistical Mechanics: Theory and Experiment*, 2007(07):P07013.

Doghieri, F., De Angelis, M. G., Baschetti, M. G., and Sarti, G. C. (2006). Solubility of gases and vapors in glassy polymers modelled through non-equilibrium phsc theory. *Fluid phase equilibria*, 241(1):300–307.

Doghieri, F. and Sarti, G. C. (1996). Nonequilibrium lattice fluids: a predictive model for the solubility in glassy polymers. *Macromolecules*, 29(24):7885–7896.

Doyle, P. and Snell, E. (1984). Random walks and electrical networks. carus math.

Ebeling, W. and Sokolov, I. M. (2005). *Statistical thermodynamics and stochastic theory of nonequilibrium systems*, volume 8. World Scientific.

Flory, P. J. (1942). Thermodynamics of high polymer solutions. *The Journal of chemical physics*, 10(1):51–61.

Flory, P. J. (1953). *Principles of polymer chemistry*. Cornell University Press.

Hashin, Z. and Shtrikman, S. (1962). A variational approach to the theory of the effective magnetic permeability of multiphase materials. *Journal of applied Physics*, 33(10):3125–3131.

Huggins, M. L. (1942). Some properties of solutions of long-chain compounds. *The Journal of Physical Chemistry*, 46(1):151–158.

Kamiya, Y., Hirose, T., Mizoguchi, K., and Naito, Y. (1986). Gravimetric study of high-pressure sorption of gases in polymers. *Journal of Polymer Science Part B: Polymer Physics*, 24(7):1525–1539.

Kanehashi, S. and Nagai, K. (2005). Analysis of dual-mode model parameters for gas sorption in glassy polymers. *Journal of Membrane Science*, 253(1):117–138.

Kirkpatrick, S. (1971). Classical transport in disordered media: scaling and effective-medium theories. *Physical Review Letters*, 27(25):1722.

Kirkpatrick, S. (1973). Percolation and conduction. *Reviews of modern physics*, 45(4):574.

Kittel, C. (2005). *Introduction to solid state physics*. Wiley.

Laatikainen, M. and Lindstrom, M. (1987). General sorption isotherm for swelling materials. *ACTA POLYTECHNICA SCANDINAVICA-CHEMICAL TECHNOLOGY SERIES*, (178):105–116.

Landauer, R. (1952). The electrical resistance of binary metallic mixtures. *Journal of Applied Physics*, 23(7):779–784.

Maass, P. and Rinn, B. (2001). Equilibrium and non-equilibrium dynamics in random-energy landscapes. *Philosophical Magazine B*, 81(9):1249–1261.

Maass, P., Rinn, B., and Schirmacher, W. (1999). Hopping dynamics in random energy landscapes: an effective medium approach. *Philosophical Magazine B*, 79(11-12):1915–1922.

Mathieu, P. (2008). Quenched invariance principles for random walks with random conductances. *Journal of Statistical Physics*, 130(5):1025–1046.

Mauze, G. and Stern, S. (1982). The solution and transport of water vapor in poly (acrylonitrile): a re-examination. *Journal of Membrane Science*, 12(1):51–64.

Meroz, Y., Sokolov, I. M., and Klafter, J. (2010). Subdiffusion of mixed origins: when ergodicity and nonergodicity coexist. *Physical Review E*, 81(1):010101.

Mi, Y., Zhou, S., and Stern, S. (1991). Representation of gas solubility in glassy polymers by a concentration-temperature superposition principle. *Macromolecules*, 24(9):2361–2367.

Newstead, G. (1959). General circuit theory.

Paterson, R., Yampol'skii, Y., Fogg, P. G., Bokarev, A., Bondar, V., Ilinich, O., and Shishatskii, S. (1999). Iupac-nist solubility data series 70. solubility of gases in glassy polymers. *Journal of Physical and Chemical Reference Data*, 28(5):1255–1450.

Putintsev, N. and Putintsev, D. (2004). Method for determining the parameters of the lennard-jones potential. In *Doklady Physical Chemistry*, volume 399, pages 278–282. Springer.

Raucher, D. and Sefcik, M. D. (1983). Sorption and transport in glassy polymers: Gas—polymer—matrix model. ACS Publications.

Rinn, B., Braunschweig, U., Maass, P., and Schirmacher, W. (2000). Effective-medium approximation for energy-dependent hopping on a lattice. *Physica Status Solidi B Basic Research*, 218(1):93–98.

Sarti, G. C. and Doghieri, F. (1998). Predictions of the solubility of gases in glassy polymers based on the nelf model. *Chemical Engineering Science*, 53(19):3435–3447.

Schrödinger, E. (1992). *What is life?: With mind and matter and autobiographical sketches*. Cambridge University Press.

Sinai, Y. G. (1970). Dynamical systems with elastic reflections. *Russian Mathematical Surveys*, 25(2):137–189.

Stern, S. and Kulkarni, S. (1982). Solubility of methane in cellulose acetate—conditioning effect of carbon dioxide. *Journal of Membrane Science*, 10(2-3):235–251.

Wiener, O. (1912). Der abhandlungen der mathematisch-physischen klasse der konigl. *Sachsischen Gesellshaft der Wissenschaften*, 32:509–604.

Witte, P. v. d., Dijkstra, P., Berg, J. v. d., and Feijen, J. (1996). Phase behavior of polylactides in solvent-nonsolvent mixtures. *Journal of Polymer Science, Part B: Polymer physics*, 34(15):2553–2568.

Yuge, Y. (1977). Three-dimensional site percolation problem and effective-medium theory: A computer study. *Journal of Statistical Physics*, 16(4):339–348.

Selbständigkeitserklärung

Hiermit erkläre ich, die Dissertation selbstständig und nur unter Verwendung der angegebenen Hilfen und Hilfsmittel angefertigt zu haben.

Ich habe mich nicht anderwärts um einen Doktorgrad in dem Promotionsfach beworben und besitze keinen entsprechenden Doktorgrad.

Die Promotionsordnung der Mathematisch-Naturwissenschaftlichen Fakultät, veröffentlicht im Amtlichen Mitteilungsblatt der Humboldt Universität zu Berlin Nr. 21 am 06. Juli 2009, habe ich zur Kenntnis genommen.

Albano Laziale, den 22. Dezember 2019 Federico Camboni

List of publications

- F.Camboni, Igor M. Sokolov: *Sorption of small molecules in polymeric media*, Physica A 464 (2016) 54-63
- F.Camboni, A.Koher, I.M.Sokolov: *Diffusion of small particles in a solid polymeric medium*, Phys. Rev. E 88, 022120 (2013); (arXiv:1210.6816)
- F.Camboni, I.M.Sokolov: *Normal and anomalous diffusion in random potential landscapes*, Phys. Rev. E 85, 050104(R) (2012); (arXiv:1205-2543)
- E.Agliari, A.Barra, F.Camboni: *Notes on ferromagnetic diluted p-spin model*, Rep. in Math. Phys. 68, 1, (2011); (arXiv:0912.5173)
- E.Agliari, A.Barra, R.Burioni, F.Camboni, P.Contucci: *Effective interactions in group competition with strategic diffusive dynamics*, arXiv:0905.3813
- A.Barra, F.Camboni, P.Contucci: *Dilution robustness for mean field ferromagnets*, J.Stat.Mech. (2009) P03028; (arXiv:0812.1568)
- F.Camboni, A.Barra, E.Agliari: *Criticalitiy in diluted ferromagnet*, J.Stat.Mech. (2008) P10003; (arXiv:0804.4503)